UNIVERSITY OF TURKU

MYOCARDIAL BLOOD FLOW AND CORONARY ANATOMY IN SUSPECTED OBSTRUCTIVE CORONARY ARTERY DISEASE

A Hybrid Imaging Study

Iida Stenström

TURUN YLIOPISTON JULKAISUJA – ANNALES UNIVERSITATIS TURKUENSIS
SARJA - SER. D OSA - TOM. 1523 | MEDICA - ODONTOLOGICA | TURKU 2020

UNIVERSITY OF TURKU

MYOCARDIAL BLOOD FLOW AND CORONARY ANATOMY IN SUSPECTED OBSTRUCTIVE CORONARY ARTERY DISEASE

A Hybrid Imaging Study

Iida Stenström

TURUN YLIOPISTON JULKAISUJA – ANNALES UNIVERSITATIS TURKUENSIS
SARJA - SER. D OSA – TOM. 1523 | MEDICA – ODONTOLOGICA | TURKU 2020

University of Turku

Faculty of Medicine
Department of Cardiology and Cardiovascular Medicine
Doctoral Programme in Clinical Research
Heart Center and Turku PET Centre, Turku University Hospital

Supervised by

Professor Antti Saraste, MD, PhD
Heart Center
University of Turku and
Turku University Hospital
Turku, Finland

Professor Juhani Knuuti, MD, PhD
Turku PET Centre
University of Turku and
Turku University Hospital
Turku, Finland

Reviewed by

Docent Sari Kivistö
Department of Radiology
HUS Medical Imaging Center
Helsinki University Hospital and
University of Helsinki
Helsinki, Finland

Docent Pertti Jääskeläinen
Heart Center
University of Eastern Finland and
Kuopio University Hospital
Kuopio, Finland

Opponent

Professor Juhani Junttila
Director of Medical Research Center Oulu
Oulu University Hospital and
University of Oulu
Oulu, Finland

The originality of this publication has been checked in accordance with the University of Turku quality assurance system using the Turnitin OriginalityCheck service.

ISBN 978-951-29-8298-1 (PRINT)
ISBN 978-951-29-8299-8 (PDF)
ISSN 0355-9483 (Print)
ISSN 2343-3213 (Online)
Painosalama Oy, Turku, Finland 2020

UNIVERSITY OF TURKU
Faculty of Medicine
Department of Cardiology and Cardiovascular Medicine
Heart Center and Turku PET Centre, Turku University Hospital
IIDA STENSTRÖM: Myocardial Blood Flow and Coronary Anatomy in Suspected Obstructive Coronary Artery Disease – A Hybrid Imaging Study
Doctoral Dissertation, 127 pp.
Doctoral Programme in Clinical Research
December 2020

ABSTRACT

Coronary computed tomography angiography (CTA) is an accurate noninvasive imaging modality for detecting coronary atherosclerosis and to rule out obstructive coronary artery disease (CAD). Myocardial perfusion imaging (MPI) with positron emission tomography (PET) allows the quantification of myocardial blood flow (MBF). The quantification of MBF enables the assessment of the hemodynamical significance of a coronary stenosis seen on coronary CTA, as well as the assessment of the function of the microvasculature. Hybrid imaging with coronary CTA and PET combines information on coronary anatomy and function, but its clinical value has not been extensively studied.

In this study, the effect of a selective hybrid imaging protocol on downstream referrals to invasive coronary angiography (ICA) as well as its prognostic value in patients with suspected CAD were investigated. An assessment of MBF was performed only if a suspected significant stenosis was seen on coronary CTA. In addition, the prevalence of coronary microvascular dysfunction (CMD) was prospectively investigated in chest pain patients by using a combination of coronary CTA, PET perfusion imaging, and ICA.

Obstructive CAD was excluded in approximately one half of the patients by coronary CTA alone, and MBF was normal in approximately one half of the patients who also underwent PET MPI. In these patients, downstream referrals to ICA and revascularization procedures were rare and the rates of acute coronary syndrome or death were low during the follow-up of 3.6 years. The prevalence of CMD was low (1%) in the absence of CAD.

Selective hybrid imaging with coronary CTA and PET may potentially reduce the number of unnecessary ICAs and is useful in the risk stratification of patients with suspected CAD. The prevalence of CMD is relatively low in patients with chronic chest pain.

KEYWORDS: computed tomography, coronary artery disease, coronary microvascular dysfunction, hybrid imaging, positron emission tomography

TURUN YLIOPISTO
Lääketieteellinen tiedekunta
Kardiologia ja kardiovaskulaarilääketiede
Sydänkeskus ja Turun PET-keskus, Turun yliopistollinen keskussairaala
IIDA STENSTRÖM: Sydänlihaksen verenvirtaus ja sepelvaltimoiden anatomia ahtauttavaa sepelvaltimotautia epäiltäessä – Hybridikuvantamistutkimus
Väitöskirja, 127 s.
Turun kliininen tohtoriohjelma
Joulukuu 2020

TIIVISTELMÄ

Sepelvaltimoiden tietokonetomografialla (TT) voidaan todeta luotettavasti sepelvaltimoiden ateroskleroosimuutokset ja sulkea pois ahtauttava sepelvaltimotauti. Sydänlihaksen verenvirtauksen mittaus positroniemissiotomografiaa (PET) käyttämällä mahdollistaa TT-tutkimuksessa nähtyjen ahtaumien toiminnallisen merkityksen sekä pienten sepelvaltimoiden toiminnan arvioinnin. PET-TT-hybridikuvantamisen avulla on mahdollista tutkia sekä sepelvaltimoiden anatomiaa että toimintaa, mutta sen hyötyä sepelvaltimotaudissa on tutkittu vain vähän.

Kliinisissä tutkimuksissa tutkittiin valikoivan PET-TT-hybridikuvantamisen vaikutusta potilaiden jatkotutkimuksiin ja menetelmän ennustearvoa oireisilla potilailla, jotka lähetettiin tutkimuksiin ahtauttavan sepelvaltimotaudin epäilyn vuoksi. Sydänlihaksen verenvirtauksen mittaus suoritettiin ainoastaan, mikäli TT-tutkimuksessa havaittiin mahdollisesti hemodynaamisesti merkitsevä ahtauma. Lisäksi pienten sepelvaltimoiden toimintahäiriön esiintyvyyttä pitkäaikaisen rintakivun yhteydessä selvitettiin etenevässä tutkimuksessa, jossa potilaille tehtiin sepelvaltimoiden TT, sydänlihaksen verenvirtauksen mittaus PET-menetelmällä sekä kajoava sepelvaltimoiden varjoainekuvaus.

Sepelvaltimoiden TT-tutkimuksen perusteella ahtauttava sepelvaltimotauti voitiin sulkea pois puolella potilaista. Puolella potilaista, joilla todettiin ahtauma TT-tutkimuksessa, sydänlihaksen verenvirtaus rasituksessa oli kuitenkin normaali. Näillä potilailla kajoava sepelvaltimoiden varjoainekuvaus tai revaskularisaatio tehtiin vain harvoin ja sydänkohtauksen tai kuoleman riski oli 3.6 vuoden seurannan aikana pieni. Lisäksi havaittiin, että pienten sepelvaltimoiden toimintahäiriö ilman sepelvaltimotautia on harvinainen (1%).

Valikoiva PET-TT -hybridikuvantaminen voi vähentää kajoavien varjoainekuvausten määrää ja on hyödyllinen riskinarvioinnissa niillä potilailla, joilla epäillään ahtauttavaa sepelvaltimotautia. Pienten sepelvaltimoiden toimintahäiriö on rintakipupotilailla suhteellisen harvinainen löydös.

AVAINSANAT: hybridikuvantaminen, pienten sepelvaltimoiden toimintahäiriö, positroniemissiotomografia, tietokonetomografia, sepelvaltimotauti

Table of Contents

Abbreviations

CABG	Coronary artery bypass graft
CAD	Coronary artery disease
CBF	Coronary blood flow
CCS	Chronic coronary syndromes
CFR	Coronary flow reserve
CMD	Coronary microvascular dysfunction
CMR	Cardiac magnetic resonance
CT	Computed tomography
CTA	Computed tomography angiography
CTP	Computed tomography myocardial perfusion
ECG	Electrocardiography
FFR	Fractional flow reserve
FFR_{CT}	Computed tomography-derived fractional flow reserve
HDL	High-density lipoprotein
ICA	Invasive coronary angiography
LAD	Left anterior descending
LCX	Left circumflex
LDL	Low-density lipoprotein
LV	Left ventricle
MBF	Myocardial blood flow
MPI	Myocardial perfusion imaging
MVA	Microvascular angina
PCI	Percutaneous coronary intervention
PET	Positron emission tomography
RCA	Right coronary artery
SPECT	Single photon emission computed tomography
UAP	Unstable angina pectoris

List of Original Publications

This dissertation is based on the following original publications, which are referred to in the text by their Roman numerals:

I Stenström I, Maaniitty T, Uusitalo V, Ukkonen H, Kajander S, Mäki M, Nammas W, Bax JJ, Knuuti J, Saraste A. Absolute Stress Myocardial Blood Flow After Coronary CT Angiography Guides Referral to Invasive Angiography. *JACC Cardiovasc Imaging*, 2019;12:2266-7.

II Maaniitty T, Stenström I, Bax JJ, Uusitalo V, Ukkonen H, Kajander S, Mäki M, Saraste A, Knuuti J. Prognostic Value of Coronary CT Angiography With Selective PET Perfusion Imaging in Coronary Artery Disease. *JACC Cardiovasc Imaging*, 2017;10:1361-70.

III Stenström I, Maaniitty T, Uusitalo V, Pietilä M, Ukkonen H, Kajander S, Mäki M, Bax JJ, Knuuti J, Saraste A. Frequency and Angiographic Characteristics of Coronary Microvascular Dysfunction in Stable Angina: A Hybrid Imaging Study. *Eur Heart J Cardiovasc Imaging*, 2017;18:1206-13.

1 Introduction

Coronary arterial system is responsible for providing blood flow and oxygen to the myocardium. The system is complex and there is a subtle balance between the functions of macro- and microcirculation (Camici & Crea, 2007). Structural or functional abnormalities in epicardial arteries, prearterioles, or intramural arterioles may lead to myocardial ischemia, which occurs when the myocardial blood flow (MBF) is insufficient in relation to the oxygen demand of the myocardium.

Coronary artery disease (CAD) is the most common manifestation of atherosclerosis. In the course of time, intimal lipid accumulation may cause narrowing of the epicardial artery lumen and evolve into a flow-limiting stenosis (Libby & Theroux, 2005). Coronary computed tomography angiography (CTA) enables noninvasive visualization of the coronary artery lumen and wall, as well as the detection of atherosclerotic plaque (Achenbach, 2006). However, the degree of a stenosis seen on anatomical imaging does not directly correlate with the hemodynamic significance (Meijboom, van Miegham et al., 2008). Noninvasive functional imaging aims to detect myocardial ischemia, which may be caused by a flow-limiting atherosclerotic lesion and coronary microvascular dysfunction (CMD). These conditions share a similar symptom profile including exercise related chest pain and dyspnea (Camici & Crea, 2007). Myocardial perfusion imaging (MPI) with positron emission tomography (PET) enables the quantification of MBF and can be used in combination with coronary CTA to obtain information on both anatomy and function (Gaemperli et al., 2012). Hybrid imaging combines data from two separate imaging modalities, both of which are independently contributing to the image formation.

CAD is the leading cause of death globally, and a chronic coronary syndrome (CCS) with stable symptoms can evolve to an acute coronary syndrome at any time. Thus, the identification of patients at high risk of an acute coronary syndrome or death is crucial for the optimization of treatment. Hybrid imaging with PET and coronary CTA is a rather novel combination that may be beneficial in the detection of obstructive CAD and CMD, guidance of treatment, and risk stratification.

This thesis is comprised of clinical studies investigating the use of hybrid imaging with coronary CTA and PET in symptomatic patients with suspected CAD.

2 Review of the Literature

2.1 Anatomy and physiology of the coronary circulation

2.1.1 Anatomy of the coronary arterial system

The coronary arterial system provides blood flow to the myocardium. The large epicardial arteries, prearterioles and intramural arterioles compose the three compartments of this arterial network (Camici & Crea, 2007). The epicardial arteries constitute the macrocirculation, whereas the small arteries, together with capillaries, form the microcirculation. The regions differ in function and, in fact, their differentiation is impossible on the basis of anatomy alone. The diameter of the proximal compartment arteries varies from approximately 500 μm to 5 mm. The diameters of the intermediate and distal compartment vessels range from approximately 100 to 500 μm and to less than 100 μm, respectively (Mathew et al., 2019).

Epicardial coronary arteries originate from the ascending aorta above the aortic valve. Typically, the left coronary artery supplies the anterior ventricular septum and the anterior and lateral wall of the left ventricle (LV), whereas the right coronary artery (RCA) supplies the right ventricle. The dominance of the coronary artery system is determined by the artery that supplies the posterior descending artery and the posterolateral branch. These arteries supply the inferoseptal and inferior segments of the LV. In 80-85% of the cases, the system is right dominant, in other words, the posterior descending artery and the posterolateral branch arise from the RCA, whereas in 15-20% they arise from the LCX. Co-dominance is observed in around 5% of the patients. The left main coronary artery bifurcates into the left anterior descending (LAD) and left circumflex (LCX) arteries, which further divide into smaller branches (Kini et al., 2007). The vessel arrangement of the microcirculation is not anatomically anchored but, rather, is adaptive by nature and responds to functional demands with structural angioadaptation (Pries et al., 2005).

Contemporary imaging modalities do not allow the direct visualization of the coronary arterial system in its entirety and beyond epicardial arteries (Pries & Reglin, 2017). An anatomical evaluation of the epicardial artery lumen and wall can be

performed either noninvasively with coronary CTA or with invasive coronary angiography (ICA) (Knuuti et al., 2020).

Histologically, the wall of an epicardial coronary artery is three-layered with intima, media, and adventitia. Tunica intima consists of an endothelial cell monolayer supported by internal elastic lamina and has no capillaries or lymphatic vessels. The media of an epicardial coronary artery consists mainly of smooth muscle cells, and the external elastic lamina separates it from adventitia, which is composed of connective tissue, nerve fibers, and small vessels, *vasa vasorum*. The media in prearterioles and arterioles consists of smooth muscle cells alone, thus enabling the changes in lumen size through smooth muscle cell contraction. Capillaries, on the other hand, have no media but only an endothelial cell lining and basement membrane (Waller et al., 1992).

2.1.2 Physiology of coronary circulation

In myocardial tissue, oxygen extraction varies between 60–80% at rest, and therefore, its ability to increase oxygen extraction to meet increased metabolic demands is limited. An increase in coronary blood flow (CBF) is required when myocardial oxygen consumption is elevated, for example, during physical activity. The increase can be up to four- to fivefold in the absence of microcirculatory dysfunction. The term coronary flow reserve (CFR) is used to describe the capacity to increase CBF in response to stress and is given as the ratio of hyperemic to rest MBF. In fact, CFR is a composite measure that takes into consideration possible epicardial stenosis and its severity, as well as the dysfunction of the microvasculature (Mathew et al., 2019).

CBF shows great phasic variations and, distinctively, most of the flow happens during diastole. An increase in the coronary arterial inflow is observed with a perfusion gradient towards the endocardial layers in the absence of LV compression on intramyocardial microvessels. During exercise, the duration of diastole shortens and, consequently, the duration of effective CBF decreases. This may result in reduced oxygen delivery in patients with obstructive CAD (Duncker et al., 2015).

In addition to the duration of the diastole, the two other significant factors are the coronary perfusion pressure and coronary vascular resistance (Schelbert, 2010). The pressure gradient across the coronary vasculature constitutes the effective perfusion pressure that is essential for the CBF, with input pressure being the diastolic aortic pressure at valvular plane (Duncker et al., 2015). Coronary vascular resistance is composed of several external and internal components, the most important of which are the extravascular compressive forces and the state of the resistance vessels. The extravascular compressive forces follow the cardiac cycle and are highest during systole, causing intramyocardial microvessel compression

and redistribution of blood flow from subendocardial to subepicardial layers (Duncker et al., 2015). The microcirculation is the main component of coronary vascular resistance since only approximately 5% pressure drop happens in the epicardial arteries in the absence of a stenosis at rest (Camici & Crea, 2007).

Autoregulation is a distinctive feature of coronary circulation and it ensures that CBF is kept constant over a wide range of perfusion pressures under resting conditions. Keeping CBF steady with a low perfusion pressure protects the myocardium from ischemia and, conversely, with a high perfusion pressure, it protects endothelium and prevents myocardial edema. This is achieved by the changes in microvascular vessel diameter and include myogenic, metabolic, endothelial, and neurohumoral mechanisms (Duncker et al., 2015).

The change in the diameter of the resistance vessels is the most important factor in the immediate regulation of CBF. Mostly, the extramyocardial prearterioles respond to hemodynamic changes in, for example, flow and intravascular pressure and sustain pressure, at the origin of arterioles within a narrow pressure scale. As the aortic pressure increases, they undergo myogenic constriction (Camici & Crea, 2007; Mathew et al., 2019).

Endothelium plays a key role in the regulation of CBF by modulating the vascular tone. Nitric oxide is the most important vasodilator released from the endothelium and it mediates the vasodilatation of epicardial arteries, whereas the endothelium-dependent vasodilatation of coronary microvessels is mediated by the endothelium-derived hyperpolarizing factor (Sechtem et al., 2020). A powerful vasoconstrictor, on the other hand, is endothelin-1 which is a key modulator of the vasomotor tone. The production of prostaglandin, prostacyclin and thromboxane becomes more important when the production of nitric oxide is impaired for example in atherosclerosis. Neurohumoral receptor activation via acetylcholine, angiotensin, bradykinin, and norepinephrine affects the balance between vasodilators and vasoconstrictors.

The most distal compartment, the intramural arterioles, balances the MBF and oxygen consumption via metabolic regulation, i.e., they dilate when metabolites from the myocardium are released in response to enhanced oxygen consumption (Duncker et al., 2015). Consequently, the dilatation of the arterioles decreases the pressure in distal prearterioles, resulting in an increase in shear stress, which provokes a flow-dependent dilatation in the larger prearterioles and conductance arteries. Metabolic regulators of CBF include carbon dioxide, adenosine, and adenosine triphosphate acting as vasodilators (Deussen et al., 2006). Adenosine predominantly dilates the coronary arterioles up to 100 μm and is produced especially when the oxygen supply-to-demand ratio is impaired (Deussen et al., 2006).

2.2 Coronary artery disease

2.2.1 Pathophysiology of CAD and flow-limiting stenosis

Atherosclerosis is a progressive immunoinflammatory disease of medium-sized and large arteries, characterized by intimal lesions to which coronary arteries and especially their bifurcations are particularly prone to (Antoniadis et al., 2015; Libby & Theroux, 2005). CAD is the most common manifestation of atherosclerosis, with others being ischemic stroke and peripheral vascular disease (Bentzon et al., 2014).

The atherosclerotic process is dynamic by nature, with the number and level of severity of the risk factors defining the evolution of the disease (Liu et al., 2012; Vartiainen et al., 1994). Traditional risk factors of atherosclerosis include age, gender, smoking, hypertension, diabetes, high serum low-density lipoprotein (LDL) level, low serum high-density lipoprotein (HDL) level, and family history of premature CAD (Castelli et al., 1986; Wilson et al., 1998).

The fundamental event in the course of atherosclerosis is the accumulation of LDL into the intima where LDL can undergo various modifications, such as oxidation (Libby et al., 2000). The modified LDL particles stimulate pro-inflammatory cytokine production, which increases the expression of leukocyte adhesion molecules responsible for capturing leukocytes from blood (Gimbrone & García-Cardeña, 2016; Libby et al., 2000). After transendothelial migration with the help of chemoattractants, monocytes differentiate into macrophages and take up modified LDL particles until they turn into foam cells, which are distinctive to both early and late atherosclerotic lesions (Falk, 2006; Gimbrone & García-Cardeña, 2016).

Diffuse intimal thickening, found in atherosclerotic-prone arteries as early as in neonates, is a physiologic response to blood flow (Nakashima et al., 2002). Intimal xanthomas or fatty streaks, seen already in childhood develop via extracellular deposition of lipids in the outer layer of the intimal thickening (Nakashima et al., 2007; Virmani et al., 2000). Pathological intimal thickening is the first stage of progressive atherosclerotic lesions with microcalcification within lipid pools in addition to absence of viable smooth muscle cells. Infiltration of macrophages starts with pathological intimal thickening and is progressively seen in a fibroatheroma, which is formed after the development of a necrotic core and a fibrous cap (Otsuka et al., 2015; Yahagi et al., 2016). Traditionally, a thin-cap fibroatheroma is thought to be the precursor lesion to acute coronary syndrome.

Atherosclerotic coronary stenosis alters the epicardial resistance conditions by reducing the diameter of the artery lumen. Stenosis becomes flow-limiting when causing a decline in post-stenotic pressure, which usually occurs when the internal luminal diameter is reduced by approximately 50% or more (Duncker et al., 2015).

The vasodilation of the coronary resistance vessels via autoregulation compensates the lower perfusion pressure, but the compensatory mechanism becomes exhausted when the stenosis reaches the critical luminal diameter of 90% (Duncker et al., 2015). The impairment in maximal CBF and reduction in CFR in exercise- and stress-induced myocardial ischemia, that is, an insufficient MBF in relation to the oxygen demand of the myocardium, are typically limited to the subendocardial layers of the heart when caused by a flow-limiting stenosis.

2.2.2 Clinical scenarios of chronic coronary syndromes

The latest European Society of Cardiology (ESC) Guidelines have been revised to focus on chronic coronary syndromes (CCS) instead of stable CAD to emphasize the dynamic nature of atherosclerotic plaque accumulation and to classify the clinical presentations of CAD to acute coronary syndrome and CCS. The clinical scenarios of suspected or established CCS have been categorized as follows: i) patients with suspected CAD and 'stable' anginal symptoms, and/or dyspnea, ii) patients with new onset of heart failure (HF) or left ventricular dysfunction and suspected CAD, iii) asymptomatic and symptomatic patients with stabilized symptoms <1 year after an acute coronary syndrome, or patients with recent revascularization, iv) asymptomatic and symptomatic patients >1 year after initial diagnosis or revascularization, v) patients with angina and suspected vasospastic or microvascular dysfunction, and vi) asymptomatic subjects in whom CAD is detected at screening (Knuuti et al., 2020). All phases of the disease involve different risks for future cardiovascular events. The risk may vary over time and it can be reduced by controlling cardiovascular risk factors through lifestyle modifications, medical therapy, and revascularization.

The underlying cause of an acute coronary syndrome is coronary artery thrombosis as a result of plaque rupture, plaque erosion, or calcified nodule (Tomaniak et al., 2020). Until recently, studies have focused on the search for the so-called vulnerable plaque. Lately, it has been observed that it is not the vulnerable plaque but the vulnerable patient with the vulnerable plaque, that is essential to recognize. Atherosclerosis is an inflammatory disease affecting the whole body, not just a single segment of a coronary artery (Libby & Pasterkamp, 2015; Tomaniak et al., 2020).

2.2.3 Diagnosis and general approach

The general approach in patients with angina and suspected CAD includes six consecutive steps according to the current ESC Guideline (Knuuti et al., 2020). Step 1 includes the assessment of symptoms to exclude patients with acute coronary

syndrome. The patient's general condition, quality of life and other potential causes of the symptoms are evaluated in step 2. In step 3, basic testing and assessment of LV function are performed, followed by the estimation of the clinical likelihood of obstructive CAD in step 4, and further diagnostic tests in selected patients in step 5. Once the diagnosis is confirmed, step 6 involves the evaluation of the patient's event risk, which has a significant impact on subsequent therapeutic decisions.

The traditional clinical classification of suspected anginal symptoms categorizes chest pain into typical angina, atypical angina and nonanginal chest pain. Typical angina is constricting discomfort in the front of the chest or in the neck, jaw, shoulder or arm; is precipitated by physical exertion, and relieved by rest or nitrates within 5 minutes. Atypical angina meets two of these criteria and nonanginal chest pain only one or none. Nevertheless, recent data shows that only 10–15% of the patients with suspected CAD present typical chest pain (Douglas et al., 2015; SCOT-HEART investigators, 2015; Reeh et al., 2019).

The basic testing includes standard laboratory biochemical testing, a resting electrocardiography (ECG), and a resting echocardiography. The latter is used to define LV ejection fraction, which typically is normal in patients with CCS (Daly et al., 2003). A suspicion of ischemic myocardial damage may arise if the patient has decreased systolic or diastolic LV function and/or regional wall motion abnormalities (Daly et al., 2006). The assessment of LV function, especially LV ejection fraction, plays a key role in risk assessment (Knuuti et al., 2020). Decreased diastolic LV function may also indicate myocardial ischemia or CMD (Knuuti et al., 2020; Shaw et al., 2009).

In diagnosing obstructive CAD, the performance of the available imaging modalities is dependent on the prevalence of the disease in the population. Diagnostic testing is most useful when the likelihood of the disease is intermediate. Thus, performing the diagnostic test in patients with extremely low or extremely high pre-test probability, is not advisable. Pre-test probability of obstructive CAD can be assessed on the basis of age, gender, and the nature of the symptoms (Diamond & Forrester, 1979). The pre-test probabilities have recently been updated in the recent Guideline since the prevalence of obstructive CAD in patients with suspected CAD has in several studies been shown to be lower than earlier reported (Foldyna et al., 2019). Overestimation of pre-test probability is an important contributory factor for the low diagnostic yield of noninvasive and invasive testing.

In cases where the diagnosis of CAD is uncertain after clinical evaluation and assessment of pre-test probability, the current ESC Guidelines recommend noninvasive functional imaging or coronary CTA as the initial diagnostic test (Knuuti et al., 2020). If the clinical likelihood of CAD is high and the patient has symptoms unresponsive to medical therapy, or angina at a low level of exercise, proceeding directly to ICA may be considered. The role of exercise ECG has

changed in recent years as having inferior diagnostic performance and limited power to rule in or rule out obstructive CAD (Knuuti et al., 2018). Based on recent studies, the current ESC Guidelines recommend the use of an imaging diagnostic test instead of exercise ECG as the initial test for diagnosing obstructive CAD, but the latter may be considered if there is a need for complementary assessment of symptoms, exercise tolerance, arrhythmias or blood pressure response (Knuuti et al., 2020). Diagnostic accuracy, clinical likelihood, patient characteristics including possible contraindications for certain tests, local expertise, and availability of tests are relevant factors contributing to the selection of the appropriate noninvasive test, and in all cases, clinical benefits should exceed the projected risks of the test itself (Knuuti et al., 2014).

ICA is required for diagnostics if noninvasive testing is inconclusive. However, it may be indicated in order to assess the need for revascularization after noninvasive testing suggestive of significant stenosis and/or ischemia. ICA has traditionally been considered the gold standard in the anatomical imaging of coronary artery stenoses as it provides high-resolution imaging of the artery lumen. However, ICA lacks the ability to assess the functional relevance of an atherosclerotic plaque. Thus, the current ESC Guidelines recommend fractional flow reserve (FFR) measurements for stenoses of 50–90% if noninvasive proof of ischemia is not available (Knuuti et al., 2020; Toth et al., 2014). FFR is a pressure-derived index, defined as the pressure gradient across a coronary lesion during adenosine-induced vasodilatation, and a threshold of <0.80 in FFR measurements has been shown to be useful in finding lesions that would benefit from revascularization (Adjedj et al., 2016). To assess microvascular dysfunction, indicies of microvascular resistance and hyperemic microvascular resistance may be determined during ICA. However, their clinical use is currently limited due to the requirement of technical expertise and specialist resources (Sara et al., 2015). As an invasive test, ICA carries out a risk for complications with the composite rate of death, MI or stroke of 0.1–0.2%, although complication rates have decreased due to technical improvements, such as the use of radial artery access (Arora et al., 2007; Mason et al., 2018). Visualization of the plaque structure and vessel remodeling invasively requires complementary testing with intravascular ultrasound or optical coherence tomography of which the first is a sound-based imaging technique providing grey-scale or color-coded images of the artery wall *in vivo*, and the latter is based on infrared light emission (Neumann et al., 2019). IVUS and OCT are mainly used to optimize revascularization with PCI, but IVUS is also useful in assessing the severity of stenoses in the left main coronary artery (Neumann et al., 2019).

Event risk is a major contributory factor for treatment decisions, and event risk assessment is recommended for every patient with suspected or recently diagnosed CAD with the goal of identifying patients at high risk who would benefit from

revascularization besides the control of symptoms as described below. Determination of the event risk relies on clinical evaluation, assessment of LV function by resting echocardiography, noninvasive assessment of ischemia or assessment of coronary anatomy noninvasively or invasively. Findings that correspond to a high event risk have been identified for each imaging modality (Knuuti et al., 2020), as described below in more detail.

2.2.4 Treatment of CCS

2.2.4.1 Lifestyle and pharmacological management

The aim in the management of CCS is to reduce symptoms and to improve prognosis, which are achieved by lifestyle changes, medical care, and interventions in well-selected patients. Primary care providers play an essential role in the field of prevention, since maintaining a healthy lifestyle significantly decreases the risk of cardiac events and deaths in the future. Lifestyle recommendations for patients with CCS include smoking cessation, healthy diet, physical activity, healthy weight, and taking medication as prescribed (Knuuti et al., 2020). However, adherence to a healthy lifestyle is known to be a challenge (Booth et al., 2014; Chow et al., 2010; Chowdhury et al., 2013; Wood et al., 2008).

Typically, pharmacological management is initiated with one or two anti-ischemic drugs combined with medication for secondary prevention. Beta-adrenergic blockers or calcium channel blockers are recommended as the first choice of anti-ischemic drugs. The first have been associated with a reduction in adverse events in selected patients with MI or chronic heart failure with reduced ejection fraction, but the latter lack evidence in reducing mortality. Immediate relief of anginal symptoms is achieved with rapidly acting formulations of nitroglycerin, whereas long-acting nitrate formulations may be used in second-line anti-ischemic therapy. Secondary prevention of obstructive CAD includes an antithrombotic drug and a cholesterol lowering medication, which are crucial in the prevention of atherothrombotic events. Aspirin is recommended for prevention of ischemic events in patients with obstructive CAD, especially in patients with a history of MI or revascularization. Temporary dual antiplatelet therapy with an oral $P2Y_{12}$-inhibitor in addition to aspirin is used after MI and/or percutaneous coronary intervention (PCI) (Knuuti et al., 2020). Statins are recommended in all patients with CCS and combination of ezetimibe is recommended if the goal is not reached. In addition, proprotein convertase subtilisin-kexin type 9 inhibitors may be combined to the combination of statin and ezetimibe in selected patients with a very high risk (Knuuti et al., 2020). Angiotensin-converting enzyme inhibitors have been shown to reduce

mortality, stroke, and heart failure in patients with CAD combined with LV dysfunction, and diabetes (Knuuti et al., 2020).

2.2.4.2 Revascularization in CCS

The role of optimal medical therapy in patients with CCS is undeniable. However, revascularization by PCI or coronary artery bypass graft (CABG) plays a significant additional role in symptom relief and improvement of prognosis in high-risk patients. Unlike in acute coronary syndrome, the optimal use of revascularization in stable CAD remains controversial. Consensus has been reached on the importance of the evaluation of the functional significance of the stenosis and documentation of ischemia by noninvasive functional imaging or FFR before revascularization (Neumann et al, 2019; Tonino et al., 2009). According to the current ESC guideline on myocardial revascularization, indications for revascularization in patients with CCS receiving guideline-recommended medical treatment are persistence of symptoms despite medical treatment and/or the improvement of prognosis (Neumann et al., 2019). For prognosis, indications for revascularization in CCS are left main disease with stenosis >50%, proximal LAD stenosis >50%, two- or three-vessel disease with stenosis >50% with impaired LV function (LV ejection fraction ≤35%), large area of ischemia detected by functional testing (>10% LV) or abnormal invasive FFR, single remaining patent coronary artery with stenosis >50% (Neumann et al., 2019). For symptom relief, indication for revascularization is hemodynamically significant coronary stenosis in the presence of limiting angina or angina equivalent with insufficient response to optimized medical therapy (Neumann et al., 2019). The SYNTAX score can be used in assessment of the anatomical complexity of CAD and to guide the decision on the type of revascularization in some cases (Neumann et al., 2019).

In the DEFER study, patients referred to PCI with non-ischemic FFR values >0.75 were randomized to undergo PCI or to continue with solely medical therapy alone (Pijls et al., 2007). Medical therapy alone was non-inferior to PCI, and interestingly, during the 15 years of follow-up, PCI showed a higher event rate, mainly due to target-vessel MI with low adverse event rates in both groups (Zimmermann et al., 2015). The FAME trial was a randomized comparison of angiographically guided PCI and FFR-guided PCI where the threshold for treatment for FFR was raised to 0.80, and the FFR-guided PCI resulted in lower rates of MI and death during the 1-year follow-up (Tonino et al., 2009).

In a number of meta-analyses, PCI has been compared with initial medical therapy in patients with stable CAD, and no or modest benefits in mortality and MI for the invasive strategy have been found. However, in the FAME 2 study, a lower rate of MI and urgent revascularization was observed during the 5-year follow-up,

with the PCI specifically targeting stenoses with FFR <0.80 (Xaplanteris et al., 2018). Moreover, incremental decrease of mortality and MI has been reported when using CABG or new-generation drug-eluting stents (Windecker et al., 2014).

Revascularization on top of optimal medical therapy relieves anginal symptoms, reduces the use of anti-anginal drugs, and improves exercise capacity as well as quality of life. However, the benefit of symptom control may be of short term (Hueb et al., 2010; Weintraub et al., 2008; Xaplanteris et al., 2018). The recent randomized ORBITA trial compared PCI with a sham procedure in patients with stable single-vessel CAD with preserved LV function, accompanied with moderate anginal symptoms, and found no significant improvement in exercise capacity with PCI (Al-Lamee et al., 2018). Due to the limited trial size, short observation time, and insufficient power to assess end points, no definite conclusions can be drawn. Hence, the study implies of a significant placebo component in the clinical effects subject to bias.

In the ISCHEMIA trial, a total of 5,179 patients were randomly divided to an initial invasive strategy and medical therapy or to an initial conservative strategy and angiography in case the medical therapy failed. Patients were followed up for a median time of 3.2 years and it was observed that the initial invasive strategy did not reduce the risk of ischemic cardiovascular events or death (Maron et al., 2020). However, unlike stated in the initial study design, not all patients had undergone noninvasive functional imaging with PET, single photon emission computed tomography (SPECT), echocardiography, or cardiac magnetic resonance (CMR), but instead, patients with stress ECG were also enrolled although no preliminary data exists on the possible ability of this method to identify patients potentially benefiting from revascularization (Maron et al., 2020). Nevertheless, the ISCHEMIA trial suggests that medical therapy is a safe option for patients with an ischemic heart disease. The trial does not mitigate the clinical value of accurate diagnosis of CAD and estimation of risk, as these are important factors in determining the need of therapy, either medical or revascularization.

2.3 Coronary microvascular dysfunction

2.3.1 Pathophysiology of CMD

CMD refers to the whole subset of disorders affecting coronary microcirculation. It has recently been noted for its capability to induce myocardial ischemia and even non-ST-elevation acute coronary syndromes independent of or coexisting with obstructive CAD (Knuuti et al., 2020; Roffi et al., 2016). Several structural and functional abnormalities have been associated with CMD. Different combinations of abnormalities occur depending on the patient population and possible underlying

conditions (Camici et al., 2015; Kaski et al., 2018). Correlation and causality have been observed with endothelial dysfunction, microvascular spasm, and luminal obstruction (Pries & Reglin, 2017). In addition, a large number of different hypotheses on the pathophysiological mechanisms exist. However, the pathophysiological chain has not been established in any of these (Pries & Reglin, 2017).

Microvascular remodeling is a structural abnormality leading to microvascular obstruction via luminal narrowing of the intramural arterioles and capillaries, as well as capillary rarefaction, the loss of microcirculatory arterioles and capillaries. CMD resulting from structural changes has been observed in patients with risk factors for CAD and with different cardiomyopathies (Suzuki et al., 1994; Tanaka et al., 1987).

Functional abnormalities may lead to impaired vasodilation or increased vasoconstriction. The mechanisms include endothelial dysfunction (Egashira et al., 1993; Vanhoutte et al., 2017), primary vascular smooth muscle cell dysfunction with reduced response to endothelium-independent vasodilators (e.g., adenosine, dipyridamole and papaverine) in patients with traditional CAD risk factors (Campisi et al., 1998; Di Carli et al., 2003; Hamasaki et al., 2000; Pitkänen et al., 1996), and microvascular spasm with augmented α-adrenoceptor activation responses (Baumgart et al., 1999). New hypotheses on the pathophysiology of CMD, including degraded endothelial surface layer, compromised conduction, and impaired metabolic feedback, have recently been suggested (Pries & Reglin, 2017).

2.3.2 Classification of CMD and the interplay between CMD and atherosclerosis

Camici and Crea have presented a widely cited classification of CMD based on the clinical setting in which it occurs: i) CMD in the absence of obstructive CAD and myocardial diseases, ii) CMD in the presence of myocardial diseases, iii) CMD in the presence of obstructive CAD, and iv) iatrogenic CMD (Camici & Crea, 2007). Furthermore, Taqueti and Di Carli have suggested a simplified classification of CMD based on the extent of atherosclerosis, severity of CMD, and factors that augment the clinical risk (Taqueti & Di Carli, 2018). This classification is thought to better describe CMD as a spectrum with possibly coexisting nonobstructive or obstructive CAD.

CMD in the absence of atherosclerosis and myocardial diseases has been observed in patients with traditional risk factors for CAD such as arterial hypertension (Hamasaki et al., 2000; Laine et al., 1998), diabetes (Nahser et al., 1995; Nitenberg et al., 1993), and dyslipidemia (Dayanikli et al., 1994; Kaufmann et al., 2000). In addition, CMD has been associated with certain myocardial diseases such as aortic stenosis (Rajappan et al., 2003) and nonischemic cardiomyopathies

(Majmudar et al., 2015; Neglia et al., 2002), as well as Anderson-Fabry's disease, amyloidosis, and myocarditis (Camici and Crea, 2007).

CMD with nonobstructive atherosclerosis possibly represents the largest subgroup of patients with CMD and may be classified as an independent entity with unique prognostic and therapeutic implications (Taqueti & Di Carli, 2018). There is substantial evidence that diabetes and prediabetes are conductive to changes in the regulation of vascular tone before the occurrence of obstructive CAD and that patients with diabetes and impaired CFR have a worse outcome compared to those with preserved CFR (Di Carli et al., 2003; Yokoyama et al., 1997). In patients with chronic kidney disease, a gradual increase in CMD severity with decreasing glomerular filtration rate has been observed (Chade et al., 2006; Charytan et al., 2018).

In patients with CMD and obstructive atherosclerosis, microcirculatory reserve is impaired. Thus, the functional significance of upstream stenosis is exacerbated, leading to a possible increase in the severity of ischemia. Recent evidence regarding CMD has highlighted some critical diagnostic and prognostic issues. FFR values measured to define the hemodynamic significance of a stenosis may be higher in patients with CMD due to the altered microvascular resistance which may lead to interpretations that underestimate the significance of a stenosis (Sechtem et al., 2020). Reduced CFR values may identify patients at high risk for adverse events not related to angiographic findings (Taqueti et al., 2015). A comprehensive evaluation of both epicardial and microvascular compartments before revascularization may be useful since an increase in adverse events has been observed in patients with normal FFR but abnormal CFR after deferral of revascularization (van de Hoef et al., 2014).

2.3.3 Symptoms and signs of CMD

Anginal symptoms caused by CMD cannot be differentiated with certainty from those triggered by an obstructive epicardial disease without conducting further imaging studies (Knuuti et al., 2020) Thus, microvascular angina (MVA) is not typically suspected until the presence of obstructive CAD has been excluded by anatomical imaging. Up to 40% of patients with symptoms indicative of ischemia do not have obstructive CAD on ICA (Ong et al., 2012; Patel et al., 2010). MVA is often presented as retrosternal and effort-induced chest pain or discomfort sometimes accompanied with dyspnea. Anginal episodes may be prolonged, occur after stress, at rest or during cold-exposure, and respond poorly to sublingual or oral nitrates (Kaski et al., 2018; Knuuti et al., 2020). Regional LV wall motion abnormalities develop infrequently during stress in patients with CMD (Mygind et al., 2016; Sara et al., 2015). Patients with CMD may also be asymptomatic. Despite the similar clinical presentation, the prevalence of CMD is higher in female population, and

especially in postmenopausal women (Murthy, Naya, et al., 2014). In a typical scenario, the symptoms of MVA differ from those of vasospastic angina in which symptoms occur predominantly during rest with intact effort tolerance and the episodes adhere to a circadian pattern, with episodes predominantly occurring during night and early morning hours (Beltrame et al., 2017).

2.3.4 Risk stratification and diagnosis of CMD

The association of angina and nonobstructive atherosclerosis with an increased risk of adverse events has been shown (Jespersen et al., 2012) and extended with recent data based on the documentation of abnormalities in the microcirculation with invasive and noninvasive techniques (Murthy et al., 2012; Pepine et al., 2010; van de Hoef et al., 2014). Moreover, the most recent evidence shows that the prognosis in patients with CMD is worse than originally thought and in some comparable to the outcome of patients with obstructive CAD. At present, a comprehensive invasive diagnostic workup to study the role of CMD or vasomotor coronary disorders according to ESC Guidelines is seldom implemented outside research populations in patients with chest pain or angina equivalent and angiographically normal or nonobstructed coronary arteries. Thus, these patients are at the risk of undergoing repeated and inconclusive diagnostic tests, which lead to increased healthcare costs and may result in patient dissatisfaction, depression, and procedural complications due to unnecessary repeated ICAs (Arora et al., 2007; Asbury et al., 2004; Mason et al., 2018; Vermeltfoort et al., 2009). Currently, the development of noninvasive imaging techniques has enabled more widespread diagnostics of CMD.

International standardization of the diagnostic criteria for MVA was suggested by Ong et al. defining the criteria for suspected MVA as follows: i) symptoms of myocardial ischemia, ii) absence of obstructive CAD (<50% diameter reduction or FFR >0.80) by coronary CTA or ICA, iii) objective evidence of myocardial ischemia, and iv) evidence of impaired coronary microvascular function (Ong et al., 2018). Objective evidence of ischemia includes ischemic ECG changes during an episode of chest pain or stress-induced chest pain and/or ischemic ECG changes in the presence or absence of transient/reversible abnormal myocardial perfusion and/or wall motion abnormality. Evidence of CMD includes impaired CFR, coronary microvascular spasm during acetylcholine testing, abnormal coronary microvascular resistance indices, and coronary slow-flow phenomenon.

The current ESC Guidelines for the diagnosis and management of CCS present the diagnostics of CMD as divided in the separate testing of the two main mechanisms of dysfunction, namely impaired microcirculatory conductance and arteriolar dysregulation (Ford et al., 2018; Knuuti et al., 2020). The first can be diagnosed by measuring CFR or minimal microcirculatory resistance. Measurement

of CFR can be performed noninvasively with transthoracic Doppler echocardiography, magnetic resonance imaging or PET, and in the catheterization laboratory setting by measuring the microcirculatory resistance by combining intracoronary pressure with thermodilution-based data (to calculate the index of microvascular resistance) or Doppler flow velocity (to calculate hyperemic microvascular resistance). They both allow the calculation of CFR and are measured using intravenous vasodilators such as adenosine or regadenoson. Values of index of microvascular resistance ≥25 units or CFR between ≤2.0 and ≤2.5, depending on the methodology used, are indicative of microcirculatory dysfunction (Ong et al., 2018). Diagnosis of arteriolar dysregulation on the other hand, requires assessment of the function of the endothelium and smooth muscle cells with intracoronary acetylcholine infusion which triggers paradoxical arteriolar vasoconstriction in the presence of dysfunctional endothelium and abnormal smooth muscle cell function.

2.3.5 Treatment of CMD

Treatment of CMD remains a challenge due to the lack of randomized outcome trials regarding treatment strategies and, consequently, evidence-based recommendations. Until recently, the diagnostic criteria of CMD have been unclear, and a substantial proportion of the older studies have been conducted on patients with chest pain and no obstructive CAD rather than CMD specifically. In addition, noninvasive and invasive diagnosis of CMD has been available for only a short period of time.

The current ESC Guidelines recommend considering treatment options based on the dominant mechanism of CMD (Knuuti et al., 2020). With CFR and index of microvascular resistance values suggestive of CMD and a negative acetylcholine provocation test, angiotensin-converting enzyme inhibitors, statins, and beta-blockers accompanied with lifestyle management, are recommended. A positive acetylcholine test without severe epicardial vasoconstriction is suggestive of microvascular spasm, and these patients may be treated with calcium channel blockers and long-acting nitrates together with risk factor control and lifestyle management (Ong et al., 2015). The CorMiCa trial studied the effects of a stratified treatment plan with 151 patients randomized to stratified medical treatment, which was based on CFR, index of microvascular resistance, and acetylcholine test, versus a standard-care group with a sham interventional diagnostic procedure. After one-year follow-up, the stratified medical treatment resulted in significant and sustained angina improvement, but no difference was observed in outcomes (Ford et al., 2020).

Some small randomized and placebo-controlled studies on angiotensin-converting enzyme inhibitors the results have shown improvement in microvascular function (Pauly et al., 2011), but not all (Schlaifer et al., 1997). Evaluation of treatment with statins lacks randomized, placebo-controlled trials, and other studies

are controversial with either promising results (Caliskan et al., 2007), or results that have no statistical significance (Eshtehardi et al., 2012). Combinations of statins with angiotensin-converting enzyme inhibitors or calcium channel blockers have shown promising results (Pizzi et al., 2004; Zhang et al., 2014). The results on the effect of short-acting nitrates on microvascular angina have mostly showed no positive effect (Russo et al., 2013). Beta-blockers, metformin, ranolazine, and nicorandil have also been studied (Bairey Merz et al., 2016; Chen et al., 1997; Jadhav et al., 2006; Lanza et al., 1999).

2.4 Coronary computed tomography angiography

2.4.1 Technology of coronary CTA

Coronary CTA enables noninvasive visualization of the coronary arteries by utilizing X-rays in the form of computed tomography (CT), and contrast media (Achenbach, 2006). Technological evolution of the CT systems during the past decades has enabled the high-resolution anatomical imaging of coronary arteries to become a routine clinical application. Indications for coronary CTA include the ruling out of CCS in patients with low to intermediate pre-test probability of obstructive CAD, imaging of coronary artery anatomy in patients undergoing valvuloplasty, imaging of coronary anomalies, aneurysms, fistulae or myocardial bridging, and assessment of CABG grafts or stents >3,5mm, of which the first is the most frequent indication (Schroeder et al., 2008).

The current ESC Guideline recommends refraining from coronary CTA if the patient has extensive coronary calcification, irregular heart rate, significant obesity or inability to co-operate with breath-hold commands (Knuuti et al., 2020). Patients with known severe allergy to an iodinated contrast agent, pregnancy, respiratory failure, or severe heart failure should be excluded. Impaired renal function is a relative contraindication to coronary CTA and preventive measures such as intravenous fluid volume loading, should be considered (Abbara et al., 2016). However, only a low incidence of persistent renal dysfunction after coronary CTA in patients with suspected CAD has been observed (Maaniitty et al., 2016).

In coronary CTA, the X-ray tube and the detector system move around the patient simultaneously to form the image by measuring the attenuation of the radiation. Multi-detector CT scanners allow multiple adjacent slices to be acquired concurrently which significantly reduces the overall examination time in addition to iterative techniques. Short overall image acquisition time is crucial for image quality and lower radiation dose. Minimum requirements for coronary CTA are a 64-slice CT with the width of each detector element ≤0.75 mm and a rotation speed of ≤500 ms. To improve temporal resolution, systems with up to 320 simultaneously acquired

slices, rotation time 250 ms, and a combination of two X-ray tubes are available in different combinations (Abbara et al., 2016). A typical data set consists of 200–300 transaxial slices which creates to a continuous volume of data. Intravenous iodine contrast agent is used to achieve vascular enhancement during the scan for the visualization of coronary artery lumen (Abbara et al., 2016).

High image quality with high spatial and temporal resolution is essential for accurate detection and exclusion of CAD (Achenbach, 2006). Spatial resolution represents the capability of distinguishing structures with different densities. It can be optimized through thinner detector rows, thinner reconstructed slice thickness, and modification of X-ray tube output (Abbara et al., 2016). Increase in image contrast especially for iodine-enhanced CT imaging, can be achieved by reducing the tube potential. Among various cardiac imaging techniques, CT is unique with its isotropic spatial resolution, that is, equally high through-plane and in-plane spatial resolution, allowing the generation of images in any plane with preserved spatial resolution. However, spatial resolution of coronary CTA is 0.5-0.6 mm in all three dimensions, which is considerably lower compared to ICA (0.1-0.2 mm) (Rossi et al., 2014). Temporal resolution represents the minimum time needed to generate one axial image and can be optimized through higher rotation speed, multicycle reconstruction algorithms, dual-source CT, and movement corrected reconstruction methods.

Until recently, high radiation dose has been one of the greatest limitations of coronary CTA with the dose being between 8 and 21 mSv without any means for reduction in the 64-slice CT (Einstein, 2008). Prospective ECG triggering and new reconstruction algorithms have allowed substantial reduction in the radiation dose without any significant effect on image quality. In prospective ECG triggering, the tube output is triggered by the patient's ECG and X-ray exposure is demarcated to the phase of interest. In contrast, retrospective ECG-gated image reconstruction allows reconstruction of images at any time instant of the cardiac cycle enabling also functional assessment of ventricles and valves. Other contributing factors on lowering the radiation dose are longer detectors, faster imaging protocols, and reduction in tube potential. With contemporary CT scanners and prospective ECG triggering, the radiation dose can be as low as 1–4 mSv and even lower with high-end technology (Benz et al., 2015; Kajander et al., 2009; Stocker et al., 2018).

Artifacts are a major negative contributor to image quality. Rapid and irregular heart rate together with breath-hold problems may cause motion and misalignment artifacts resulting in steps in the CT data set. During cardiac cycle, the motion radius of a coronary artery is larger than its diameter. Thus, ECG-synchronized protocol is needed to assure that stacks of data are acquired during the precise same phase (Abbara et al., 2016). Mid-diastole between the rapid passive filling and atrial contraction as well as the end of ventricular systole are optimal for acquisition of

motion free images (Abbara et al., 2016). In addition, breath-hold problems are a major contributor to motion and misalignment artifacts and a proper breath-holding technique should be practiced beforehand. To extend the length of the motion free mid-diastolic phase, heart rate of <60–65 beats/min is recommended, which in most cases calls for orally or intravenously administered beta blockade (Abbara et al., 2016). A substantial proportion of patients with suspected CAD have atrial fibrillation, which currently is a contraindication for coronary CTA. However, it has been shown that dual source scanners identified obstructive CAD with acceptable sensitivity, specificity, and negative predictive value in patients with atrial fibrillation (Marwan et al., 2010). In addition, no evidence of increased amount of stress testing or subsequent ICA in patients with atrial fibrillation has been observed. However, the radiation and contrast agent exposure are higher (Korosoglou et al., 2018). Sublingual nitroglycerine is recommended to all patients undergoing coronary CTA in the absence of contraindications since it dilates coronary arteries and thereby improves image quality. Artifacts related to coronary artery calcification are common, and refrainment of coronary CTA is recommended if calcification is extensive (Hoffman et al., 2006). Blooming artifacts are caused by the partial volume effect make calcifications seem larger than actually are, which is likely to lead to an overestimation of the stenosis (Hoffmann et al., 2006). A beam-hardening artifact may appear when the X-ray beam passes through a dense area, such as calcification, which is interpreted as a less attenuating material due to the lower energy photon absorption resulting in a dark area in the image (Hoffmann et al., 2006).

2.4.2 Coronary CTA in the diagnosis, guidance of treatment and risk stratification of CAD

Coronary CTA enables the visualization of the coronary artery lumen and artery wall, as well as the detection of atherosclerotic plaque, both calcified and non-calcified. It also allows the detection of nonobstructive atherosclerosis, which cannot be evaluated with other noninvasive imaging methods (Achenbach, 2006; Hoffmann et al., 2006).

Coronary CTA is a rather novel imaging modality, and consequently, new major recommendations regarding coronary CTA are included in the current ESC Guidelines for the diagnosis and management of CCS (Knuuti et al., 2020). Coronary CTA together with noninvasive functional imaging is recommended as the initial test for the evaluation of CAD in symptomatic patients for whom the clinical assessment is not sufficient. If another noninvasive test is equivocal or non-diagnostic, coronary CTA should be considered as an alternative to ICA.

Coronary CTA has demonstrated high sensitivity (95–99%) for detection of obstructive CAD in studies with a 50% luminal narrowing as the cut-off value and

the degree of stenosis in ICA as the gold standard (Budoff et al., 2008; Meijboom, Meijs et al., 2008). The negative predictive value of coronary CTA is close to 100% and it is applicable to the exclusion of obstructive CAD. On the other hand, specificity (64–83%) and positive predictive value are lower, owing to the overestimation of the angiographic disease severity, especially in the presence of calcifications and artifacts. This is accentuated when the patient has high pre-test probability, leading to subsequent imaging and exposure to radiation, which could be avoided with proper patient selection.

It has been repeatedly shown that the degree of coronary artery stenosis on anatomical imaging does not directly correlate with the hemodynamic significance and ischemia. Actually, only approximately 50% of the ≥50% diameter reduction due to stenosis in ICA significantly affect the coronary flow based on FFR measurements (Meijboom, Van Mieghem, et al., 2008). Thus, functional testing for the detection of ischemia, preferably noninvasively, is recommended before revascularization (Neumann et al., 2019; Tonino et al., 2009).

In addition to the assessment of atherosclerosis in native arteries, coronary CTA enables imaging of coronary stents and bypass grafts. Imaging of metal coronary stents and assessment of possible in-stent restenosis is complicated due to artifacts. However, the diagnostic accuracy has improved along with the development of new CT technology (Dai et al., 2018; de Graaf et al., 2010; Wykrzykowska et al., 2010). Coronary CTA provides a good visualization method for the assessment of arterial and venous bypass grafts, which are less prone to cardiac movement. Graft stenosis can be detected with high accuracy, but the assessment of distal stenosis and anastomosis can be challenging (de Graaf et al., 2011; Meyer et al., 2007).

Coronary CTA is also an important tool for the risk assessment of future cardiac events. It has been repeatedly shown that there is a correlation between the extent of these findings and the risk of future adverse events including all-cause death, cardiovascular death, MI, UAP requiring hospitalization, and coronary revascularization (Bamberg et al., 2011; Bittencourt et al., 2014; Cho et al., 2018; Chow et al., 2011; Dougoud et al., 2014; Gaemperli et al., 2008; Hadamitzky et al., 2009; Hadamitzky, Täubert et al., 2013; Hou et al., 2012; Hulten et al., 2011; Min et al., 2007; Nakazato et al., 2014; Ostrom et al., 2008). Coronary CTA findings are graded as high-risk if they include three-vessel disease with proximal stenosis, left main disease, or proximal anterior descending disease (Knuuti et al., 2020). On the other hand, normal coronary arteries in coronary CTA are suggestive of a good prognosis (Dougoud et al., 2014; Hadamitzky, Täubert et al., 2013; Hulten et al., 2011; Min et al., 2011; Nakazato et al., 2014). In the SCOT-HEART trial, a significantly lower rate of cardiovascular death or MI was observed in patients for whom coronary CTA was performed in addition to routine testing (Adamson et al., 2019; SCOT-HEART investigators, 2015; Williams et al., 2016). One possible

explanation for these results is the detection of nonobstructive CAD by coronary CTA, and consequently, the more effective preventive therapy.

At the Turku University Hospital, coronary CTA is performed as the initial test for the assessment of coronary atherosclerosis in patients with intermediate pre-test probability of obstructive CAD, and an assessment of MBF with PET is performed selectively if obstructive CAD is suspected based on coronary CTA. The incremental prognostic value of coronary CTA has been studied over SPECT MPI and LV ejection fraction with favorable results (Chow et al., 2011; van Werkhoven et al., 2009).

A hemodynamically significant stenosis causing myocardial ischemia is associated with a worse prognosis. In addition, vulnerable plaques and acute coronary syndromes resulting from their erosion or rupture may contribute to the process in some patients. Coronary CTA enables the assessment of the coronary plaque morphology, and it has been suggested that certain plaque characteristics are associated with a worse prognosis of the extent and severity of CAD, including the presence of a thin-cap fibroatheroma, low-CT-attenuation plaques, positive vessel remodeling, spotty calcification, and a napkin-ring sign (Bamberg et al., 2011; Gaemperli et al., 2008; Hou et al., 2012; Maurovich-Horvat et al., 2014; Motoyama et al., 2009; Otsuka et al., 2014).

Various coronary risk scores have been derived from the anatomical imaging findings of coronary CTA or ICA independent of patient clinical variables with the attempt to quantify the complexity of CAD (de Araújo Gonçalves et al., 2013; de Graaf et al., 2014; Hadamitzky, Achenbach et al., 2013; Sianos et al., 2005; Uusitalo et al., 2017). Compared to clinical-based scores (Conroy et al., 2003; D'Agostino et al., 2008), anatomy-based scores are exposed to intra- and inter-observer variability. The anatomy-based scores move the assessment of risk further down the treatment pathway, but provide probably a better estimate on individual cardiovascular risk in the future.

Coronary CTA tends to overestimate the severity of coronary stenoses, and consequently, increases downstream referral to ICA and revascularization with no improvement in mortality. In the recent PROMISE trial, the referral rate to ICA increased by almost 50% as compared to routine provocative testing (Bittencourt et al., 2016; Douglas et al., 2015; Nielsen et al., 2014). Selective referral to ICA with coronary CTA as the gatekeeper was studied in a randomized clinical trial. The selective approach reduced the use of ICA and resulted in a greater diagnostic yield with a comparable 1-year MACE rate (Chang et al., 2019).

The current Guidelines recommend ischemia-testing, preferably noninvasively, before revascularization decisions (Neumann et al., 2019). Thus, noninvasive functional imaging may be needed after a suspected obstructive stenosis has been detected in coronary CTA in order to confirm the functional relevance of the

stenosis. In addition, the CT first approach does not provide any information about the state of the coronary microvasculature, and consequently, patients with MVA might be missed. A combination of anatomical and functional imaging, on the other hand, gives a complete overview of both the epicardial arteries and microvasculature.

2.5 Noninvasive functional imaging of CAD and CMD

The primary aim of cardiac functional imaging is to detect myocardial ischemia, which is most often caused by an obstructive flow-limiting stenosis. Other conditions that may cause myocardial ischemia are CMD and epicardial vasospastic disease, which should be kept in mind as alternative causes of chest pain. The traditional techniques for the imaging of myocardial ischemia are stress echocardiography and SPECT MPI. In addition, PET and CMR imaging are used to an increasing extent. Two different noninvasive CT-based functional techniques, computed tomography myocardial perfusion (CTP) imaging and computed tomography-derived fractional flow reserve (FFR_{CT}), are included in the latest developments. According to the current ESC Guidelines, either noninvasive functional testing or coronary CTA are equally recommended as the initial test to diagnose CAD in symptomatic patients, and the selection of the test is based on the clinical likelihood of CAD, other patient characteristics, local expertise, and the availability of the tests (Knuuti et al., 2020). In addition, functional imaging for myocardial ischemia is recommended if coronary CTA has shown equivocal CAD or is not diagnostic.

2.5.1 Nuclear imaging techniques

Two nuclear imaging modalities, SPECT and PET, are available for noninvasive assessment of myocardial perfusion. Physical exercise or pharmacological agents are used to detect possible abnormalities in myocardial perfusion. During stress, a hemodynamically significant stenosis limits the increase in MBF leading to a reversible perfusion defect. In contrast, a scar caused by MI produces a persistent or fixed perfusion defect both during rest and stress. Stress-only protocols have lately been increasingly used with selective rest perfusion imaging only if a perfusion defect is detected in stress imaging (Chang et al., 2010; Gowd et al., 2014).

In stress imaging, the stress condition can be induced with physical exercise or pharmacological agents. Physical exercise can only be used with tracers with a long half-life. The physical stress enables the simultaneous assessment of symptoms, echocardiographic images, functional capacity, blood pressure, and ECG, and are thus recommendable in patients with sufficient exercise capability. PET tracers have a shorter half-life and, thus, pharmacological agents are used. Adenosine,

regadenoson, and dipyridamole are vasodilators that increase myocardial perfusion, the first two by stimulating A_{2A} receptors and the last one by inhibiting the cellular reuptake of endogenously produced adenosine (Henzlova et al., 2016). Contraindications for adenosine or regadenoson stress testing are known hypersensitivity to adenosine or regadenoson, severe bronchospastic lung disease, second- or third-degree AV block without a functioning pacemaker, sinus node disease, systolic blood pressure <90 mmHg or >200 mmHg, diastolic blood pressure >110 mmHg, recent use of dipyridamole-containing medications, and unstable angina or acute coronary syndrome (Henzlova et al., 2016). Dipyridamole shares these contraindications with the exception that AV block and sinus bradycardia are only relative contraindications. In addition, ingestion of caffeinated foods and beverages within 24 hours must be avoided (Henzlova et al., 2016). Currently the quantitative MBF values achieved using different stressors have not been studied. Only one quantitative cardiac PET study using a paired design has been published; in which using ^{82}Rb PET, regadenoson achieved only 80% of maximal hyperemia as compared to dipyridamole (Johnson & Gould, 2015). Dobutamine may be used in patients with contraindications to vasodilator stress agents. However, it is less studied than the vasodilator stress in the evaluation of patients with suspected CAD (Henzlova et al., 2016). Dobutamine is a beta receptor agonist and stimulates myocardial perfusion by increasing the metabolic demand and, if needed, atropine may be given simultaneously to increase heart rate and myocardial contractility.

2.5.1.1 SPECT MPI

SPECT MPI is the most established technique for cardiac functional imaging worldwide. It is based on the administration of a radiotracer into peripheral circulation during rest and exercise or pharmacological stress. ^{201}Thallium (^{201}Tl) and the technetium-99m (^{99m}Tc)-labeled tracers sestamibi and tetrofosmin are the most common SPECT tracers. A potassium analog ^{201}thallium relies on sodium/potassium transport in myocardial uptake whereas sestamibi and tetrofosmin as lipophilic cations cross the cell membrane passively and their mitochondrial retention is dependent on blood flow. These radiotracers are actively internalized by the viable myocardial cells in proportion to regional MBF, emitting high-energy photons that are detected and three-dimensionally localized by the SPECT camera. Thus, SPECT images represent regional tracer uptake reflecting relative MBF. In addition, the dilatation of the LV, or increased uptake in the lung in stress images are suggestive of stress-induced ventricular dysfunction in patients with severe CAD. ^{201}Tl has a longer half-life associated with a higher radiation burden of around 20 mSv, lower photon energy resulting often in attenuation artifacts, and lower injected activity as compared with ^{99m}Tc which is the most commonly used radiopharmaceutical with

the radiation exposure of around 10 mSv. Stress-only imaging and new technology at least halves the radiation dose (Einstein, 2008; Knuuti et al., 2014).

The four main components allow the conversion of the gamma rays emitted by the injected radiotracer into three dimensional images: the collimator, the scintillating crystal, the photon detectors, and the dedicated electronics. The collimators are the primary determinants of spatial resolution by limiting the number of detected photons to those coming from a pre-specified range of directions in space. The crystal is the real detecting component of the camera emitting visible light when hit by the high-energy photons. The photon detectors convert the visible light into electronic signals and amplify the signal in addition to defining the most precise localization of the scintillation event. The digital pixels of the final image array are amplified from these electric pulses. A typical SPECT camera is formed of two scintillation cameras rotating around the patient attached to a gantry at a 90° angle. Multiple myocardial projections (usually 64) are acquired and the whole imaging session lasting around 20–25 min. Finally, the process of image reconstruction allows the creation of three-dimensional images that show the radiotracer's distribution in the myocardium followed by the filtering to reduce image noise (Hyafil et al., 2019).

The images are analyzed in the short axis, horizontal long axis, or vertical long axis views, and in a polar map with a relative way of analysis. The assumption in the relative analysis is that the region of the highest tracer uptake is normally perfused, and others are compared to this reference. The visual analysis is often complemented with semiquantitative analysis with summed scores. The myocardium is divided into segments which are further numerically graded based on their relative tracer uptake. A per-patient summed score can be generated by adding up the segmental values. There have been attempts to quantify MBF with the use of SPECT (Hsu et al., 2014; Shrestha et al., 2017). SPECT MPI studies can be performed in an ECG-gated mode to obtain parameters of LV function in addition to myocardial perfusion (Henzlova et al., 2016).

Cardiac nuclear imaging techniques are well validated in terms of the diagnosis and prognosis of CCS. In a recent meta-analysis, a pooled sensitivity for SPECT MPI was 87% and specificity 70% when CAD was defined as stenosis >50% in angiography (Knuuti et al., 2018). In addition, sensitivity of 73–74% and specificity of 79–83% have been observed when defining CAD functionally with FFR (Knuuti et al., 2018; Takx et al., 2015).

Shaw and Iskandrian have extensively reviewed previous SPECT studies regarding the prognostic value of SPECT imaging in almost 70,000 patients (Shaw & Iskandrian, 2004). In this review, it was reported that patients with normal perfusion findings had annual event rate of 0.6% as compared to the annual event rate of 5.9% in patients with high-risk SPECT findings.

A reversible stress induced perfusion defect of ≥10% of the total LV myocardium is associated with an annual rate of cardiovascular death or MI >3%, which represents high event risk (Shaw et al., 2014). Retrospective analyses indicate that these patients might benefit from revascularization (Hachamovitch et al., 2003; Hachamovitch et al., 2011). However, the recent ISCHEMIA trial showed contradictory results (Maron et al., 2020). A normal SPECT MPI study on the other hand, is associated with a good prognosis (Smulders et al., 2017), a comparable result with other noninvasive functional tests.

Limitations of this imaging method are low-resolution images, relative elevated radiation burden, and time-consuming imaging stages. In patients with multivessel disease or CMD, the reduction in myocardial perfusion is typically global. SPECT MPI is based on relative analysis, e.g. the assumption is that the region with the highest tracer uptake is normally perfused and the others are compared to this reference. If the reduction in the myocardial perfusion is global, which is typically the case in multivessel disease or CMD, it may be undetected with SPECT imaging. In terms of cost-effectiveness of SPECT MPI, the greatest value is achieved in the higher range of intermediate pre-test probability of CAD (Trägårdh et al., 2017).

2.5.1.2 PET MPI

PET is an advanced nuclear imaging technique representing the gold standard for the evaluation of coronary vasodilator function and allowing the measurement of absolute MBF and CFR. PET differentiates from SPECT with different detection principle, absolute quantification of MBF, higher spatial resolution, and shorter-lived positron emitting radioisotopes, which increase the flexibility of imaging protocols and lowering the radiation exposure. Quantification of MBF in mL/g/min allows the evaluation of CMD and better analysis of multivessel disease as compared with SPECT MPI (Bengel et al., 2009). In addition to ischemia, PET MPI provides information on myocardial viability similar to SPECT MPI.

PET imaging aims to define the distribution of the tracer in the body accurately by producing a three-dimensional image volume. This is generated over time to describe the time-activity curves and to investigate the kinetics of the tracer uptake and release from different tissues and blood at rest and during pharmacological stress. In this manner, information about the presence or absence, location and extent of myocardial ischemia can be obtained (Bengel et al., 2009).

Cyclotrons accelerate protons and deuterons, which interact with the target atoms producing radioisotopes. When decaying, the proton converts into a neutron and a positron is emitted. Interaction with a positron and an electron results in the annihilation of both particles, and two photons are emitted in opposite directions each with energy of 511 keV. The emission of the pair of annihilation photons results

in higher detection efficiency, higher spatial resolution and easier correction for attenuation of photons as compared to the radionuclide emitting single gamma-ray photons (Bengel et al., 2009).

For the measurement of MBF by PET, three tracers are commonly used: ^{15}O-labeled water ($H_2{}^{15}O$), ^{13}N-labeled ammonia ($^{13}NH_3$), and ^{82}Rubidium (^{82}Rb) (Saraste et al., 2012). The radiation exposure is around 1–4 mSv which is considerably lower than in SPECT imaging and is due to the shorter radioactive half-live of PET perfusion tracers. ^{15}O-water molecule is metabolically inert and freely diffusible and an ideal flow tracer since it has a linear relation to MBF. The tracer does not accumulate into the myocardium, and thus visual image analysis cannot be performed. ^{15}O has a half-life of 112 seconds and the PET scan is started immediately after the tracer injection. ^{15}O-labeled water is currently not U.S Food and Drug Administration approved.

Nitrogen-13 (^{13}N)-labeled ammonia is also feasible for the quantification of MBF and due to the relatively high retention fraction, it is possible to perform the visual image analysis and ECG-gated evaluation of LV volumes and ejection fraction. The half-life is around 10 minutes and stress imaging can be performed 30 minutes after rest scan to allow the tracer decay (Knuuti et al., 2009). Rubidium-82 (^{82}Rb) does not need an on-site cyclotron and is the most widely used radiotracer in cardiac PET imaging. It has a short half-life of 76 seconds. It has a nonlinear extraction fraction and high positron range making the quantitation and image quality less optimal.

In a recent meta-analysis, a pooled sensitivity of 90% and specificity of 85% was reported when CAD was defined as stenosis >50% in angiography (Knuuti et al., 2018). In addition, sensitivity of 89% and specificity of 85% have been observed when defining CAD functionally with FFR (Knuuti et al., 2018; Takx et al., 2015). Two meta-analyses consisting mainly of studies with ^{82}Rb PET found pooled sensitivities of 84% and 90% and specificities of 81% and 88%, respectively, in the detection of obstructive CAD (Jaarsma et al., 2012; Mc Ardle et al., 2012). ^{13}N-ammonia PET enables flow quantification. Consequently, improved accuracy and sensitivity have been observed in comparison to relative MPI analysis, similarly to studies with ^{15}O-water PET (Fiechter, Ghadri, Gebhard et al., 2012; Hajjiri et al., 2009; Lee et al., 2016; Muzik et al., 1998). A high per-patient sensitivity of 95%, specificity of 91%, and accuracy of 92%, have been observed in a study with ^{15}O-water PET MPI with absolute quantification of stress MBF and ICA with FFR when feasible for the detection of obstructive CAD (Kajander et al., 2011). In this study, a relative analysis was also conducted with the corresponding values 74%, 73%, and 73%, showing better diagnostic accuracy when using an absolute scale. The absolute stress MBF value <2.5 was considered abnormal based on earlier receiver operating characteristic analysis (Kajander et al., 2010). More recently, Danad et al. pooled

data from three sites and studied the diagnostic performance of stress MBF and myocardial flow reserve in patients undergoing both quantitative ^{15}O-water PET MPI and ICA with FFR when feasible and found a bit lower cut-off value of 2.3 mL/g/min for stress MBF with per-patient sensitivity, specificity, and accuracy of 89%, 84%, and 86%, respectively, for obstructive CAD (Danad, Uusitalo et al., 2014). The study showed inferior diagnostic performance of myocardial flow reserve when compared to stress MBF with per-patient sensitivity of 86%, specificity of 72%, and accuracy of 78%, when the identified cut-off value of 2.5 for myocardial flow reserve was used. The optimal cut-off values of MBF for the detection of obstructive CAD may vary depending on the technique used (Knuuti et al., 2009).

In addition to diagnostic accuracy, prognosis has also been studied extensively. The extent and severity of the perfusion abnormalities correlate with the increase in the likelihood of cardiac events, as shown in a multicenter study with a population of 7,061 patients and a follow-up of 2.2 years (Dorbala et al., 2013). In a recent meta-analysis it was demonstrated that a normal PET study has a high negative predictive value for cardiac death, major cardiovascular adverse events and all-cause mortality with a low annual risk of cardiac death of 0.39%, thus almost reaching the level of normal age-matched population (A. Chen et al., 2017). Similar results were obtained in another recent meta-analysis (Smulders et al., 2017).

The prognostic value of CFR, the ratio between hyperemic and resting MBF, has been extensively investigated in single-center studies with PET imaging. Herzog et al. investigated the prognostic value of CFR using quantitative ^{13}N-ammonia PET in 256 patients during the mean follow-up of 5.5 years (Herzog et al., 2009). In the analysis, both quantitative and semiquantitative methods were used to analyze CFR and summed stress scores, respectively. CFR <2.0 was considered abnormal and added a threefold increase in adverse events as was observed in patients with or without relative perfusion defects. In addition, it was observed that, in patients with normal perfusion findings and abnormal CFR, the predictive value of CFR was sustained only for the first three years of follow-up.

In addition, results from several clinical registries using ^{82}Rb PET have shown the ability of CFR to detect patients at low or high risk for adverse events besides clinical evaluation, LV ejection fraction, or semiquantitative measures of stress imaging (Fukushima et al., 2011; Murthy, Lee et al., 2014; Murthy et al., 2011; Ziadi et al., 2011). In addition, integration of CFR and maximal MBF may pinpoint unique prognostic phenotypes (Gupta et al., 2017). In a recent meta-analysis, Green et al. observed the need for prognostic studies regarding CFR in special subgroups due to the heterogeneity of the study population (Green et al., 2019). The flow range is extensive, wherefor a graded flow range instead of a definite threshold for normal versus abnormal may be applied (Gould et al., 2013).

The quantification of MBF and assessment of CFR allow the identification of patients with CMD, especially in combination with coronary CTA when obstructive CAD can be excluded. Gould et al. have proposed a comprehensive quantitative perfusion analysis by PET instead of the clinically used protocols since the latter do not quantify accurately vasodilator-induced subepicardial to subendocardial perfusion gradients due to limitations in the spatial resolution (Gould & Johnson, 2018; Sara et al., 2015). The comprehensive analysis would include regional absolute stress flow, relative stress flow, CFR, and quantitative subendocardial perfusion gradients.

Limitations of PET perfusion imaging include the limited availability of the PET tracers and scanners, and higher expenses. The need of an on-site cyclotron is a major limitation, which does not concern studies conducted with ^{82}-Rb and potentially in the future with ^{18}F-labelled tracers.

2.5.2 Other noninvasive functional imaging techniques

Stress echocardiography combines echocardiography with exercise or pharmacologic stress and is used for the detection of CAD, assessment of the severity of a valve disease, or to study the viability of the myocardium. Stress echocardiography enables the detection of reduced myocardial wall thickening and regional wall motion abnormalities with a semiquantitative visual scoring. Physical stressors enable the simultaneous assessment of symptoms, echocardiographic images, blood pressure, and ECG (Sicari et al., 2009). Dobutamine is the preferred pharmacological stressor, but the vasodilator drugs adenosine and dipyridamole may also be used. No differences in sensitivity or specificity between the physical and pharmacological stressors have been observed (Heijenbrok-Kal et al., 2007). The pooled sensitivity of stress echocardiography was 85% and specificity 82% when obstructive CAD was defined as ≥50% luminal narrowing (Knuuti et al., 2018). Ultrasound contrast agents have improved the diagnostic accuracy (Plana et al., 2008; Senior et al., 2017) and can be used in assessment of myocardial perfusion. However, microbubble use is not U.S Food and Drug Administration approved for perfusion. This method enables the assessment of the microvasculature and has been validated against PET (Mygind et al., 2016; Vogel et al., 2005). The prognostic value of stress echocardiography is similar to nuclear MPI and CMR, and a normal stress echocardiogram is associated with a low annual event risk (Metz et al., 2007). However, the risk of adverse events increases proportionally to the extent of wall motion abnormalities (Marwick et al., 2001; Sicari et al., 2003; Yao et al., 2003). Stress echocardiography findings have been observed to guide referral to ICA and revascularization decisions especially in patients with markedly abnormal results (Yao et al., 2010). Advantages of the method are good availability, lack of radiation exposure, and low cost. One of the

greatest limitations is its dependence of the operator's expertise. In addition, transthoracic pulsed-wave Doppler echocardiography performed on proximal LAD can be used to assess MBF and to calculate coronary flow velocity reserve (Saraste et al., 2001; Shah et al., 2018).

CMR imaging allows the simultaneous assessment of the structure and the function of the cardiovascular system and the myocardium. Stress CMR enables the assessment of myocardial perfusion and LV wall motion in response to stress induced by a vasodilator or dobutamine (Le et al., 2017). In first-pass perfusion stress CMR imaging, the reduced signal increase during the first pass of the gadolinium contrast agent is indicative of a hemodynamically significant stenosis. Dobutamine stress CMR imaging is typically based on the visual assessment of low-signal areas with abnormal perfusion. However, the development of semiquantitative and quantitative CMR perfusion analyses is ongoing (van Dijk et al., 2017). The detection of scars in the myocardium, indicative of a prior MI, can be performed with persistent gadolinium enhancement in delayed magnetic resonance imaging. In a recent meta-analysis, pooled sensitivity and specificity of 90% and 80%, respectively, were observed for the detection of CAD (Knuuti et al., 2018). The prognostic value is similar to that of nuclear MPI and stress echocardiography (Greenwood, Herzog, et al., 2016; Jahnke et al., 2007; Lipinski et al., 2013). Normal stress CMR findings are associated with a low event risk (Gargiulo et al., 2013; Lipinski et al., 2013). CMR provides prognostic information in patients with myocardial scarring and no perfusion abnormalities in stress testing (Steel et al., 2009). CE-MARC II trial showed that CMR guided care resulted in a lower number of unnecessary ICAs compared to standard care. No statistically significant difference was observed between CMR and SPECT strategies, or the rates of cardiovascular death, MI, unplanned revascularization, or hospital admission for cardiovascular cause (Greenwood, Ripley et al., 2016). CMR MPI has been studied in the identification of patients with CMD (Liu et al., 2018; Thomson et al., 2015), but more studies are needed to assess the clinical utility of CMR in this indication. Advantages of the method are the lack of radiation exposure and operator dependency. As to its limitations, stress CMR has low availability, high expenses, and requires high expertise.

Two noninvasive functional methods, FFR_{CT} and CTP imaging, have been developed to complement coronary CTA. FFR_{CT} uses computational fluid dynamics to estimate the impact of a stenosis on flow and pressure by identifying enhancement gradients. FFR_{CT} can be performed on standard coronary CTA scans and requires no vasodilator use. FFR_{CT} has shown approximately 85% accuracy compared to invasive FFR (Nørgaard et al., 2014) with an increase in specificity when compared to coronary CTA alone. The use of proprietary software restricts the widespread utilization of the method (Taylor et al., 2013). However, open source methods have

been developed (Kishi et al., 2018). Nonischemic FFR_{CT} findings have been associated with a good prognosis in small studies (Douglas et al., 2016; Nørgaard et al., 2018). In addition, promising results in terms of guiding referral to ICA (Jensen et al., 2018; Nørgaard et al., 2018; Sand et al., 2018) and revascularization (Collet, Miyazaki, et al., 2018; Collet, Onuma et al., 2018) have been observed. A low ratio of coronary CTA-derived luminal volume to myocardial mass has been observed to independently predict ischemia in nonobstructive CAD, and a lower ratio has been detected in patients with MVA (Nørgaard et al., 2014; Grover et al., 2017).

CTP utilizes the passage of iodinated contrast agent into the myocardium and attenuates X-ray photons proportionally to its concentration during vasodilator stress. Static imaging at the expected peak of the contrast bolus, or dynamic CT imaging by acquisition of multiple images during both contrast wash-in and wash-out can be used (Danad et al., 2016). Coronary CTA combined with stress CTP has been compared with coronary CTA alone, SPECT, and CMR with promising results (Bamberg et al., 2014; Rochitte et al., 2014; Takx et al., 2015). However, the method is not in widespread clinical use and has not been validated in prospective studies. Some data exists on the prognostic value of coronary CTA combined with CTP (M. Y. Chen et al., 2017; van Assen et al., 2019) and on the incremental prognostic value of CTP over coronary CTA (Nakamura et al., 2019). CTP is not used to assess CMD in clinical practice (Mathew et al., 2019).

2.6 Hybrid imaging with coronary CTA and myocardial perfusion imaging

2.6.1 Different approaches of hybrid imaging in CAD

Hybrid imaging combines and fuses data from two separate imaging modalities with a significant contribution from both modalities to the image information. In other words, the data provided by the fusion of imaging data cannot be gathered with a solely stand-alone or side-by-side interpretation of the data sets. It has been suggested that hybrid imaging should be differentiated from combination imaging where the other modality only contributes to improved image quality and does not independently contribute to the formation of the image, for example, in the case of SPECT with unenhanced CT where the latter is used for attenuation correction only. In imaging of CAD, the potential of hybrid imaging lies in the combination of anatomical and functional data, which can be achieved by combining coronary CTA with either SPECT or PET (Gaemperli et al., 2012). In addition, the combination of coronary CTA and CMR has been studied (Groothuis et al., 2013; Scheffel et al., 2010; van Werkhoven et al., 2010), but the technology is still under development (von Spiczak et al., 2018). Recently, the fusion of coronary CTA and 3D speckle-

tracking stress and rest echocardiography has also been studied (Maffessanti et al., 2017). The most important aspect is to use dedicated software for accurate fusion of the two datasets, which are usually presented as three-dimensional reconstructions, although special hybrid scanner devices are available.

Although hybrid imaging with PET/CT or SPECT/CT sounds ideal, the optimal use of different modalities and the optimal patient selection needs further clarification. Factors to be considered are the radiation dose, cost issues, and possible side-effects of the pharmacological agents. As a highly technical procedure, the work needs to be done for translation into a widely adapted clinical routine (Piccinelli, 2020). The high cumulative radiation burden has been considered as a major limitation. However, technological advancements and iterative reconstruction algorithms have allowed cardiac hybrid imaging with a low radiation dose (Benz et al., 2015).

Several early studies on the diagnostic accuracy in the detection of CAD and the incremental value of hybrid imaging as compared to either modality alone showed promising results for coronary CTA and SPECT (Gaemperli et al., 2011; Rispler et al., 2007; Sato et al., 2010; Schaap et al., 2014) as well as for coronary CTA and PET (Danad et al., 2013; Groves et al., 2009; Kajander et al., 2010; Namdar et al., 2005).

A recent prospective controlled single-center head-to-head comparative study assessed PET/CT, SPECT/CT, and coronary CTA with ICA and FFR, and the results showed no incremental diagnostic value of the hybrid imaging techniques compared to stand-alone imaging, which was a secondary endpoint (Danad et al., 2017). A meta-analysis of earlier studies with the assessment of PET/CT, SPECT/CT, and CT/CMR as compared to stand-alone coronary CTA showed improved diagnostic specificity for detection of obstructive CAD. However, a limited increase in the overall diagnostic performance was observed (Rizvi et al., 2018). In contrast to the prospective study by Danad et al., ICA with a quantitative coronary analysis was used as the reference standard instead of FFR.

Hybrid imaging is not of benefit for all patients. Thus, a selective imaging approach has been introduced, allowing the complementary imaging in patients for whom the first modality provides abnormal or equivocal results (Kaufmann & Buechel, 2016; Saraste et al., 2012). This leads to the discussion of whether the anatomical or the functional imaging should be performed first. It could be suggested, that the approach with coronary CTA first would be utilized in patients with a low to moderate pre-test probability of obstructive CAD, owing to the high negative predictive value and relatively low positive predictive value of coronary CTA. This would enable the exclusion of obstructive CAD reliably, without neglecting the possible existence of nonobstructive atherosclerosis and the need for secondary prevention. However, the coronary CTA first approach is not able to

identify patients with CMD. Therefore, MPI first approach might be beneficial in patients with higher pre-test probability, and the complementary coronary CTA would allow the accurate localization of the culprit lesion. In the case of SPECT, the MPI first strategy may be problematic in patients with a three-vessel disease or CMD because of a possible false-negative finding due to the semiquantitative nature of SPECT.

Limited amount of data exists of the selective hybrid imaging approach. Engbers et al. studied selective SPECT/CT imaging for the detection of obstructive CAD in a single-center study with 5,018 consecutive patients without history of CAD who underwent a stress SPECT and coronary artery calcium scoring (Engbers et al., 2017). If the stress SPECT findings were abnormal, a rest SPECT and a coronary CTA were performed if feasible. In 52% of the patients, obstructive CAD was excluded by stress SPECT and the absence of coronary artery calcium.

In addition, limited amount of data exists on the cost-effectiveness of cardiac hybrid imaging. Lorenzoni et al. have studied the cost-effectiveness of stand-alone or combined noninvasive imaging for the diagnosis of CCS (Lorenzoni et al., 2019). The results suggest that noninvasive strategies combining coronary CTA with stress imaging if the first test showed inconclusive results, are cost-effective in patients with low prevalence of obstructive CAD.

2.6.2 Impact of hybrid imaging on patient management

Traditionally, noninvasive tests have been evaluated by their accuracy in the detection of obstructive CAD with reference to ICA. Consequently, noninvasive testing has primarily been seen as a gatekeeper for further invasive testing. Especially in hybrid imaging, the potential of a combination of two imaging modalities outperforms this way of thinking. Noninvasive hybrid imaging provides information of the location, severity, and extent of atherosclerosis and ischemia, which can be used in guiding and tailoring treatment, for example, the decision on the type of revascularization. Data concerning patient management after hybrid imaging is limited and consists mostly of protocols in which hybrid imaging has been performed to all patients (Benz et al., 2018; Danad, Raijmakers, et al., 2014; Liga et al., 2016; Pazhenkottil, Nkoulou, Ghadri, Herzog, Küest et al., 2011; Schaap et al., 2013).

Pazhenkottil et al. studied the impact of fused SPECT/CT on the subsequent treatment strategy in 318 consecutive patients, with 21% of patients having known CAD (Pazhenkottil, Nkoulou, Ghadri, Herzog, Küest, et al., 2011). Matching pathological hybrid imaging findings were observed in 16% of the patients, with a referral rate to ICA and revascularization rate per angiogram of 61% and 68%. Unmatched pathological hybrid imaging findings were found in 23% with referral to

ICA and revascularization rate per angiogram of 20% and 53%, respectively. Normal hybrid imaging findings were observed in 61% and no ICAs were performed in this group. The yield of CAD by ICA after hybrid imaging was 90% in the matched group with revascularization rate per angiogram of 68% compared with the unmatched group, 80% and 53% respectively.

Fiechter et al. studied 62 patients with known or suspected CAD by using hybrid SPECT/CT (Fiechter, Ghadri, Wolfrum et al., 2012). Matching pathological findings were observed in 37% of the patients, with a referral rate to ICA of 100% and 91% were revascularized. The corresponding figures in patients with unmatched and normal findings (63%) were 13% and 60%, respectively. The yield of CAD by ICA was 96% in the overall study population.

Schaap et al. analyzed 107 patients who were prospectively enrolled and underwent hybrid SPECT/CT prior to ICA (Schaap et al., 2013). Patients with prior PCI or CABG were excluded. The study outcome was categorized as no revascularization, PCI or CABG, and treatment decisions were made in two steps: first, based on hybrid SPECT/CT, and second, based on SPECT and ICA. A direct comparison of the effects of hybrid SPECT/CT versus traditional work-up using SPECT and ICA on the choice of treatment strategy was performed. A high overall percentage agreement (92%) was observed in the primary outcome measure evaluating the decisions on revascularization. However, the percentage agreement was lower (74%) for the secondary outcomes regarding the method of revascularization. Compared to the study by Pazhenkottil et al. the revascularization rate of patients with matched findings was remarkably higher (90%) with no obvious explanation.

Danad et al. studied the downstream treatment strategy in 375 patients with all patients undergoing PET/CT hybrid imaging retrospectively (Danad, Raijmakers, et al., 2014). Patients with a history of PCI, CABG or MI were excluded from the study. Obstructive CAD was excluded in 182 patients of whom 16 had abnormal perfusion, and 10 ICAs and no revascularizations were performed. Of all patients, 193 had equivocal or obstructive CAD on coronary CTA, and of these patients, 110 had normal MPI and 83 had abnormal MPI. In these subgroups, the referral rates to ICA and rates of revascularization per angiogram were 37% and 20%, and 83% and 64%, respectively. In other words, when patients with equivocal or obstructive coronary CTA results were pooled together, the referral rate for patients with normal perfusion was 37%, compared to 83% in patients with abnormal perfusion findings. The authors concluded that PET/CT hybrid imaging findings were strong predictors of referral to ICA and subsequent revascularizations. In patients with obstructive CAD on coronary CTA and normal or abnormal perfusion, the yield of CAD in ICA was 32% and 69%, respectively.

Liga et al. investigated 252 patients who underwent hybrid SPECT/CT or PET/CT, and ICA in an EVINCI substudy (Liga et al., 2016). Revascularization rates of 70%, 36%, and 10% were reported for matched, mismatched, and normal hybrid imaging findings, respectively. In addition, 4,284 myocardial segments were analyzed of which 23% were pathological. After image fusion, 25% were reclassified from the standard coronary distribution to another territory. In 18% of the patients, this led to a reassignment of an entire perfusion defect to another territory. However, the final diagnosis was changed in 4% of patients only. In 84% of these cases, the abnormality was changed to a territory subtended by a hemodynamically significant stenosis.

In addition, a recent retrospective analysis by Benz et al. studied the capability of hybrid SPECT/CT to identify those patients who would benefit from early revascularization: the study population consisted of 414 patients with known or suspected CAD (Benz et al., 2018). In patients with normal findings, no revascularizations were performed. Of the patients with CAD observed on coronary CTA (79%), 23% patients had a matched perfusion finding and 49% of these patients were revascularized. Of the patients with an unmatched perfusion finding (77%), 5% were revascularized. In patients with a matched finding, early revascularization was associated with a significantly lower rate of death, MI, UAP requiring hospitalization, and late revascularization during a median follow-up of 6.0 years. In contrast, early revascularization did not change the outcome in patients with an unmatched finding. However, in patients without early revascularization and unmatched findings, the presence of high-risk CAD was associated with a significantly worse outcome controversially to patients with matched findings.

2.6.3 Patient outcome after hybrid imaging

In order to safely adapt a new clinical routine, such as SPECT/CT or PET/CT hybrid imaging, an evaluation of prognostic data must be performed. A few studies have addressed this issue and no data is available on the selective approach described earlier in this thesis (Ghadri et al., 2013; Pazhenkottil et al., 2018; Pazhenkottil, Nkoulou, Ghadri, Herzog, Buechel et al., 2011; Schenker et al., 2008; van Werkhoven et al., 2009).

Ghadri et al. investigated 462 patients referred for evaluation of known or suspected CAD by SPECT combined with coronary calcium imaging (Ghadri et al., 2013). A matched pathological hybrid imaging finding (perfusion defect and coronary calcification) was detected in 22% of the patients and an unmatched finding in 59%. A matched hybrid imaging finding was an independent predictor of MACE on univariate and multivariable analysis.

Schenker et al. investigated 621 patients without known CAD who completed the combined rest-stress ^{82}Rb PET MPI and coronary artery calcium scoring (Schenker et al., 2008). During a follow-up of 1.4 years, patients with or without ischemia on PET showed a stepwise increase in their event risk with increasing coronary artery calcium scores.

Van Werkhoven et al. studied the incremental prognostic value of coronary CTA over MPI in 517 patients with suspected CAD who underwent both coronary CTA and SPECT MPI with a three-month interval (van Werkhoven et al., 2009). During the follow-up of 1.8 years, it was shown that coronary CTA provided complementary information of atherosclerosis when used in combination with MPI and also improved risk stratification. The annual event rate for patients with no or nonobstructive atherosclerosis and normal SPECT MPI findings was 1.0%. The event rate was moderately increased in patients with either abnormal perfusion or a significant ≥50% stenosis, 3.7% and 3.8%, respectively. Highest annual event rate (9.0%) was observed in patients with both abnormal SPECT MPI findings and a significant stenosis.

Pazhenkottil et al. studied the prognostic predictive value of hybrid SPECT/CT in 335 patients referred for evaluation of known or suspected CAD (Pazhenkottil, Nkoulou, Ghadri, Herzog, Buechel, et al., 2011). During a median follow-up of 2.8 years, it was observed that patients with matching hybrid imaging findings had the worst outcome, with the annual event rate of death or MI being 6.0%. In patients with unmatched and normal findings, the corresponding values were 2.8% and 1.3%, respectively. In 2018, Pazhenkottil et al. expanded their previous study with a larger patient population of 375 patients and a longer follow-up of 6.8 years, and were able to confirm the excellent risk stratification ability of cardiac hybrid imaging (Pazhenkottil et al., 2018). Patients with matched, unmatched and normal hybrid imaging findings showed annual event rates of all-cause death and MI of 7.0%, 3.7%, and 1.2%, respectively.

3 Aims

The purpose of this observational study was to evaluate the clinical value of hybrid imaging with coronary CTA and PET in the assessment of symptomatic patients with suspected obstructive CAD. The detailed objectives in this thesis are as follows:

1. To evaluate the impact of a hybrid imaging protocol with selective assessment of stress MBF after coronary CTA on referral to ICA and revascularization decisions (Study I).
2. To investigate the prognostic value of a hybrid imaging protocol with selective assessment of stress MBF after coronary CTA (Study II).
3. To study the frequency and angiographic characteristics of CMD (Study III).

4 Materials and Methods

4.1 Turku cardiac CTA registry

The Turku cardiac CTA registry is a retrospectively assembled registry comprehending all consecutive patients who have undergone cardiac CTA imaging at Turku PET Centre since 2006. The majority of the patients were referred to coronary CTA due to clinical indications for suspected obstructive CAD. In these patients, the pre-test probability of CAD was estimated to be 15–85% based on age, gender and type of chest pain. Other indications for referral to coronary CTA included, e.g., examination of the etiology of heart failure, atrial fibrillation or other arrhythmias, exploration of congenital coronary artery defects, or preoperative studies. These patients, however, were excluded from Studies I–III. For some patients, obstructive CAD had been previously documented, or they had undergone revascularization (PCI or CABG), and these patients were excluded from Studies I–III.

The collection and recording of the data for the registry were done retrospectively and mainly manually. Baseline patient characteristics were obtained from the electronic medical record system and they included the following: indication for coronary CTA, referring department, age, gender, weight, height, previous or current smoking, prediabetes or diabetes, hypertension, dyslipidemia, family history of CAD in first-degree relatives, type of chest pain, dyspnea on exertion, possible preceding test results (LV ejection fraction by echocardiography, ECG findings and stress capability by exercise testing, and laboratory blood test results), cardiovascular medication, prior myocardial infarction or coronary revascularization, atrial fibrillation, and existence of a cardiac pacemaker. Information about previous smoking, diabetes, hypertension, dyslipidemia, and family history was collected as anamnestic data from the electronic medical record system. Additionally, regarding prediabetes, diabetes, and dyslipidemia, the criteria set out in the clinical guidelines were applied to specific laboratory measurements, when available, in case anamnestic information was missing. Prediabetes was defined as impaired fasting glucose (fasting plasma glucose 6.1–6.9 mmol/L), impaired glucose tolerance (2-hour plasma glucose 7.8–11.0 mmol/L in a 75 g oral glucose tolerance test), or blood hemoglobin A1c 6.0–6.4% (Goldenberg et al.,

2013). Diabetes was defined as fasting plasma glucose ≥7.0 mmol/L in at least two measurements, 2-hour plasma glucose ≥11.1 mmol/L after a 75 g oral glucose tolerance test, plasma glucose >11 mmol/L in the case of symptoms of hyperglycemia, or blood hemoglobin A1c ≥6.5% (Goldenberg et al., 2013). Dyslipidemia was defined as plasma LDL >3.0 mmol/L, plasma HDL <1.0 mmol/L in men and <1.2 mmol/L in women, or triglycerides >1.7 mmol/L. In addition, any patient receiving medical therapy for these conditions was defined as having diabetes or dyslipidemia.

Data on the coronary CTA and PET procedures included information on premedication (beta blocker, nitrate), contrast agent volume and concentration, X-ray tube voltage, CT dose-length product, injected PET tracer radioactivity, and heart rate and blood pressure during adenosine stress. Initially, each coronary CTA and PET study was analyzed and reported in a standardized manner for clinical purposes by an experienced physician. The data on coronary arteries were collected based on standardized coronary artery system (Leipsic et al., 2014). In addition to the degree of diameter luminal stenosis, presence and composition of a coronary plaque was recorded (Leipsic et al., 2014). Furthermore, information about the presence of an image artifact, coronary dominance, and overall image quality were obtained. Total and per-vessel Agatston coronary calcium scores were recorded, if available. Standardized segmental (17-segment system) and territorial (LAD, LCX, and RCA) quantitative MBF values (mL/g/min) were recorded (Cerqueira et al., 2002). MBF in each of the three myocardial territories was categorized (normal, mildly reduced, moderately reduced, or severely reduced) based on the presence of local PET perfusion defects and the individual coronary anatomy on CTA and/or hybrid images.

Subsequent patient management information regarding ICA, PCI, CABG, changes in medication and laboratory results within six months after coronary CTA was obtained retrospectively from the imaging database, imaging reports, and electronic medical records. The follow-up data on all-cause mortality, cardiac mortality, MI, and UAP, blinded to imaging data, was obtained from the registries of the Centre for Clinical Informatics of the Turku University Hospital, the Finnish National Institute for Health and Welfare, and Statistics Finland. The adverse events were manually confirmed by the investigators using the electronic medical records according to the criteria of the ESC Guidelines (Hamm et al., 2011).

4.2 Study design and patient population

4.2.1 Study design

This thesis consists of three studies (I–III). In addition, some previously unpublished results are included. Studies I and II were conducted retrospectively, whereas Study III is of a prospective nature. In Studies I – III, the referral of patients to coronary CTA was clinically indicated on the basis of their symptoms suggestive of obstructive CAD. The imaging studies were conducted during 2007–2011 at the Turku University Hospital.

The objective in Study I was to evaluate referrals to ICA and revascularization decisions within six months after a hybrid imaging study with selective assessment of stress MBF after coronary CTA in patients with suspected CAD. In addition, the occurrence of cardiovascular mortality and nonfatal myocardial infarction (MI) was studied. Study II investigated the prognostic value of the selective hybrid imaging protocol imaging in patients with suspected CAD.

In Studies I and II, the imaging studies followed the hospital's standard protocol regarding PET/CT hybrid imaging. The coronary CTA scan was performed with a hybrid PET/CT scanner on the basis of clinical suspicion of obstructive CAD. Instantly after the scan, the attending physician performed an initial evaluation of the coronary CTA scan to determine whether a PET study was needed to assess MBF. If obstructive CAD was excluded by coronary CTA (no atherosclerosis or <50% stenosis), no further testing was performed. If obstructive CAD was suspected based on the coronary CTA, an assessment of MBF using PET with ^{15}O-water as tracer was performed during adenosine stress in order to study the hemodynamic significance of the stenosis. Clinicians were informed about the findings of the PET/CT imaging. Decisions on referral to ICA and revascularization were at the discretion of treating physicians.

The objective of Study III was to evaluate the frequency and angiographic characteristics of CMD in patients with suspected obstructive CAD. The prospective study protocol in Study III included coronary CTA and assessment of rest and stress MBF with PET/CT hybrid scanner in all patients. Furthermore, as part of the study protocol, all patients underwent ICA, on average, 29 days (range 2–178 days) after the first imaging study.

Studies I–III were approved by the local Ethics Committee of the Hospital District of Southwest Finland and they comply with the Declaration of Helsinki. In Studies I and II, the Ethics Committee of the Hospital District of Southwest Finland waived the need for written informed consent for retrospective evaluation of clinically collected data. Permission from the National Institute for Health and Welfare (Finland) was gained for the purpose of collecting patient information. In

Study III, informed consent was collected from all patients. The trial was registered prospectively in a publicly accessible database (http://www.clinicaltrials.gov. Unique identifier: NCT00627172).

4.2.2 Patient population

Basic patient characteristics for Studies I–III are shown in Table 1. In Study I, 721 symptomatic patients were evaluated at the Turku University Hospital during the period from 2008 to 2011. These patients had been referred to PET/CT imaging due to suspected CAD and were retrospectively evaluated in case of successfully completed coronary CTA. Fifty-one patients did not adhere to the selective hybrid imaging protocol and were addressed separately, and thus, the final study population comprised 670 patients.

In Study II, the study population consisted of 957 consecutive patients referred to PET/CT imaging due to suspected CAD at the Turku University Hospital during 2007–2011. Fifty-two patients were excluded from Study II because of nondiagnostic imaging results and 41 patients due to their failure to adhere to the imaging protocol. Thus, the final study population consisted of 864 patients. In this population, 191 patients had routinely undergone both coronary CTA and assessment of MBF with PET. The imaging results of these patients were reclassified according to the hospital's standard protocol described above, and PET imaging results were taken into account only if obstructive CAD was suspected on the basis of coronary CTA.

In Study III, a total of 200 outpatients were prospectively recruited during 2007–2011 at the Turku University Hospital. Consecutive patients with stable chest pain or equivalent symptoms and intermediate pre-test probability (20–90%) of obstructive CAD were considered for inclusion. The assessment of the pre-test probability of CAD was based on age, gender, type of chest pain, and the result of the bicycle ergometer exercise ECG (exercise ECG was not mandatory, but it was performed in 184 patients). Eleven patients for whom the PET study failed were excluded from the final study population (n = 189). One patient with a significant three-vessel disease in ICA, but non-diagnostic coronary CTA due to motion artifacts, was included. Eleven patients (10 with normal coronary CTA and 1 with nonobstructive atherosclerosis in the LAD) refused to undergo ICA but were included. No cardiac events took place between PET/CT and ICA.

Table 1. Basic patient characteristics in Studies I–III.

Variable	Study I	Study II	Study III
Number of patients	n = 670	n = 864	n = 189
Age (mean ± SD), years	61 ± 10	61 ± 9	62 ± 7
Male gender, %	42	45	55
Risk factors for CAD, %			
Current smoking	13	13	14
Previous smoking	18	20	25
Prediabetes	15	17	23
Diabetes	13	14	15
Hypertension	53	54	56
Dyslipidemia	59	62	75
Family history of CAD	45	46	51
Medication, %			
Beta blocker	44	48	62
Lipid lowering drug	38	43	63
Antiplatelet drug	48	55	78
Anticoagulant	7	6	n/a
Long-acting nitrate	9	9	11
Diuretic	19	18	13
ACE inhibitor	19	19	21
ARB	15	15	13
Calcium channel blocker	14	14	12
Antiarrhythmic agent	2	2	1

ACE = angiotensin-converting enzyme; ARB = angiotensin receptor blocker; CAD = coronary artery disease; SD = standard deviation

The exclusion criteria in Studies I–III included previous coronary revascularization, MI or obstructive CAD documented as >50% stenosis by ICA, acute coronary syndrome, as well as PET/CT as a part of pre-operative evaluation or for the purpose of studying the etiology of cardiomyopathy or heart failure. Patients with a contraindication to coronary CTA (iodine hypersensitivity, irregular heart rhythm, severe renal dysfunction (eGFR <30 mL/min/1.73m2), inadequate patient co-operation, and pregnancy) or in Study III, contraindication to PET imaging with adenosine-infusion (atrioventricular conduction block, unstable bronchospastic

pulmonary disease, untreated congestive heart failure, acute coronary syndrome, hypotension or uncontrolled hypertension, hypersensitivity to adenosine, and pregnancy) were excluded. In addition, patients with pre-test probability <20% or >90% according to the ESC Guidelines of 2013 were excluded from Study III.

4.3 Data acquisition and analysis

4.3.1 Imaging data acquisition

4.3.1.1 Coronary CTA imaging

In Studies I–III, coronary CTA and PET scans were conducted with a 64-row hybrid PET/CT scanner (GE Discovery VCT or GE D690, General Electric Medical Systems, Waukesha, Wisconsin, US). Isosorbide dinitrate aerosol (1.25 mg in Studies I–II) or sublingual nitrate (800 µg in Studies II–III) was administered prior to the coronary CTA scan. If necessary, the patient was also given intravenous metoprolol up to 30 mg to reach target heart rate <60 beats per minute before the scan. Agatston coronary calcium score was measured prior to coronary CTA. An intravenously administered low-osmolal iodine contrast agent was used (48–145 mL of 320 to 400 mg iodine/mL in Study I; 48–155 ml of 320 to 400 mg iodine/mL in Study II; 50–96 mL of 350 to 400 mg iodine/mL iomeprol, iohexol or iobitridol in Study III). The CT collimation was 64 × 0.625 mm, the gantry rotation time was 350 ms, the tube current was 600–750 mA, and the voltage was 100–120 kV, depending on the patient's size. Prospective ECG-triggering for CTA was applied, when feasible, in order to reduce the radiation dose. The presence, extent, and severity of coronary atherosclerosis were evaluated by experienced physicians according to the 17-vessel system by using the GE ADW Workstation (General Electric, Piscataway, New Jersey, US). Both reoriented single plane and multiplanar reconstructions were used (Leipsic et al., 2014).

4.3.1.2 PET imaging

In Studies I–II, a quantitative assessment of MBF during adenosine infusion was performed during the same visit if obstructive CAD was suspected based on the initial interpretation of the coronary CTA. In Study III, the assessment of MBF with PET was performed to all patients immediately after coronary CTA, and both at rest and during adenosine-induced stress. In PET imaging, ^{15}O-labeled water was used as a radiotracer, and adenosine infusion (140 µg/kg/min) was used to induce vasodilator stress. Caffeine intake was prohibited for 12–24 hours prior to the

imaging studies. Due to logistic reasons or caffeine use, the assessment of MBF was performed in some patients in the days or weeks following coronary CTA. The PET data was quantitatively analyzed using the Carimas software version 1.1.0 (developed at Turku PET Centre, Turku, Finland) in standardized 17 segments according to the American Heart Association recommendations (Nesterov et al., 2009). The GE IQfusion software (GE ADW 4.4 Workstation, General Electric Medical Systems, Waukesha, Wisconsin) was used to create PET/CT fusion images. The analysis was performed by an experienced physician and recorded in a standardized reporting system.

4.3.1.3 Invasive coronary angiography

In Study III, ICA was carried out in addition to PET/CT imaging. Coronary angiograms were performed in Turku University Hospital with a Siemens Axiom Artis coronary angiography system (Siemens, Erlangen, Germany). The measurement of FFR was performed for stenoses with intermediate severity (30–80%), when feasible, using a ComboMap pressure/flow instrument and 0.014 inch BrightWire pressure guidewires (Volcano Corp, Rancho Cordova, CA, USA). The pressure was measured distally to the lesion during maximal hyperemia induced by 18 μg intracoronary boluses of adenosine with simultaneous measurement of aortic pressure. FFR was calculated as the ratio between the mean distal pressure and mean aortic pressure. A quantitative analysis of coronary angiograms was performed by an experienced reader, using software with an automated edge detection system (Quantcore, Siemens, Munich, Germany) and blinded to the results of PET, coronary CTA, and FFR.

4.3.2 Collection of clinical data and data analysis

In addition to the methods of data collection described earlier, prospectively filled questionnaires were also utilized, and the authors had direct access to all data in Study III.

In Studies I–II, the patients were divided into two categories on the basis of the most severe stenosis detected on coronary CTA. The first group consisted of patients for whom obstructive CAD was excluded by coronary CTA alone. The patients in the second group had a stenosis indicative of obstructive CAD requiring a further examination with PET. In Study II, for the patients with routinely performed coronary CTA and assessment of MBF with PET, the categorization of coronary CTA was made as if the patients had followed the hospital's standard protocol. In other words, the assessment of MBF with PET was taken into consideration only if the coronary CTA was suggestive of obstructive CAD. Based on a previous

validation, the value of absolute stress MBF ≤ 2.4 mL/min/g in at least one of the standard 17 segments was considered abnormal (Danad, Uusitalo, et al., 2014).

In Study I, the primary end point was ICA or revascularization performed within six months after the PET/CT. Other ICAs and revascularizations were considered as late events not triggered by the PET/CT. Indications for ICA and revascularization were also evaluated. In addition, the occurrence of cardiovascular mortality and non-fatal MI were studied. The individual follow-up time ranged from the initial coronary CTA until the end of 2015.

Primary end points in Study II were all-cause death, MI and UAP. The individual follow-up time ranged from the initial coronary CTA until the end of 2013. Information on possible ICA or revascularization within six months after coronary CTA was collected, but these were not included as adverse events.

In Study III, significant obstructive CAD was defined as either ≥ 50% stenosis on ICA or FFR <0.8. When FFR was available, stenoses with FFR ≥0.8 were classified as non-significant, regardless of the degree of luminal narrowing. Nonobstructive atherosclerosis was defined as the presence of coronary calcium or atherosclerotic plaque on the coronary CTA in the absence of significant obstructive CAD on ICA. The threshold for abnormal stress MBF, <2.4 mL/g/min, was based on a previous validation (Danad, Uusitalo, et al., 2014). CMD was defined as diffusely abnormal absolute MBF during adenosine stress in myocardial regions supplied by the main coronary arteries (LAD, LCX, and RCA) in the absence of corresponding epicardial obstructive CAD. CFR was calculated as the ratio of stress-to-rest MBF in each region. Coronary vascular resistance was calculated as the mean arterial pressure divided by global MBF, and the mean of systolic and diastolic blood pressure measurements at three and six minutes after adenosine administration was used to calculate the mean arterial pressure.

4.4 Statistical methods

4.4.1 Study I

Continuous variables are shown as means ± standard deviation (SD) or medians with corresponding 25th–75th percentiles. Categorical variables are shown as percentages. The independent-samples Mann-Whitney U test was used to compare the continuous variables, and the 2-sided Pearson chi-square test or Fisher's exact test was used for the categorical variables. The chi-square test or Fisher's exact test was used to compare the differences in referral rates to ICA and revascularizations between the different imaging finding groups. The combined event rate of cardiovascular death and MI was used as an end point, and annual combined event rates were compared using the Cox proportional hazards model. A p-value <0.05

was considered statistically significant. The Cox proportional hazards model was applied to analyze the predictors of referral to ICA and the predictors of events. The presence of abnormal stress MBF, age, gender, presence of typical angina pectoris, diabetes, and coronary calcium score >0 were included in the univariable analysis. Covariates with a p-value ≤0.05 in the univariable regression analysis were included in the multivariable analysis. The statistical analyses were performed with IBM SPSS Statistics Software version 24 (IBM Corporation, Armonk, New York, US).

4.4.2 Study II

Continuous variables are shown as means ± SD or medians with corresponding 25th–75th percentiles. Categorical variables are shown as percentages. The independent-samples Mann-Whitney U test or Kruskal-Wallis test was used to compare the continuous variables and the 2-sided Pearson chi-square test or Fisher's exact test was used for the categorical variables. Annual event rates (all-cause mortality, and the composite of mortality, MI, or UAP) were compared using Poisson regression analysis. A p-value <0.05 was considered statistically significant. Kaplan-Meier curves were generated and pooled log-rank tests were conducted (Mantel-Cox). The Cox proportional hazards model was applied to identify the predictors of adverse events and death; covariates with a p-value ≤0.10 in the univariable regression analysis were included in the multivariable analysis. The statistical analyses were conducted with IBM SPSS Statistics for Windows version 22.0 (IBM Corporation, Armonk, New York).

4.4.3 Study III

Continuous variables are shown as means ± SD. The Shapiro-Wilk test was used to assess the normality of distribution of the continuous variables. The two-tailed independent-samples t-test or Mann-Whitney U test was used to compare the continuous variables between two groups. The Kruskal-Wallis test followed by pairwise comparisons was used two compare the continuous variables between multiple groups. The two-sided chi-square test or Fisher's exact test was used to compare the categorical variables. Spearman's rank-order correlation coefficient was used to assess the relationship between two continuous variables. Univariate and multivariable linear regression analyses were performed to study the effects of possible predictors of coronary hemodynamics. A p-value <0.05 was considered statistically significant. The statistical analyses were conducted with software IBM SPSS Statistics Software version 22.0 (IBM Corporation, Armonk, New York, NY, USA).

5 Results

5.1 Assessment of stress MBF after coronary CTA and referral to ICA (Study I)

5.1.1 Patient characteristics, adherence to the protocol and imaging findings

In Study I, 721 symptomatic outpatients referred to coronary CTA due to suspected obstructive CAD were evaluated. Fifty-one patients (7%) did not complete the selective PET/CT protocol due to contraindication for adenosine (n = 22), direct referral to ICA after coronary CTA (n = 11), referral to other functional tests (n = 6), or technical reasons (PET failed or was not available, n = 12). Thus, the final study population consisted of 670 symptomatic patients who had completed the selective hybrid imaging protocol (Figure 1).

Patient characteristics of Study I are shown in Table 2. The mean age was 61 years and 283 (42%) patients were male. Typical angina pectoris was experienced by 19% of the patients, whereas 70% presented atypical angina pectoris, non-anginal chest pain, or dyspnea.

Obstructive CAD was excluded in 417 (62%) patients on the basis of the coronary CTA alone (Figure 1). Among these, 217 (52%) had no coronary atherosclerosis and 200 (48%) had nonobstructive atherosclerosis. After the initial evaluation of coronary CTA images, a suspicion of obstructive CAD led to an assessment of stress MBF with PET in 253 (38%) patients. Among them, the coronary CTA showed two-vessel obstructive CAD in 42 (17%) and three-vessel obstructive CAD in 41 (16%) patients. Stress MBF findings were normal in 114 (45%) patients and abnormal in 139 (55%) patients. In the latter group, the median number of abnormal segments per patient was 9 (25th–75th percentile: 5–13). The mean global stress MBF was lower in patients with abnormal than those with normal PET (2.3 ± 0.8 mL/g/min vs. 3.8 ± 1.0 mL/g/min, $p < 0.001$). Taken together, there was (i) no obstructive CAD based on coronary CTA alone in 62%, (ii) suspected obstructive CAD with normal PET findings in 17%, and (iii) suspected obstructive CAD with abnormal PET findings in 21% of the patients (n = 670).

Table 2. Patient characteristics in Study I.

Variable	No OCAD	Suspected OCAD and normal MBF	Suspected OCAD and abnormal MBF	p-value*	p-value**
Number of patients	n = 417	n = 114	n = 139		
Age (mean ± SD), years	59 ± 10	66 ± 8	63 ± 9	< 0.001	0.009
Male gender, %	36	36	68	0.925	< 0.001
Risk factors for CAD, %					
Current or previous smoking	29	33	39	0.446	0.036
Prediabetes	13	18	21	0.119	0.044
Type 2 diabetes	9	16	23	0.040	< 0.001
Hypertension	43	69	71	< 0.001	< 0.001
Dyslipidemia	54	61	71	0.170	0.002
Family history of CAD	44	47	43	0.652	0.757
Primary symptom, %					
Typical AP	15	23	26	0.051	0.014
Atypical AP, nonanginal chest pain or dyspnea	72	66	67	0.167	0.348
Other	13	11	7	0.901	0.093
Medication, %					
Beta blocker	38	52	55	0.007	0.003
Lipid lowering drug	31	41	53	0.044	< 0.001
Antiplatelet drug	42	50	63	0.150	< 0.001
Anticoagulant	7	8	9	0.593	0.451
Long-acting nitrate	7	11	14	0.077	0.012
Diuretic	16	25	25	0.015	0.047
ACE inhibitor	16	21	26	0.188	0.016
Angiotensin receptor blocker	11	21	23	0.005	0.004
Calcium channel blocker	10	22	19	0.001	0.075
Antiarrhythmic agent	2	2	2	1.000	1.000

*CAD excluded by coronary CTA vs. normal MBF, **CAD excluded by coronary CTA or normal MBF vs. abnormal MBF. ACE = angiotensin-converting enzyme; AP = angina pectoris; CAD = coronary artery disease; CTA = computed tomography angiography; ECG = electrocardiography; OCAD = obstructive coronary artery disease; PET = positron emission tomography; SD = standard deviation

Typical angina was more common in patients with abnormal stress MBF than those with normal stress MBF or no obstructive CAD on the coronary CTA (Table 2). Patients with abnormal stress MBF were also more often smokers or had diabetes, hypertension or dyslipidemia. Furthermore, antithrombotic, lipid lowering, anti-ischemic and blood pressure lowering medications were more common in patients with abnormal than those with normal MBF. Exercise ECG had been performed on 466 patients, but a positive ECG finding was not associated with abnormalities in PET.

The mean radiation doses of coronary CTA, PET and combined PET/CT were 7.9 ± 3.7 mSv, 0.97 ± 0.10 mSv and 9.1 ± 4.0 mSv, respectively.

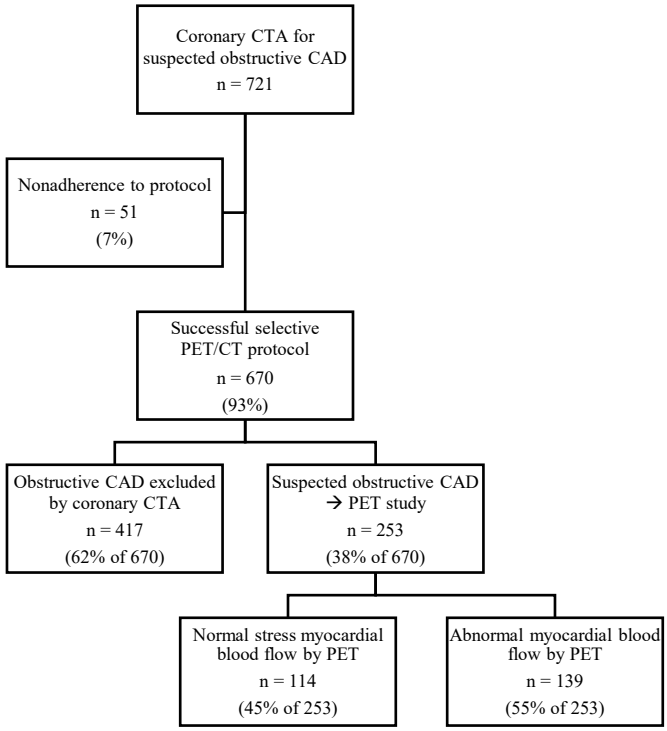

Figure 1. Imaging findings with a selective hybrid imaging strategy with PET and coronary CTA in patients with suspected obstructive coronary artery disease (CAD).

5.1.2 Referral to ICA and revascularization

The rates of referral to ICA and revascularizations within six months after PET/CT are shown in Figure 2A.

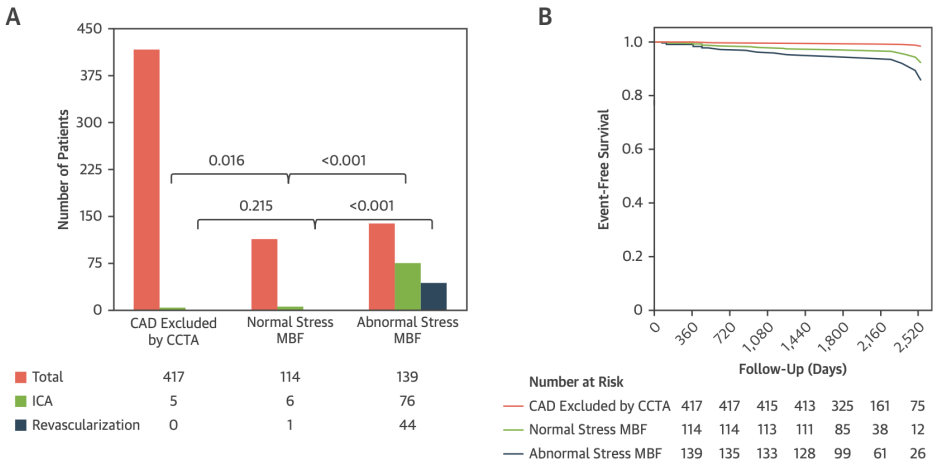

Figure 2. (A) Rates of invasive coronary angiography (ICA) and revascularization after coronary computed tomography angiography (CTA) and selective assessment of absolute stress myocardial blood flow (MBF) by positron emission tomography (PET) within 6 months. (B) Event-free long-term survival among patients with abnormal stress MBF by PET versus patients with obstructive coronary artery disease (CAD) excluded by coronary CTA ($p < 0.001$) alone or normal stress MBF ($p = 0.308$). Originally published in Stenström et al. *JACC Cardiovasc Imaging* 2019;12:2266-7. Reprinted by permission from Elsevier.

Of those 417 patients for whom CAD was excluded by the coronary CTA alone, five (1%) patients with nonobstructive atherosclerosis in the coronary CTA were referred to ICA. All of these patients continued to have chest pain after PET/CT and it was the indication for subsequent referral to ICA. ICA showed no obstructive CAD and no revascularizations were performed in this category.

Of the patients with suspected obstructive CAD in coronary CTA, but normal absolute stress MBF (n = 114), six (5%) patients were referred to ICA due to continuous symptoms. ICA showed obstructive CAD in three cases, while the others had nonobstructive CAD. Revascularization was performed for one (1%) out of the 114 patients. In this patient, ICA showed coronary artery spasm, but also anatomically significant (>70%) stenoses in the LCX and the RCA which were treated by PCI.

Of the 139 patients with abnormal stress MBF by PET, 76 (55%) were referred to ICA and revascularization was performed on 44 (32%), including 39 PCIs and 5 CABGs. To rephrase it, the revascularization rate was 58%. Abnormal stress MBF in a particular myocardial region corresponding to a stenosis seen on the coronary CTA was more common in the revascularized than non-revascularized patients (Table 3, 88% vs. 60%; p = 0.006, Stenström et al., unpublished results). All 44

revascularized patients showed either a stenosis of ≥70% on ICA, a stenosis associated with FFR of <0.8, or a stenosis of >50% in combination with ischemia in the same territory by noninvasive testing.

Table 3. Prevalence of a high-risk coronary anatomy, MBF <2.4 ml/g/min in ≥3 segments and MBF <2.4 ml/g/min in a region matching with stenosis on coronary CTA in revascularized vs. not revascularized patients after documented abnormal stress MBF and invasive coronary angiography.

	Abnormal stress MBF Revasc + (n = 44)	**Abnormal stress MBF Revasc – (n = 32)**	**p-value**
High risk anatomy*	66%	69%	0.795
≥3 ischemic segments	95%	83%	0.130
Matching stenosis and ischemia	88%	60%	0.006

* High-risk anatomy: >50% stenosis in the left main, proximal left anterior descending coronary artery or obstructive three-vessel disease
CTA= coronary computed tomography, MBF= myocardial blood flow
Stenström et al., unpublished results.

In the univariable analysis, predictors of referral to ICA were abnormal absolute stress MBF, coronary calcium score >0, male gender, diabetes, typical angina, and age older than 65 years. In multivariable Cox regression analysis, abnormal stress MBF was the only independent predictor of ICA referral ($p < 0.001$).

Patients with abnormal MBF not referred to ICA

There were 63 patients with abnormal MBF who were not referred to ICA within six months. As shown in Table 4, these patients were less likely to have a high-risk anatomy by coronary CTA (38% vs. 67%, $p = 0.001$) or a perfusion defect in a myocardial region corresponding to a stenosis seen on coronary CTA (60% vs. 76%, $p = 0.044$) than the patients who were referred to ICA (Stenström et al., unpublished results).

Based on medical records, the motives for not to refer a patient to ICA despite abnormal stress MBF were adequate control of symptoms by medical therapy (71%) and the patient's unwillingness to undergo ICA (10%). In addition, the benefit of revascularization in the presence of abnormal stress MBF without corresponding stenosis in the coronary CTA was considered uncertain in 19% of patients.

Sixteen ICAs were performed later than six months after the PET/CT imaging, and seven of these resulted in revascularization (5 PCIs and 2 CABGs). Hence, the

rates of late referral to ICA and late revascularization were 26% and 11%, respectively, in this group with abnormal coronary CTA and PET.

Table 4. Prevalence of a high-risk coronary anatomy, MBF <2.4 ml/g/min in ≥3 segments and MBF <2.4 ml/g/min in a region matching with stenosis on coronary CTA in patients referred vs. not referred to invasive coronary angiography after documented abnormal stress MBF.

Variable	Abnormal stress MBF ICA + (n = 76)	Abnormal stress MBF ICA – (n = 63)	p-value
High risk anatomy*	67%	38%	0.001
≥3 ischemic segments	90%	78%	0.066
Matching stenosis and ischemia	76%	60%	0.044

* High-risk anatomy: >50% stenosis in the left main, proximal left anterior descending coronary artery or obstructive three-vessel disease
CTA= computed tomography angiography, MBF=myocardial blood flow
Stenström et al., unpublished results.

5.1.3 Patient follow-up

During the median follow-up time of 5.2 years (25th–75th percentile 4.5–6.4 years), 8 cardiovascular deaths and 12 non-fatal MIs occurred. One patient (with abnormal MBF) experienced both MI and cardiovascular death during the follow-up. Thus, the combined annual rate of cardiovascular death or MI was 0.53% in this category.

The annual event rate was 0.13% including 2 deaths and 1 MI, in patients with obstructive CAD excluded by coronary CTA alone. In those patients who underwent PET imaging, the annual event rate was 1.21%, including 6 deaths and 11 MIs. In patients with normal stress MBF, annual event rate was 0.83% including 1 death and 4 MIs. In patients with abnormal stress MBF, the annual event rate was 1.51% including 5 deaths and 7 MIs. Thus, the patients with abnormal stress MBF had a significantly higher event rate than those with either no obstructive CAD by coronary CTA or normal stress MBF (HR: 5.4; 95% CI 2.16–13.34, $p < 0.001$).

Although there was a tendency towards lesser events in those patients with abnormal stress MBF who were revascularized (n = 44; no deaths, 2 MIs, annual event rate 0.9%) than those who were not revascularized (n = 97; 5 deaths and 5 MIs, annual event rate 2.0%) this difference was not statistically significant (HR: 0.47; 95% CI 0.46–9.84, $p = 0.337$).

In the univariable analysis, statistically significant predictors of events were abnormal stress MBF, male gender, diabetes, and age older than 65 years. In the

multivariable Cox regression analysis, abnormal absolute stress MBF remained the only independent predictor ($p < 0.001$, Figure 2B).

Patients who did not adhere to the selective PET/CT protocol

Patients who were not investigated according to the hybrid imaging protocol (n = 51) had 15 (29%) ICAs of which 6 (12%) resulted in revascularization (5 PCIs and 1 CABG). There occurred 3 cardiovascular deaths and 1 MI in patients among the nonadherents.

5.2 Prognostic value of coronary CTA with selective assessment of stress MBF (Study II)

5.2.1 Patient characteristics and imaging findings

Basic patient characteristics are shown in Table 1. A total of 864 patients successfully completed the selective PET/CT protocol for suspected CAD and thus formed the final study population for the prognostic analysis. Typical angina pectoris was recorded in 23% of the patients, whereas 65% had atypical angina pectoris, nonanginal chest pain, or dyspnea on exertion, and the rest with other symptoms.

In 462 (53%) patients, obstructive CAD was excluded with the information gained from the coronary CTA alone (Figure 3). The study was interpreted as normal in 260 patients and revealed nonobstructive atherosclerosis in 202 patients. Of the 402 (47%) patients with suspected obstructive CAD based on coronary CTA, 74 (18%) patients had two-vessel and 55 (14%) patients three-vessel obstructive CAD. In the PET study, 195 (49%) of the 402 patients had normal stress MBF and 207 (51%) reduced stress MBF. The radiation dose was 8.2 ± 4.0 mSv from coronary CTA and 0.97 ± 0.11 mSv from PET imaging.

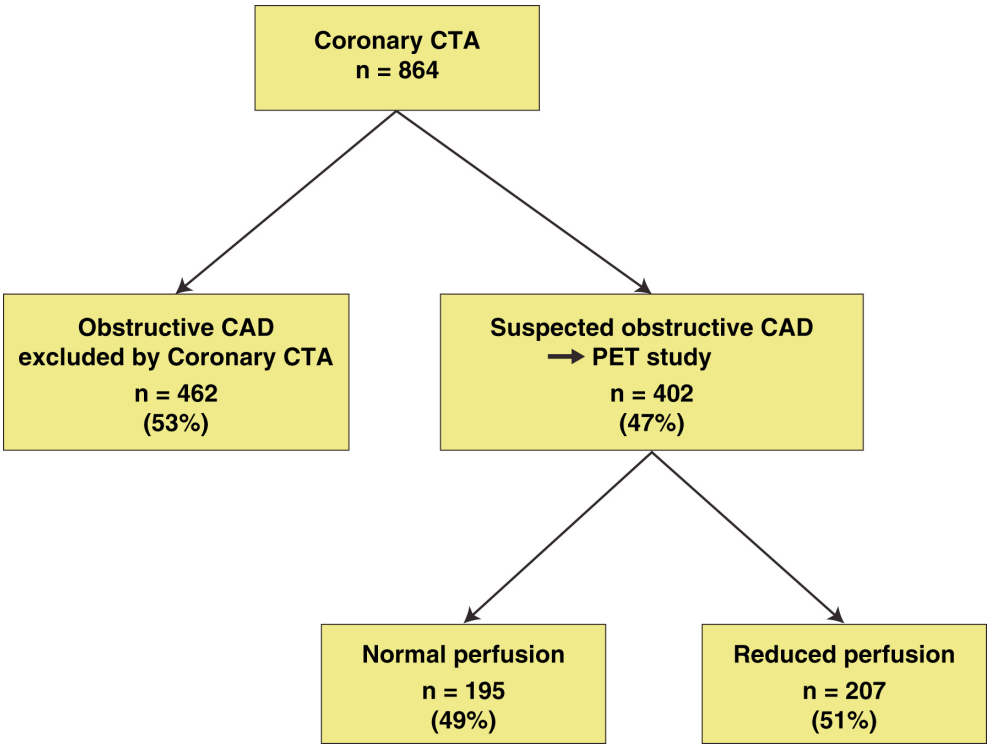

Figure 3. Imaging findings of selective hybrid imaging strategy with coronary CTA and PET in patients with suspected obstructive coronary artery disease (CAD). Originally published in Maaniitty et al. *JACC Cardiovasc Imaging* 2017;10:1361-70. Reprinted by permission from Elsevier.

5.2.2 Prognosis after coronary CTA with selective assessment of stress MBF

The patients were followed until the end of 2013 and the median follow-up time was 3.6 years (interquartile range 2.7 to 4.8 years). During this time, 31 adverse events occurred, including 16 deaths, 10 MIs, and 5 UAPs. In addition, two deaths occurred in patients with an earlier nonfatal event. Thus, the total number of deaths was 18. Consequently, the annual rate of all combined adverse events was 0.95% and the annual rate of all-cause mortality was 0.54%.

In patients with normal coronary arteries based on coronary CTA (n = 260), there were 3 deaths, 1 MI, and no UAPs during the follow-up. The combined annual rate of adverse events was 0.42% and the annual rate of all-cause mortality was 0.31% (Figure 4). In 202 patients with nonobstructive atherosclerosis, there were 3 deaths

and no other events. Therefore, the annual rates of adverse events and all-cause mortality were both 0.42%. There was no significant difference in the occurrence of adverse events or deaths between the patients with nonobstructive atherosclerosis and those with normal coronary arteries (0.42 vs. 0.42%; p = 0.99; and 0.42 vs. 0.31%; p = 0.71, respectively).

There were 12 deaths, 9 MIs, and 5 UAPs in patients with suspected obstructive CAD in the coronary CTA and subsequent assessment of MBF with PET (n = 402). In these patients, the annual combined adverse event rate was significantly higher than in those 462 patients in whom obstructive CAD was excluded by coronary CTA alone (1.50% vs. 0.42%; p = 0.003). However, the annual rate of all-cause mortality was statistically not significantly different (0.73% vs. 0.36%; p = 0.15).

Of the 402 patients with suspected CAD on coronary CTA, 207 (51%) patients had abnormal MBF by PET. Among these patients with abnormal MBF, there were 9 deaths, 8 MIs, and 5 UAPs, whereas in the patients with normal MBF (n = 195), there were only 3 deaths and 1 MI. The annual rate of adverse events was 5 times higher in the patients with abnormal MBF compared to the patients with normal PET study (2.5% vs. 0.50%; p = 0.004). The annual rates of all-cause mortality in patients with reduced MBF and in patients with normal MBF were 1.07% and 0.38%, respectively (p = 0.12).

The rate of adverse events and the annual rate of all-cause mortality, were comparable between patients with suspected obstructive coronary stenosis, but normal MBF, and patients in whom obstructive CAD was excluded by the coronary CTA alone (0.50% vs. 0.42%, p = 0.77; and 0.38% vs. 0.36%, p = 0.94, respectively). Survival according to PET/CT findings is shown in Figure 4. There was no difference in annual rates of adverse events or all-cause mortality between the revascularized or non-revascularized patients (2.1% vs. 2.8%; p = 0.57; and 0.52% vs. 1.5%; p = 0.17, respectively). Hence, the patients with or without early revascularization were pooled together for prognostic analyses, however, coronary revascularization was not considered as an end point.

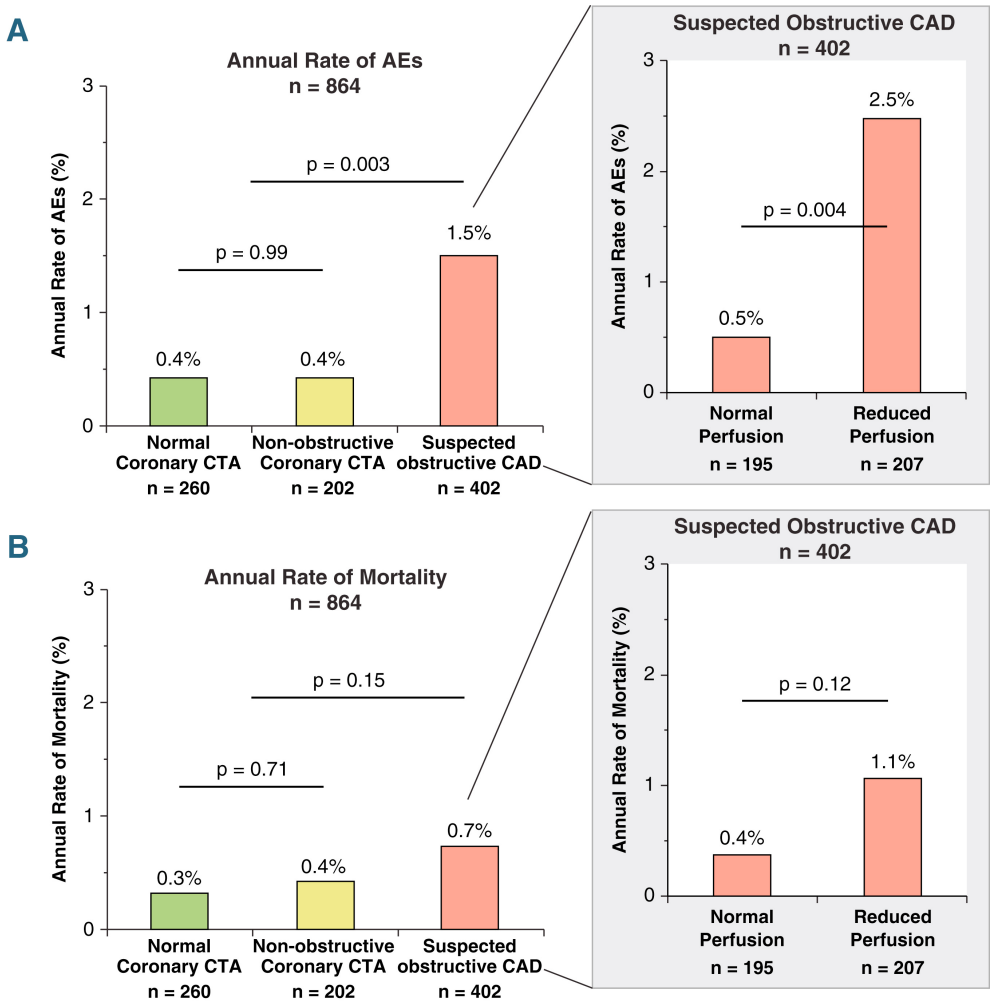

Figure 4. (A) Patients with obstructive CAD excluded by coronary CTA alone and patients with suspected obstructive CAD but normal MBF had low and comparable (p = 0.77) annual rates of adverse events (AE). (B) In contrast, patients with reduced MBF had significantly worse outcome. Originally published in Maaniitty et al. JACC Cardiovasc Imaging 2017;10:1361-70. Reprinted by permission from Elsevier.

The independent prognostic value of the imaging findings was studied using the Cox proportional hazards model. In the univariable analysis, statistically significant predictors of adverse events were increasing age and abnormal MBF by PET, while male gender and presence of pre-diabetes or diabetes predicted adverse events at a significance level of 0.10. In the multivariable Cox regression analysis, abnormal MBF and increasing age were found to be independent predictors of adverse events.

5.3 CMD in CCS (Study III)

5.3.1 Patient characteristics

Basic patient characteristics are shown in Table 1. The final study population comprised 189 patients with suspected obstructive CAD. The mean age was 62 years, 55% of the patients were male, and traditional risk factors for CAD were common. Atypical angina pectoris or nonanginal chest pain was recorded in 50% of the patients, followed by typical angina pectoris in 37%. Average pre-test probability of CAD was 65%. Based on the coronary CTA and ICA, 43 patients (23% of all patients) had normal coronary arteries, 76 (40%) had nonobstructive atherosclerosis, and 70 (37%) had obstructive CAD. Of the patients with obstructive CAD, 40% had one-vessel, 23% two-vessel, and 37% three-vessel disease.

5.3.2 Prevalence and clinical characteristics of CMD

In 119 (63%) patients, the absolute MBF during adenosine stress was normal (≥2.4 mL/g/min) in the myocardium supplied by the LAD, LCX, and RCA (Figure 5). Regional abnormalities in stress MBF explained by epicardial coronary stenosis were observed in 38 (20%) patients. Diffuse abnormalities (<2.4 mL/g/min) in the absolute stress MBF in the myocardium supplied by all major coronary arteries were found in 32 (17%) patients. In 15 (8% of all patients) of these, reduced MBF was explained by obstructive three-vessel CAD and was suggestive of balanced ischemia. In 17 (9% of all patients) patients, the diffuse abnormality of stress MBF was not explained by epicardial obstructive CAD, and these patients were diagnosed with CMD according to our definition.

Only 1% (n = 2) of all patients had CMD in the presence of normal epicardial coronary anatomy. CMD associated with nonobstructive atherosclerosis was recorded in 3% of all patients (n = 5) and CMD coexisting with obstructive CAD in 5% of all patients (n = 10). Thus, based on the fusion of perfusion maps with individual coronary anatomy, the diffusely abnormal stress MBF was not explained by the presence of obstructive CAD alone. Of the patients with coexisting CMD and obstructive CAD, three had one-vessel disease and seven had two-vessel disease.

Symptom presentation showed similar distribution in patients with and without CMD. The patients with CMD were more commonly male than patients without CMD, but there were no differences in the number of smokers or prevalence of prediabetes, diabetes, hypertension, dyslipidemia, family history of premature CAD, or the number of risk factors. The proportion of patients on lipid lowering medication (mainly statins) was lower in patients with than those without CMD, but for other medications the groups were similar. The number of risk factors was similar (mean

3.1 and 3.4, respectively, p = 0.468) in patients with or without CMD. Two representative cases are shown in Figures 2 and 3 of the original publication III.

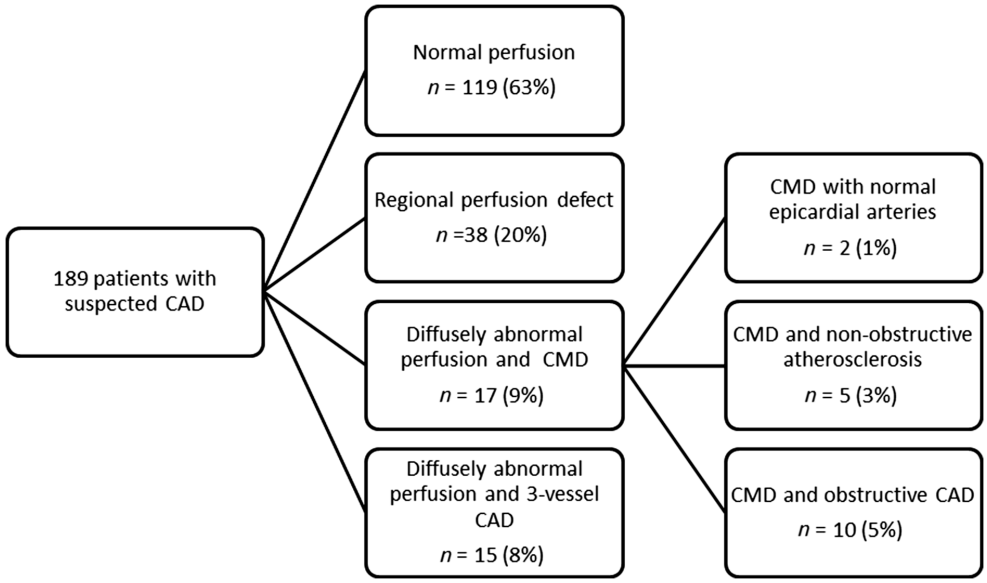

Figure 5. Prevalence of coronary microvascular dysfunction (CMD) based on myocardial perfusion imaging and coronary angiography. CMD was defined as diffusely abnormal MBF (myocardial blood flow <2.4 mL/g/min within the regions of three main coronary arteries) that was not explained by obstructive epicardial coronary artery disease (CAD). The results are shown as numbers (n) and percentages of all patients (n = 189). Originally published in Stenström et al. *Eur Heart J Cardiovasc Imaging* 2017;18: 1206-13. Reprinted by permission from Oxford University Press.

5.3.3 Determinants of coronary hemodynamics

In patients with CMD and normal coronary anatomy or nonobstructive disease, stress MBF was similar in the regions supplied by all three main coronary arteries, whereas in patients with coexisting CMD and obstructive CAD, stress MBF was usually lowest within the region supplied by an obstructed coronary artery. Notably, stress MBF within the corresponding territory did not correlate with the value of coronary calcium score in the LAD, the LCX or the RCA in the absence of obstructive CAD.

Mean absolute global MBF during adenosine stress was markedly lower in patients with CMD than other patients both in the absence (n = 119) and presence (n = 70) of obstructive CAD (1.90 vs. 3.96 mL/g/min, p = 0.000 and 1.53 vs. 2.67 mL/g/min, p = 0.000, respectively, Table 5). A similar pattern was also seen with CFR (2.61 vs. 3.71, p = 0.001 and 1.72 vs. 2.69, p = 0.003).

Linear regression analysis was performed to assess the factors affecting coronary hemodynamics in patients without obstructive CAD (n = 119). Based on the univariate analysis, only female gender and the presence of nonobstructive atherosclerosis significantly predicted global stress MBF, global CFR, and coronary vascular resistance. According to multivariable analysis, female gender was related to global stress MBF, global CFR and coronary vascular resistance, whereas nonobstructive atherosclerosis was related to global stress MBF.

Table 5. Average myocardial blood flow (MBF) at rest and during adenosine stress as well as coronary flow reserve (CFR) in patients with or without coronary microvascular dysfunction (CMD) in the absence or presence of obstructive coronary artery disease (CAD).

		CMD No	**CMD Yes**	**p-value**
All patients		n = 172	n = 17	
	Rest MBF (ml/g/min)	1.08 (0.26)	0.84 (0.17)	0.000
	Stress MBF (ml/g/min)	3.51 (1.14)	1.68 (0.33)	0.000
	CFR	3.36 (1.11)	2.08 (0.63)	0.000
No atherosclerosis		n = 41	n = 2	
	Rest MBF (ml/g/min)	1.13 (0.31)	0.75 (0.15)	0.055
	Stress MBF (ml/g/min)	4.33 (1.19)	1.87 (0.01)	0.009
	CFR	3.96 (1.04)	2.56 (0.52)	0.055
Nonobstructive CAD		n = 71	n = 5	
	Rest MBF (ml/g/min)	1.08 (0.24)	0.74 (0.14)	0.001
	Stress MBF (ml/g/min)	3.74 (0.79)	1.91 (0.24)	0.000
	CFR	3.56 (0.91)	2.63 (0.54)	0.014
Obstructive CAD		n = 60	n = 10	
	Rest MBF (ml/g/min)	1.03 (0.25)	0.91 (0.17)	0.117
	Stress MBF (ml/g/min)	2.67 (0.91)*	1.53 (0.33)	0.000
	CFR	2.69 (1.05)	1.72 (0.42)**	0.003

Values are means (standard deviation), n = number, *p < 0.001 vs. nonobstructive CAD, **p = 0.03 vs. nonobstructive CAD

Originally published in Stenström et al. *Eur Heart J Cardiovasc Imaging* 2017;18:1206-13. Reprinted by permission from Oxford University Press.

6 Discussion

6.1 Assessment of MBF after coronary CTA in patient management and risk stratification

The main findings of Study I indicate that coronary CTA with selective assessment of absolute stress MBF by PET guides the referral to ICA and potentially reduces the number of unnecessary invasive procedures in patients with suspected obstructive CAD. It was shown that the referral rates to ICA were low in patients with obstructive CAD excluded by coronary CTA alone and in patients with obstructive CAD in coronary CTA but normal stress MBF by PET (1% and 5%, respectively). In contrast, in patients with abnormal stress MBF, the referral rate to ICA was 55%.

These findings are in line with previous hybrid imaging studies (Danad, Raijmakers et al., 2014; Fiechter, Ghadri, Wolfrum et al., 2012; Pazhenkottil, Nkoulou, Ghadri, Herzog, Küest, et al., 2011) reporting low referral rates to ICA in patients with normal MPI findings. Danad et al. observed a referral rate of 83% in patients with equivocal or obstructive CAD on coronary CTA and abnormal ^{15}O-H_2O PET study (Danad, Raijmakers, et al., 2014). Similar findings were observed in the SPECT studies (Fiechter, Ghadri, Wolfrum et al., 2012; Pazhenkottil, Nkoulou, Ghadri, Herzog, Küest, et al., 2011). None of the previous hybrid imaging studies investigating downstream referral to ICA have used a selective approach, instead, all patients have undergone both coronary CTA and PET or SPECT.

ICA is rarely needed for purely diagnostic reasons in detecting obstructive CAD. The diagnostic yield of ICA has been reported to be as low as 39% in a large report of elective diagnostic ICAs (Patel et al., 2010). In the abovementioned studies by Pazhenkottil et al. and Fiechter et al., the diagnostic yield was 90% and 96%, respectively. In the study by Danad et al. the yield of CAD in ICA was 69% in patients with obstructive CAD and abnormal MBF, explained partly by the exclusion of known CAD in contrast to the other two studies. Thus, hybrid imaging, and especially selective ischemia testing, appears to be a potential method for identifying patients most likely to benefit from revascularization. However, recent studies evaluating noninvasive functional testing for the assessment of intermediate stenosis

identified by coronary CTA have shown only moderate concordance with invasive FFR (Nissen et al., 2018; Sand et al., 2018).

In Study I, the revascularization rate per angiogram was low (0.2%) in the absence of obstructive CAD as compared to patients with abnormal stress MBF (58%). In the study by Danad et al., the revascularization rate per angiogram in patients with equivocal or obstructive CAD on coronary CTA and normal perfusion the was 20%, as compared to the rate of 64% in patients with abnormal stress MBF (Danad, Raijmakers et al., 2014). The study design was not selective, and thus, comparing the pooled values is not feasible. Revascularization was more common in patients with a stenosis corresponding to a perfusion abnormality, which is in line with other studies (Fiechter, Ghadri, Wolfrum et al., 2012; Liga et al., 2016; Pazhenkottil, Nkoulou, Ghadri, Herzog, Küest et al., 2011). Similar results were obtained in a study utilizing FFR_{CT} for the evaluation of intermediate coronary lesions in patients with intermediate likelihood of CAD (Jensen et al., 2018).

To assess the safety of the guidance of patient management rather than the prognostic value itself, the outcome data was analyzed with a median follow-up time of 5.2 years. Patients with abnormal absolute stress MBF had a higher annual event rate of combined cardiovascular death and MI than patients with either obstructive CAD excluded by coronary CTA alone or with normal stress MBF (1.5% vs. 0.28%). However, the event rate of patients with suspected stenosis and normal perfusion was intermediate (0.8%), which is likely explained by the established impact of nonobstructive atherosclerosis on the event risk (Hadamitzky, Täubert et al., 2013; Hoffmann et al., 2017; Min et al., 2011), thus highlighting the need for preventive therapies in this subgroup of patients (Hoffmann et al., 2017).

In Study II, the extensive analysis of the prognostic value of the selective approach showed that hybrid imaging with coronary CTA followed by selective assessment of absolute stress MBF accurately identifies patients with low and high risk of death, MI, or UAP. In approximately one half of the patients with suspected CAD, obstructive CAD could be excluded by coronary CTA alone, and it was shown that these patients have a good outcome. In patients with obstructive CAD on coronary CTA, a significant difference in the event rates was observed between the patients with normal and abnormal stress MBF findings. The outcome in patients with normal MBF was comparable to those with obstructive CAD excluded by coronary CTA alone. The event rate of patients with abnormal MBF was fivefold as compared to patients with normal MBF. These findings are in line with previous studies in which the extent and severity of myocardial ischemia has been shown to predict a worse outcome in CAD (Dorbala et al., 2013; Hachamovitch et al., 1998; Herzog et al., 2009; Shaw & Iskandrian, 2004). In addition, the excellent prognosis of patients without obstructive CAD on coronary CTA, as well as the association between obstructive CAD on coronary CTA and a worse outcome, have been

previously repeatedly reported (Chow et al., 2011; Hadamitzky et al., 2009; Min et al., 2011). In contrast to Study I, no prognostic significance was observed in the presence of nonobstructive atherosclerosis in Study II. These differences may be explained by the different endpoint selection or with the longer follow-up time in Study I. In Study II, all-cause mortality was used as an endpoint, in contrast to cardiovascular death in Study I. All-cause mortality is a reliable measure with no verification bias (Lauer et al., 1999). However, the combined endpoint of cardiovascular death and MI was thought to better fit the study design of Study I investigating the effect and safety of the selective hybrid imaging approach. In addition, the number of events was relatively small in both study populations.

The similar outcomes in revascularized and non-revascularized patients in Studies I and II are consistent with the known limited prognostic benefit of revascularization in patients with CCS (Neumann et al., 2019), considering that the extent of ischemia or the frequency of high-risk coronary anatomy were similar in these groups. However, revascularization is typically triggered by ischemia and comparisons of rather small groups are subject to bias.

The optimal use of cardiac hybrid imaging in suspected obstructive CAD has lately been a subject of conversation. In Studies I and II, it was shown in a real-life population, that the selective assessment of stress MBF guides referral to ICA and is a feasible strategy to risk-stratify patients with suspected obstructive CAD. Engbers et al. have introduced a reverse strategy where coronary CTA is performed selectively (Engbers et al., 2017). To this day, the optimal strategy remains undiscovered and the decision-making process is affected by multiple factors, such as diagnostic accuracy, radiation dose, and costs. The concept of hybrid imaging has been criticized for the increased radiation dose per patient. However, the average radiation dose of ICA is about 7 mSv and, in our selective protocol, the assessment of stress MBF was performed in just about one third of the patients with only half of the patients in this group referred to ICA, indicating that the selective protocol reduces the overall radiation dose.

The studies included in this thesis are single-center, retrospective studies and subject to some limitations due to the study design. However, the study populations are highly representative of the population in question since they include all symptomatic patients referred to coronary CTA at the hospital in question. Only 4–7% of the patients were excluded as a result of non-adherence to the imaging protocol. The pre-test probability of CAD was within the intermediate range and atypical symptoms were common, which corresponds to other studies. The immediate availability of PET perfusion imaging has probably resulted in a higher number of performed ischemia tests, as compared to a scenario with only ICA available. Although the nationwide follow-up data on ICAs, revascularizations and adverse events was complete in all patients, we were unable to assess possible

changes in medical therapies after PET/CT. Appropriate use of preventive and anti-ischemic medication after coronary CTA may partially explain the low rate of referral to ICA (Newby et al., 2018). Nevertheless, these studies are the largest to evaluate the effect of selective assessment of stress MBF after coronary CTA on patient management and risk stratification in a real-world setting.

6.2 CMD in stable angina

The main finding Study III is that CMD is relatively rare in the absence of coronary atherosclerosis in symptomatic patients with suspected obstructive CAD, when identified as abnormal vasodilator capacity by PET perfusion imaging. In this study population, only 1% of the patients had CMD without any coronary atherosclerosis. However, the coexistence of CMD and atherosclerosis was more common with 3% of patients having nonobstructive CAD and 5% having obstructive CAD. In Study III, a large prospective cohort of symptomatic patients was studied, representing patients with intermediate pre-test probability of obstructive CAD who are typically referred to noninvasive functional imaging. In this study, hybrid imaging with PET/CT was used to study both the anatomy and the function of the coronary circulation thereby enabling the detection of CMD.

These results regarding the frequency of CMD in symptomatic patients with suspected CAD in Study III are somewhat lower than previously published in studies with invasive coronary microvascular functional testing (Ong et al., 2012; Sara et al., 2015). Sara et al. investigated responses to both acetylcholine and adenosine, and 19% of the patients were found to have both endothelium-dependent and endothelium-independent microvascular dysfunction. Adenosine, which was used in Study III, causes vasodilation via both the endothelium-dependent and endothelium-independent mechanisms and, consequently, some patients with solely endothelial dysfunction, presenting as abnormal MBF response to acetylcholine, may have been overlooked (Sara et al., 2015). In addition, the lower prevalence of CMD in Study III may be explained by different patient selection since the patients included in Study III had a low to intermediate pre-test probability of obstructive CAD. whereas patients with previous history of obstructive CAD or acute coronary syndrome were excluded. In addition, a major proportion of the patients were receiving medical therapy potentially preserving vascular function, including statin, angiotensin-converting enzyme inhibitors, and angiotensin receptor blocker medication for the treatment of underlying conditions and clinical suspicion of CAD. Of note, beta-blockers were routinely administered prior to coronary CTA. However, the effects of beta-blockers on coronary vascular function are not established (Billinger et al., 2001).

It was observed that CMD is closely associated with epicardial coronary atherosclerosis in the patients with suspected CAD, and the presence of atherosclerosis predicted reduced global stress MBF, which is analogous with the recent direction of general consensus (Sechtem et al., 2020; Taqueti & Di Carli, 2018). Of the patients with CMD, 88% were found to have coronary atherosclerosis, with almost equal proportions of nonobstructive and obstructive CAD. This is in keeping with previous observations on the association between CFR and the extent of coronary calcium (Wang et al., 2006). Typically, CMD is identified as a global reduction in MBF. However, some studies have reported regional perfusion abnormalities representing CMD (Lanza et al., 2008; Thomson et al., 2015). In Study III, four patients with coronary atherosclerosis presented with a regional perfusion defect without any corresponding significant stenosis, and the amount of coronary calcium did not correlate with regional stress MBF in these patients.

Our results indicate that hybrid PET/CT can be used in the identification of patients with CMD. Diffusely reduced CFR is a common finding and has prognostic value regarding mortality and adverse events, independently of regional ischemia (Herzog et al., 2009; Murthy, Naya, et al., 2014; Ziadi et al., 2011). In Study III, traditional atherosclerotic risk factors were common. However, no difference was observed between patients with or without CMD. CMD was prevalent both in women and men, as observed in other recent studies as well (Murthy, Naya et al., 2014; Ong et al., 2012; Sara et al., 2015).

Study III in question has some limitations. There was no control group with patients free from chest pain, and therefore, difference in the prevalence of CMD between symptomatic patients and general population could not be studied. The performance of noninvasive MBF and invasive tests in terms of detecting CMD could not be compared since no invasive coronary microvascular functional testing was performed. No follow-up data was recorded for the study population and, furthermore, the patient population is not sizeable enough to evaluate the prognostic value of CMD.

In all, CMD as an ischemia-causing entity has gained an increasing amount of attention during recent years. Invasive coronary microvascular functional testing is recommended by the current ESC Guidelines (Knuuti et al., 2020), but it is time-consuming and requires technical and specialist resources that are not widely available. Another challenge concerning patients with CMD is the lack of effective medical treatment in most of the patients. The ESC Guidelines suggest the treatment to address the dominant mechanism of microcirculatory dysfunction, however invasive procedures are only performed to few patients with suspected CMD. In this study population, prevalence of CMD was relatively low, suggesting that selective PET/CT hybrid imaging approach would be feasible in symptomatic patients with

intermediate pre-test probability of obstructive CAD. In other words, active screening for CMD is not reasonable for the time being.

6.3 Future directions

Today, the evolution of medical technology in combination with the epidemiologic shifts in cardiovascular risk factors in the population create a constant challenge for cardiovascular imaging. During the past decades, a drop in the diagnostic yield of ICA and radionuclide perfusion tests has been observed, highlighting the need for careful patient selection prior to imaging procedures in the future, together with the updated pre-test probabilities (Patel et al., 2010; Foldyna et al., 2019).

In addition, a change in the pathophysiology of acute coronary syndrome has been observed. Incidence of MIs caused by an atherothrombotic plaque rupture has decreased, while MIs caused by the imbalance between the myocardial oxygen supply and demand, as well as heart failure with preserved ejection fraction, are on the rise (Di Carli, 2020). These changes have been associated with CMD and diffuse atherosclerosis, as well as the increased prevalence of obesity, glucose intolerance, and increasing age, and these changes should be accounted for in the future.

Coronary CTA, various noninvasive functional tests, and hybrid imaging have become more available recently. Thanks to the improvements in technology, significant reductions in radiation doses have been achieved (Benz et al., 2015). The increased availability has allowed the collection of large data sets; however, in the future, randomized clinical trials are needed to study the outcomes after coronary CTA and functional testing, as well as the targeted prevention in patients with nonobstructive atherosclerosis. It has been observed that high-risk plaque characteristics seen on coronary CTA provide prognostic information besides the presence of hemodynamically significant obstructive CAD and clinical characteristics, and the more distinctive evaluation of the atherosclerotic burden may be utilized in risk-stratification in the future (Andreini et al., 2020).

The results of Studies I, II, and III indicate that selective assessment of MBF after coronary CTA is a feasible strategy in patients with suspected CAD and may be utilized more widely in clinical practice. New modalities such as FFR_{CT} and CTP are promising tools for combined imaging. In addition, deep learning and artificial intelligence have been introduced in the field of medicine and cardiovascular imaging with promising results on prognostic estimations at the individual level through the detection of complex features otherwise not noticed in combination with clinical data (Juarez-Orozco et al., 2020).

The unique feature of PET is the quantification of MBF. However, the requirement of an on-site cyclotron has limited its availability. It is currently available in Turku, Kuopio, Helsinki, and few other sites in Europe. Novel fluorine-

18-labeled tracers do not share this restriction, and studies have been conducted for the development of models for the quantification of MBF (Werner et al., 2019). More studies are warranted before clinical acceptance, but fluorine-18-labeled tracers seem to be a promising next step in the wider utilization of MBF quantification. Another recent development and target of interest in the future is the calculation of LV ejection fraction from ^{15}O-water PET (Nordström et al., 2017).

In Study III, a low prevalence of CMD was observed in patients with suspected obstructive CAD, suggesting that selective assessment of MBF after coronary CTA is a feasible option in symptomatic patients with suspected obstructive CAD. In the future, more studies are needed to investigate the pathophysiological mechanism of CMD in different disease entities in order to develop targeted treatment options.

7 Conclusions

The major findings and conclusions of Studies I–III are as follows:

1. Obstructive CAD could be excluded in 62% of the patients with suspected CAD by means of coronary CTA alone, and the referral rate to ICA was low (1%) in these patients. In patients with suspected obstructive CAD based on coronary CTA, the referral rates to ICA were 5% in patients with normal stress MBF assessed by PET and 55% in patients with abnormal stress MBF and the revascularization rates were 1% and 58%, respectively. Selective assessment of stress MBF by PET after coronary CTA guides referral to ICA and potentially reduces the number of unnecessary ICAs and revascularizations.
2. The rates of MI, UAP, or death were low in patients in whom obstructive CAD was excluded with coronary CTA alone and in patients who had normal stress MBF findings after coronary CTA. In patients with abnormal stress MBF findings, the outcome was significantly worse. Selective assessment of stress MBF by PET after coronary CTA is a safe approach for the risk stratification of patients with suspected CAD.
3. In symptomatic patients with suspected obstructive CAD, CMD was detected in 9% of the patients. The prevalence of CMD in the absence of coronary atherosclerosis was low (1%).

References

Abbara, S., Blanke, P., Maroules, C., Cheezum, M., Choi, A. D., Han B. K., Marwan, M., Naoum, C., Norgaard, B. L., Rubinshtein, R., Schoenhagen, P., Villines, T., & Leipsic, J (2016). SCCT guidelines for the performance and acquisition of coronary computed tomographic angiography: A report of the society of Cardiovascular Computed Tomography Guidelines Committee: Endorsed by the North American Society for Cardiovascular Imaging (NASCI). *Journal of Cardiovascular Computed Tomography, 10*(6), 435-449.

Achenbach, S. (2006). Computed Tomography Coronary Angiography. *Journal of the American College of Cardiology, 48*(10), 1919-1928.

Adamson, P. D., Williams, M. C., Dweck, M. R., Mills, N. L., Boon, N. A., Daghem, M., Bing, R., Moss, A. J., Mangion, K., Flather, M., Forbes, J., Hunter, A., Norrie, J., Shah, A. S. V., Timmis, A. D., van Beek, E. J. R., Ahmadi, A. A., Leipsic, J., Narula, J., . . . Berry, C. (2019). Guiding Therapy by Coronary CT Angiography Improves Outcomes in Patients With Stable Chest Pain. *Journal of the American College of Cardiology Cardiology, 74*(16), 2058-2070.

Adjedj, J., De Bruyne, B., Floré, V., Di Gioia, G., Ferrara, A., Pellicano, M., Toth, G. G., Bartunek, J., Vanderheyden, M., Heyndrickx, G. R., Wijns, W., & Barbato, E. (2016). Significance of Intermediate Values of Fractional Flow Reserve in Patients With Coronary Artery Disease. *Circulation, 133*(5), 502-508.

Al-Lamee, R., Thompson, D., Dehbi, H. M., Sen, S., Tang, K., Davies, J., Keeble, T., Mielewczik, M., Kaprielian, R., Malik, I. S., Nijjer, S. S., Petraco, R., Cook, C., Ahmad, Y., Howard, J., Baker, C., Sharp, A., Gerber, R., & Talwar, S. (2018). Percutaneous coronary intervention in stable angina (ORBITA): a double-blind, randomised controlled trial. *Lancet, 391*(10115), 31-40.

Antoniadis, A. P., Giannopoulos, A. A., Wentzel, J. J., Joner, M., Giannoglou, G. D., Virmani, R., & Chatzizisis, Y. S. (2015). Impact of local flow haemodynamics on atherosclerosis in coronary artery bifurcations. *EuroIntervention, 11* Suppl V, V18-22.

Arora, N., Matheny, M. E., Sepke, C., & Resnic, F. S. (2007). A propensity analysis of the risk of vascular complications after cardiac catheterization procedures with the use of vascular closure devices. *American Heart Journal, 153*(4), 606-611.

Asbury, E. A., Creed, F., & Collins, P. (2004). Distinct psychosocial differences between women with coronary heart disease and cardiac syndrome X. *European Heart Journal, 25*(19), 1695-1701.

Bairey Merz, C. N., Handberg, E. M., Shufelt, C. L., Mehta, P. K., Minissian, M. B., Wei, J., Thomson, L. E., Berman, D. S., Shaw, L. J., Petersen, J. W., Brown, G. H., Anderson, R. D., Shuster, J. J., Cook-Wiens, G., Rogatko, A., & Pepine, C. J. (2016). A randomized, placebo-controlled trial of late Na current inhibition (ranolazine) in coronary microvascular dysfunction (CMD): impact on angina and myocardial perfusion reserve. *European Heart Journal, 37*(19), 1504-1513.

Bamberg, F., Marcus, R. P., Becker, A., Hildebrandt, K., Bauner, K., Schwarz, F., Greif, M., von Ziegler, F., Bischoff, B., Becker, H. C., Johnson, T. R., Reiser, M. F., Nikolaou, K., & Theisen, D. (2014). Dynamic myocardial CT perfusion imaging for evaluation of myocardial ischemia as determined by MR imaging. *Journal of the American College of Cardiology: Cardiovascular Imaging, 7*(3), 267-277.

Bamberg, F., Sommer, W. H., Hoffmann, V., Achenbach, S., Nikolaou, K., Conen, D., Reiser, M. F., Hoffmann, U., & Becker, C. R. (2011). Meta-analysis and systematic review of the long-term predictive value of assessment of coronary atherosclerosis by contrast-enhanced coronary computed tomography angiography. *Journal of the American College of Cardiology*, *57*(24), 2426-2436.

Baumgart, D., Haude, M., Görge, G., Liu, F., Ge, J., Grosse-Eggebrecht, C., Erbel, R., & Heusch, G. (1999). Augmented alpha-adrenergic constriction of atherosclerotic human coronary arteries. *Circulation, 99*(16), 2090-2097.

Beltrame, J. F., Crea, F., Kaski, J. C., Ogawa, H., Ong, P., Sechtem, U., Shimokawa, H., & Bairey Merz, C. N. (2017). International standardization of diagnostic criteria for vasospastic angina. *European Heart Journal, 38*(33), 2565-2568.

Bengel, F. M., Higuchi, T., Javadi, M. S., Lautamäki, R. (2009). Cardiac Positron Emission Tomography. Journal of the American College of Cardiology, 54(1), 1-15.

Bentzon, J. F., Otsuka, F., Virmani, R., & Falk, E. (2014). Mechanisms of plaque formation and rupture. *Circulation Research, 114*(12), 1852-1866.

Benz, D. C., Gaemperli, L., Gräni, C., von Felten, E., Giannopoulos, A. A., Messerli, M., Buechel, R. R., Gaemperli, O., Pazhenkottil, A. P., & Kaufmann, P. A. (2018). Impact of cardiac hybrid imaging-guided patient management on clinical long-term outcome. *International Journal of Cardiology, 261*, 218-222.

Benz, D. C., Templin, C., Kaufmann, P. A., & Buechel, R. R. (2015). Ultra-low-dose hybrid single photon emission computed tomography and coronary computed tomography angiography: a comprehensive and non-invasive diagnostic workup of suspected coronary artery disease. *European Heart Journal, 36*(47), 3345.

Billinger, M., Seiler, C., Fleisch, M., Eberli, F. R., Meier, B., & Hess, O. M. (2001). Do beta-adrenergic blocking agents increase coronary flow reserve? *Journal of the American College of Cardiology, 38*(7), 1866-1871.

Bittencourt, M. S., Hulten, E., Ghoshhajra, B., O'Leary, D., Christman, M. P., Montana, P., Truong, Q. A., Steigner, M., Murthy, V. L., Rybicki, F. J., Nasir, K., Gowdak, L. H., Hainer, J., Brady, T. J., Di Carli, M. F., Hoffmann, U., Abbara, S., & Blankstein, R. (2014). Prognostic value of nonobstructive and obstructive coronary artery disease detected by coronary computed tomography angiography to identify cardiovascular events. *Circulation: Cardiovascular imaging*, 7(2), 282-291.

Bittencourt, M. S., Hulten, E. A., Murthy, V. L., Cheezum, M., Rochitte, C. E., Di Carli, M. F., & Blankstein, R. (2016). Clinical Outcomes After Evaluation of Stable Chest Pain by Coronary Computed Tomographic Angiography Versus Usual Care: A Meta-Analysis. *Circulation: Cardiovascular imaging, 9*(4), e004419.

Booth, J. N., Levitan, E. B., Brown, T. M., Farkouh, M. E., Safford, M. M., & Muntner, P. (2014). Effect of sustaining lifestyle modifications (nonsmoking, weight reduction, physical activity, and mediterranean diet) after healing of myocardial infarction, percutaneous intervention, or coronary bypass (from the REasons for Geographic and Racial Differences in Stroke Study). *The American Journal of Cardiology, 113*(12), 1933-1940.

Budoff, M. J., Dowe, D., Jollis, J. G., Gitter, M., Sutherland, J., Halamert, E., Scherer, M., Bellinger, R., Martin, A., Benton, R., Delago, A., & Min, J. K. (2008). Diagnostic performance of 64-multidetector row coronary computed tomographic angiography for evaluation of coronary artery stenosis in individuals without known coronary artery disease: results from the prospective multicenter ACCURACY (Assessment by Coronary Computed Tomographic Angiography of Individuals Undergoing Invasive Coronary Angiography) trial. *Journal of the American College of Cardiology Cardiology, 52*(21), 1724-1732.

Caliskan, M., Erdogan, D., Gullu, H., Topcu, S., Ciftci, O., Yildirir, A., & Muderrisoglu, H. (2007). Effects of atorvastatin on coronary flow reserve in patients with slow coronary flow. *Clinical Cardiology, 30*(9), 475-479.

Camici, P. G., & Crea, F. (2007). Coronary microvascular dysfunction. *New England Journal of Medicine*, 356(8), 830-840.

Camici, P. G., d'Amati, G., & Rimoldi, O. (2015). Coronary microvascular dysfunction: mechanisms and functional assessment. *Nature Reviews Cardiology, 12*(1), 48-62.

Campisi, R., Czernin, J., Schöder, H., Sayre, J. W., Marengo, F. D., Phelps, M. E., & Schelbert, H. R. (1998). Effects of long-term smoking on myocardial blood flow, coronary vasomotion, and vasodilator capacity. *Circulation, 98*(2), 119-125.

Castelli, W. P., Garrison, R. J., Wilson, P. W., Abbott, R. D., Kalousdian, S., & Kannel, W. B. (1986). Incidence of coronary heart disease and lipoprotein cholesterol levels. The Framingham Study. *JAMA, 256*(20), 2835-2838.

Cerqueira, M. D., Weissman, N. J., Dilsizian, V., Jacobs, A. K., Kaul, S., Laskey, W. K., Pennell, D. J., Rumberger, J. A., Ryan, T., & Verani, M. S. (2002). Standardized myocardial segmentation and nomenclature for tomographic imaging of the heart. A statement for healthcare professionals from the Cardiac Imaging Committee of the Council on Clinical Cardiology of the American Heart Association. *Circulation, 105*(4), 539-542.

Chade, A. R., Brosh, D., Higano, S. T., Lennon, R. J., Lerman, L. O., & Lerman, A. (2006). Mild renal insufficiency is associated with reduced coronary flow in patients with non-obstructive coronary artery disease. *Kidney International, 69*(2), 266-271.

Chang, H. J., Lin, F. Y., Gebow, D., An, H. Y., Andreini, D., Bathina, R., Baggiano, A., Beltrama, V., Cerci, R., Choi, E. Y., Choi, J. H., Choi, S. Y., Chung, N., Cole, J., Doh, J. H., Ha, S. J., Her, A. Y., Kepka, C., Kim, J. Y., Kim, J. W., . . . Min, J. K. (2019). Selective Referral Using CCTA Versus Direct Referral for Individuals Referred to Invasive Coronary Angiography for Suspected CAD: A Randomized, Controlled, Open-Label Trial. *Journal of the American College of Cardiology: Cardiovascular Imaging, 12*(7 Pt 2), 1303-1312.

Chang, S. M., Nabi, F., Xu, J., Raza, U., & Mahmarian, J. J. (2010). Normal stress-only versus standard stress/rest myocardial perfusion imaging: similar patient mortality with reduced radiation exposure. *Journal of the American College of Cardiology Cardiology, 55*(3), 221-230.

Charytan, D. M., Skali, H., Shah, N. R., Veeranna, V., Cheezum, M. K., Taqueti, V. R., Kato, T., Bibbo, C. R., Hainer, J., Dorbala, S., Blankstein, R., & Di Carli, M. F. (2018). Coronary flow reserve is predictive of the risk of cardiovascular death regardless of chronic kidney disease stage. *Kidney International, 93*(2), 501-509.

Chen, A., Wang, H., Fan, B., Xu, Y., Chen, W., & Dai, N. (2017). Prognostic value of normal positron emission tomography myocardial perfusion imaging in patients with known or suspected coronary artery disease: a meta-analysis. *The British Journal of Radiology, 90*(1074), 20160702.

Chen, J. W., Lee, W. L., Hsu, N. W., Lin, S. J., Ting, C. T., Wang, S. P., & Chang, M. S. (1997). Effects of short-term treatment of nicorandil on exercise-induced myocardial ischemia and abnormal cardiac autonomic activity in microvascular angina. *The American Journal of Cardiology, 80*(1), 32-38.

Chen, M. Y., Rochitte, C. E., Arbab-Zadeh, A., Dewey, M., George, R. T., Miller, J. M., Niinuma, H., Yoshioka, K., Kitagawa, K., Sakuma, H., Laham, R., Vavere, A. L., Cerci, R. J., Mehra, V. C., Nomura, C., Kofoed, K. F., Jinzaki, M., Kuribayashi, S., Scholte, A. J. , . . . Lima, J. A. C. (2017). Prognostic Value of Combined CT Angiography and Myocardial Perfusion Imaging versus Invasive Coronary Angiography and Nuclear Stress Perfusion Imaging in the Prediction of Major Adverse Cardiovascular Events: The CORE320 Multicenter Study. *Radiology, 284*(1), 55-65.

Cho, I., Al'Aref, S. J., Berger, A., Ó Hartaigh, B., Gransar, H., Valenti, V., Lin, F. Y., Achenbach, S., Berman, D. S., Budoff, M. J., Callister, T. Q., Al-Mallah, M. H., Cademartiri, F., Chinnaiyan, K., Chow, B. J. W., DeLago, A., Villines, T. C., Hadamitzky, M., Hausleiter, J., & Min, J. K. (2018). Prognostic value of coronary computed tomographic angiography findings in asymptomatic individuals: a 6-year follow-up from the prospective multicentre international CONFIRM study. *European Heart Journal, 39*(11), 934-941.

Chow, B. J., Small, G., Yam, Y., Chen, L., Achenbach, S., Al-Mallah, M., Berman, D. S., Budoff, M. J., Cademartiri, F., Callister, T. Q., Chang, H. J., Cheng, V., Chinnaiyan, K. M., Delago, A., Dunning, A., Hadamitzky, M., Hausleiter, J., Kaufmann, P., Lin, F., . . . Min, J. K. (2011). Incremental prognostic value of cardiac computed tomography in coronary artery disease using CONFIRM: COroNary computed tomography angiography evaluation for clinical outcomes: an InteRnational Multicenter registry. *Circulation: Cardiovascular imaging, 4*(5), 463-472.

Chow, C. K., Jolly, S., Rao-Melacini, P., Fox, K. A., Anand, S. S., & Yusuf, S. (2010). Association of diet, exercise, and smoking modification with risk of early cardiovascular events after acute coronary syndromes. *Circulation, 121*(6), 750-758.

Chowdhury, R., Khan, H., Heydon, E., Shroufi, A., Fahimi, S., Moore, C., Stricker, B., Mendis, S., Hofman, A., Mant, J., & Franco, O. H. (2013). Adherence to cardiovascular therapy: a meta-analysis of prevalence and clinical consequences. *European Heart Journal, 34*(38), 2940-2948.

Collet, C., Miyazaki, Y., Ryan, N., Asano, T., Tenekecioglu, E., Sonck, J., Andreini, D., Sabate, M., Brugaletta, S., Stables, R. H., Bartorelli, A., de Winter, R. J., Katagiri, Y., Chichareon, P., De Maria, G. L., Suwannasom, P., Cavalcante, R., Jonker, H., Morel, M. A., & Serruys, P. W. (2018). Fractional Flow Reserve Derived From Computed Tomographic Angiography in Patients With Multivessel CAD. *Journal of the American College of Cardiology Cardiology, 71*(24), 2756-2769.

Collet, C., Onuma, Y., Andreini, D., Sonck, J., Pompilio, G., Mushtaq, S., La Meir, M., Miyazaki, Y., de Mey, J., Gaemperli, O., Ouda, A., Maureira, J. P., Mandry, D., Camenzind, E., Macron, L., Doenst, T., Teichgräber, U., Sigusch, H., Asano, T., . . . Serruys, P. W. (2018). Coronary computed tomography angiography for heart team decision-making in multivessel coronary artery disease. *European Heart Journal, 39*(41), 3689-3698.

Conroy, R. M., Pyörälä, K., Fitzgerald, A. P., Sans, S., Menotti, A., De Backer, G., De Bacquer, D., Ducimetière, P., Jousilahti, P., Keil, U., Njølstad, I., Oganov, R. G., Thomsen, T., Tunstall-Pedoe, H., Tverdal, A., Wedel, H., Whincup, P., Wilhelmsen, L. & Graham, I. M. (2003). Estimation of ten-year risk of fatal cardiovascular disease in Europe: the SCORE project. *European Heart Journal, 24*(11), 987-1003.

D'Agostino, R. B., Vasan, R. S., Pencina, M. J., Wolf, P. A., Cobain, M., Massaro, J. M., & Kannel, W. B. (2008). General cardiovascular risk profile for use in primary care: the Framingham Heart Study. *Circulation, 117*(6), 743-753.

Dai, T., Wang, J. R., & Hu, P. F. (2018). Diagnostic performance of computed tomography angiography in the detection of coronary artery in-stent restenosis: evidence from an updated meta-analysis. *European Radiology, 28*(4), 1373-1382.

Daly, C. A., De Stavola, B., Sendon, J. L., Tavazzi, L., Boersma, E., Clemens, F., Danchin, N., Delahaye, F., Gitt, A., Julian, D., Mulcahy, D., Ruzyllo, W., Thygesen, K., Verheugt, F., Fox, K. M., & Euro Heart Survey Investigators (2006). Predicting prognosis in stable angina--results from the Euro heart survey of stable angina: prospective observational study. *BMJ (Clinical research ed.), 332*(7536), 262–267.

Daly, C., Norrie, J., Murdoch, D. L., Ford, I., Dargie, H. J., Fox, K., & group, T. T. I. B. E. T. s. (2003). The value of routine non-invasive tests to predict clinical outcome in stable angina. *European Heart Journal, 24*(6), 532-540.

Danad, I., Raijmakers, P. G., Appelman, Y. E., Harms, H. J., de Haan, S., van den Oever, M. L., Heymans, M. W., Tulevski, I. I., van Kuijk, C., Hoekstra, O. S., Lammertsma, A. A., Lubberink, M., van Rossum, A. C., & Knaapen, P. (2013). Hybrid imaging using quantitative H215O PET and CT-based coronary angiography for the detection of coronary artery disease. *Journal of Nuclear Medicine, 54*(1), 55-63.

Danad, I., Raijmakers, P. G., Driessen, R. S., Leipsic, J., Raju, R., Naoum, C., Knuuti, J., Mäki, M., Underwood, R. S., Min, J. K., Elmore, K., Stuijfzand, W. J., van Royen, N., Tulevski, I. I., Somsen, A. G., Huisman, M. C., van Lingen, A. A., Heymans, M. W., van de Ven, P. M., . . . Knaapen, P. (2017). Comparison of Coronary CT Angiography, SPECT, PET, and Hybrid Imaging for

Diagnosis of Ischemic Heart Disease Determined by Fractional Flow Reserve. *JAMA Cardiology, 2*(10), 1100-1107.

Danad, I., Raijmakers, P. G., Harms, H. J., van Kuijk, C., van Royen, N., Diamant, M., Lammertsma, A. A., Lubberink, M., van Rossum, A. C., & Knaapen, P. (2014). Effect of cardiac hybrid ^{15}O-water PET/CT imaging on downstream referral for invasive coronary angiography and revascularization rate. *European Heart Journal – Cardiovascular Imaging, 15*(2), 170-179.

Danad, I., Szymonifka, J., Schulman-Marcus, J., & Min, J. K. (2016). Static and dynamic assessment of myocardial perfusion by computed tomography. *European Heart Journal – Cardiovascular Imaging, 17*(8), 836-844.

Danad, I., Uusitalo, V., Kero, T., Saraste, A., Raijmakers, P. G., Lammertsma, A. A., Heymans, M. W., Kajander, S. A., Pietilä, M., James, S., Sörensen, J., Knaapen, P., & Knuuti, J. (2014). Quantitative assessment of myocardial perfusion in the detection of significant coronary artery disease: cutoff values and diagnostic accuracy of quantitative [(15)O]H2O PET imaging. *Journal of the American College of Cardiology, 64*(14), 1464-1475.

Dayanikli, F., Grambow, D., Muzik, O., Mosca, L., Rubenfire, M., & Schwaiger, M. (1994). Early detection of abnormal coronary flow reserve in asymptomatic men at high risk for coronary artery disease using positron emission tomography. *Circulation, 90*(2), 808–817.

de Araújo Gonçalves, P., Garcia-Garcia, H. M., Dores, H., Carvalho, M. S., Jerónimo Sousa, P., Marques, H., Ferreira, A., Cardim, N., Campante Teles, R., Raposo, L., Mesquita Gabriel, H., Sousa Almeida, M., Aleixo, A., Mota Carmo, M., Pereira Machado, F., & Mendes, M. (2013). Coronary computed tomography angiography-adapted Leaman score as a tool to noninvasively quantify total coronary atherosclerotic burden. *The International Journal of Cardiovascular Imaging, 29*(7), 1575-1584.

de Graaf, M. A., Broersen, A., Ahmed, W., Kitslaar, P. H., Dijkstra, J., Kroft, L. J., Delgado, V., Bax, J. J., Reiber, J. H., & Scholte, A. J. (2014). Feasibility of an automated quantitative computed tomography angiography-derived risk score for risk stratification of patients with suspected coronary artery disease. *The American Journal of Cardiology, 113*(12), 1947-1955.

de Graaf, F. R., Schuijf, J. D., van Velzen, J. E., Boogers, M. J., Kroft, L. J., de Roos, A., Reiber, J. H., Sieders, A., Spanó, F., Jukema, J. W., Schalij, M. J., van der Wall, E. E., & Bax, J. J. (2010). Diagnostic accuracy of 320-row multidetector computed tomography coronary angiography to noninvasively assess in-stent restenosis. *Investigative Radiology, 45*(6), 331-340.

de Graaf, F. R., van Velzen, J. E., Witkowska, A. J., Schuijf, J. D., van der Bijl, N., Kroft, L. J., de Roos, A., Reiber, J. H., Bax, J. J., de Grooth, G. J., Jukema, J. W., & van der Wall, E. E. (2011). Diagnostic performance of 320-slice multidetector computed tomography coronary angiography in patients after coronary artery bypass grafting. *European Radiology, 21*(11), 2285-2296.

Deussen, A., Brand, M., Pexa, A., & Weichsel, J. (2006). Metabolic coronary flow regulation – Current concepts. *Basic Research in Cardiology, 101*(6), 453-464.

Di Carli, M. F., Janisse, J., Grunberger, G., & Ager, J. (2003). Role of chronic hyperglycemia in the pathogenesis of coronary microvascular dysfunction in diabetes. *Journal of the American College of Cardiology, 41*(8), 1387-1393.

Diamond, G. A., & Forrester, J. S. (1979). Analysis of probability as an aid in the clinical diagnosis of coronary-artery disease. *New England Journal of Medicine, 300*(24), 1350-1358.

Dorbala, S., Di Carli, M. F., Beanlands, R. S., Merhige, M. E., Williams, B. A., Veledar, E., Chow, B. J., Min, J. K., Pencina, M. J., Berman, D. S., & Shaw, L. J. (2013). Prognostic value of stress myocardial perfusion positron emission tomography: results from a multicenter observational registry. *Journal of the American College of Cardiology, 61*(2), 176-184.

Douglas, P. S., De Bruyne, B., Pontone, G., Patel, M. R., Norgaard, B. L., Byrne, R. A., Curzen, N., Purcell, I., Gutberlet, M., Rioufol, G., Hink, U., Schuchlenz, H. W., Feuchtner, G., Gilard, M., Andreini, D., Jensen, J. M., Hadamitzky, M., Chiswell, K., Cyr, D., . . . Hlatky, M. A. (2016). 1-Year Outcomes of FFRCT-Guided Care in Patients With Suspected Coronary Disease: The PLATFORM Study. *Journal of the American College of Cardiology, 68*(5), 435-445.

Douglas, P. S., Hoffmann, U., Patel, M. R., Mark, D. B., Al-Khalidi, H. R., Cavanaugh, B., Cole, J., Dolor, R. J., Fordyce, C. B., Huang, M., Khan, M. A., Kosinski, A. S., Krucoff, M. W., Malhotra, V., Picard, M. H., Udelson, J. E., Velazquez, E. J., Yow, E., Cooper, L. S., . . . Lee, K. L (2015). Outcomes of anatomical versus functional testing for coronary artery disease. *New England Journal of Medicine, 372*(14), 1291-1300.

Dougoud, S., Fuchs, T. A., Stehli, J., Clerc, O. F., Buechel, R. R., Herzog, B. A., Leschka, S., Alkadhi, H., Kaufmann, P. A., & Gaemperli, O. (2014). Prognostic value of coronary CT angiography on long-term follow-up of 6.9 years. *The International Journal of Cardiovascular Imaging, 30*(5), 969-976.

Duncker, D. J., Koller, A., Merkus, D., & Canty, J. M. (2015). Regulation of coronary blood flow in health and ischemic heart disease. *Progress in Cardiovascular Diseases, 57*(5), 409-422.

Egashira, K., Inou, T., Hirooka, Y., Yamada, A., Urabe, Y., & Takeshita, A. (1993). Evidence of impaired endothelium-dependent coronary vasodilatation in patients with angina pectoris and normal coronary angiograms. *New England Journal of Medicine, 328*(23), 1659-1664.

Einstein, A. J. (2008). Radiation risk from coronary artery disease imaging: how do different diagnostic tests compare? *Heart, 94*(12), 1519-1521.

Engbers, E. M., Timmer, J. R., Ottervanger, J. P., Mouden, M., Oostdijk, A. H. J., Knollema, S., & Jager, P. L. (2017). Sequential SPECT/CT imaging for detection of coronary artery disease in a large cohort: evaluation of the need for additional imaging and radiation exposure. *Journal of Nuclear Cardiology, 24*(1), 212-223.

Eshtehardi, P., McDaniel, M. C., Dhawan, S. S., Binongo, J. N., Krishnan, S. K., Golub, L., Corban, M. T., Raggi, P., Quyyumi, A. A., & Samady, H. (2012). Effect of intensive atorvastatin therapy on coronary atherosclerosis progression, composition, arterial remodeling, and microvascular function. *Journal of Invasive Cardiology, 24*(10), 522-529.

Falk, E. (2006). Pathogenesis of atherosclerosis. *Journal of the American College of Cardiology, 47*(8 Suppl), C7-12.

Fiechter, M., Ghadri, J. R., Gebhard, C., Fuchs, T. A., Pazhenkottil, A. P., Nkoulou, R. N., Herzog, B. A., Wyss, C. A., Gaemperli, O., & Kaufmann, P. A. (2012). Diagnostic value of 13N-ammonia myocardial perfusion PET: added value of myocardial flow reserve. *Journal of Nuclear Medicine, 53*(8), 1230-1234.

Fiechter, M., Ghadri, J. R., Wolfrum, M., Kuest, S. M., Pazhenkottil, A. P., Nkoulou, R. N., Herzog, B. A., Gebhard, C., Fuchs, T. A., Gaemperli, O., & Kaufmann, P. A. (2012). Downstream resource utilization following hybrid cardiac imaging with an integrated cadmium-zinc-telluride/64-slice CT device. *European Journal of Nuclear Medicine and Molecular Imaging, 39*(3), 430-436.

Foldyna, B., Udelson, J. E., Karády, J., Banerji, D., Lu, M. T., Mayrhofer, T., Bittner, D. O., Meyersohn, N. M., Emami, H., Genders, T. S. S., Fordyce, C. B., Ferencik, M., Douglas, P. S., & Hoffmann, U. (2019). Pretest probability for patients with suspected obstructive coronary artery disease: re-evaluating Diamond-Forrester for the contemporary era and clinical implications: insights from the PROMISE trial. *European Heart Journal – Cardiovascular Imaging, 20*(5), 574-581.

Ford, T. J., Stanley, B., Good, R., Rocchiccioli, P., McEntegart, M., Watkins, S., Eteiba, H., Shaukat, A., Lindsay, M., Robertson, K., Hood, S., McGeoch, R., McDade, R., Yii, E., Sidik, N., McCartney, P., Corcoran, D., Collison, D., Rush, C., . . . Berry, C. (2018). Stratified Medical Therapy Using Invasive Coronary Function Testing in Angina: The CorMicA Trial. *Journal of the American College of Cardiology, 72*(23 Pt A), 2841-2855.

Ford, T. J., Stanley, B., Sidik, N., Good, R., Rocchiccioli, P., McEntegart, M., Watkins, S., Eteiba, H., Shaukat, A., Lindsay, M., Robertson, K., Hood, S., McGeoch, R., McDade, R., Yii, E., McCartney, P., Corcoran, D., Collison, D., Rush, C., & Berry, C. (2020). 1-Year Outcomes of Angina Management Guided by Invasive Coronary Function Testing (CorMicA). *Journal of the American College of Cardiology: Cardiovascular Interventions, 13*(1), 33-45.

Fukushima, K., Javadi, M. S., Higuchi, T., Lautamäki, R., Merrill, J., Nekolla, S. G., & Bengel, F. M. (2011). Prediction of short-term cardiovascular events using quantification of global myocardial

flow reserve in patients referred for clinical 82Rb PET perfusion imaging. *Journal of Nuclear Medicine, 52*(5), 726-732.

Gaemperli, O., Bengel, F. M., & Kaufmann, P. A. (2011). Cardiac hybrid imaging. *European Heart Journal, 32*(17), 2100-2108.

Gaemperli, O., Saraste, A., & Knuuti, J. (2012). Cardiac hybrid imaging. *European Heart Journal – Cardiovascular Imaging, 13*(1), 51-60.

Gaemperli, O., Valenta, I., Schepis, T., Husmann, L., Scheffel, H., Desbiolles, L., Leschka, S., Alkadhi, H., & Kaufmann, P. A. (2008). Coronary 64-slice CT angiography predicts outcome in patients with known or suspected coronary artery disease. *European Radiology, 18*(6), 1162-1173.

Gargiulo, P., Dellegrottaglie, S., Bruzzese, D., Savarese, G., Scala, O., Ruggiero, D., D'Amore, C., Paolillo, S., Agostoni, P., Bossone, E., Soricelli, A., Cuocolo, A., Trimarco, B., & Perrone Filardi, P. (2013). The prognostic value of normal stress cardiac magnetic resonance in patients with known or suspected coronary artery disease: a meta-analysis. *Circulation: Cardiovascular imaging, 6*(4), 574-582.

Ghadri, J. R., Fiechter, M., Fuchs, T. A., Scherrer, A., Stehli, J., Gebhard, C., Kläser, B., Gaemperli, O., Lüscher, T. F., Templin, C., & Kaufmann, P. A. (2013). Registry for the Evaluation of the PROgnostic value of a novel integrated imaging approach combining Single Photon Emission Computed Tomography with coronary calcification imaging (REPROSPECT). *European Heart Journal – Cardiovascular Imaging, 14*(4), 374-380.

Gimbrone, M. A., & García-Cardeña, G. (2016). Endothelial Cell Dysfunction and the Pathobiology of Atherosclerosis. *Circulation Research, 118*(4), 620-636.

Goldenberg, R., Punthakee, Z., & Canadian Diabetes Association Clinical Practice Guidelines Expert Committee. (2013). Definition, classification and diagnosis of diabetes, prediabetes and metabolic syndrome. *Canadian Journal of Diabetes, 37* Suppl 1, S8-11.

Gould, K. L., & Johnson, N. P. (2018). Coronary Physiology Beyond Coronary Flow Reserve in Microvascular Angina: JACC State-of-the-Art Review. *Journal of the American College of Cardiology, 72*(21), 2642-2662.

Gould, K. L., Johnson, N. P., Bateman, T. M., Beanlands, R. S., Bengel, F. M., Bober, R., Camici, P. G., Cerqueira, M. D., Chow, B. J., Di Carli, M. F., Dorbala, S., Gewirtz, H., Gropler, R. J., Kaufmann, P. A., Knaapen, P., Knuuti, J., Merhige, M. E., Rentrop, K. P., Ruddy, T. D., & Narula, J. (2013). Anatomic versus physiologic assessment of coronary artery disease. Role of coronary flow reserve, fractional flow reserve, and positron emission tomography imaging in revascularization decision-making. *Journal of the American College of Cardiology, 62*(18), 1639-1653.

Gowd, B. M., Heller, G. V., & Parker, M. W. (2014). Stress-only SPECT myocardial perfusion imaging: a review. *Journal of Nuclear Cardiology, 21*(6), 1200-1212.

Green, R., Cantoni, V., Acampa, W., Assante, R., Zampella, E., Nappi, C., Gaudieri, V., Mannarino, T., Cuocolo, R., Petretta, M., & Cuocolo, A. (2019). Prognostic value of coronary flow reserve in patients with suspected or known coronary artery disease referred to PET myocardial perfusion imaging: A meta-analysis. *Journal of Nuclear Cardiology.* Advance online publication. doi: 10.1007/s12350-019-02000-7.

Greenwood, J. P., Herzog, B. A., Brown, J. M., Everett, C. C., Nixon, J., Bijsterveld, P., Maredia, N., Motwani, M., Dickinson, C. J., Ball, S. G., & Plein, S. (2016). Prognostic Value of Cardiovascular Magnetic Resonance and Single-Photon Emission Computed Tomography in Suspected Coronary Heart Disease: Long-Term Follow-up of a Prospective, Diagnostic Accuracy Cohort Study. *Annals of Internal Medicine, 165*(1), 1-9.

Greenwood, J. P., Ripley, D. P., Berry, C., McCann, G. P., Plein, S., Bucciarelli-Ducci, C., Dall'Armellina, E., Prasad, A., Bijsterveld, P., Foley, J. R., Mangion, K., Sculpher, M., Walker, S., Everett, C. C., Cairns, D. A., Sharples, L. D., & Brown, J. M. (2016). Effect of Care Guided by Cardiovascular Magnetic Resonance, Myocardial Perfusion Scintigraphy, or NICE Guidelines on

Subsequent Unnecessary Angiography Rates: The CE-MARC 2 Randomized Clinical Trial. *JAMA, 316*(10), 1051-1060.

Groothuis, J. G., Beek, A. M., Brinckman, S. L., Meijerink, M. R., van den Oever, M. L., Hofman, M. B., van Kuijk, C., & van Rossum, A. C. (2013). Combined non-invasive functional and anatomical diagnostic work-up in clinical practice: the magnetic resonance and computed tomography in suspected coronary artery disease (MARCC) study. *European Heart Journal, 34*(26), 1990-1998.

Grover, R., Leipsic, J. A., Mooney, J., Kueh, S. H., Ohana, M., Nørgaard, B. L., Eftekhari, A., Bax, J. J., Murphy, D. T., Hague, C. J., Seidman, M. A., Blanke, P., Sedlak, T., & Sellers, S. L. (2017). Coronary lumen volume to myocardial mass ratio in primary microvascular angina. *Journal of Cardiovascular Computed Tomography, 11*(6), 423-428.

Groves, A. M., Speechly-Dick, M. E., Kayani, I., Pugliese, F., Endozo, R., McEwan, J., Menezes, L. J., Habib, S. B., Prvulovich, E., & Ell, P. J. (2009). First experience of combined cardiac PET/64-detector CT angiography with invasive angiographic validation. *European Journal of Nuclear Medicine and Molecular Imaging, 36*(12), 2027-2033.

Gupta, A., Taqueti, V. R., van de Hoef, T. P., Bajaj, N. S., Bravo, P. E., Murthy, V. L., Osborne, M. T., Seidelmann, S. B., Vita, T., Bibbo, C. F., Harrington, M., Hainer, J., Rimoldi, O., Dorbala, S., Bhatt, D. L., Blankstein, R., Camici, P. G., & Di Carli, M. F. (2017). Integrated Noninvasive Physiological Assessment of Coronary Circulatory Function and Impact on Cardiovascular Mortality in Patients With Stable Coronary Artery Disease. *Circulation, 136*(24), 2325-2336.

Hachamovitch, R., Berman, D. S., Shaw, L. J., Kiat, H., Cohen, I., Cabico, J. A., Friedman, J., & Diamond, G. A. (1998). Incremental prognostic value of myocardial perfusion single photon emission computed tomography for the prediction of cardiac death: differential stratification for risk of cardiac death and myocardial infarction. *Circulation, 97*(6), 535-543.

Hachamovitch, R., Hayes, S. W., Friedman, J. D., Cohen, I., & Berman, D. S. (2003). Comparison of the short-term survival benefit associated with revascularization compared with medical therapy in patients with no prior coronary artery disease undergoing stress myocardial perfusion single photon emission computed tomography. *Circulation, 107*(23), 2900-2907.

Hachamovitch, R., Rozanski, A., Shaw, L. J., Stone, G. W., Thomson, L. E., Friedman, J. D., Hayes, S. W., Cohen, I., Germano, G., & Berman, D. S. (2011). Impact of ischaemia and scar on the therapeutic benefit derived from myocardial revascularization vs. medical therapy among patients undergoing stress-rest myocardial perfusion scintigraphy. *European Heart Journal, 32*(8), 1012-1024.

Hadamitzky, M., Achenbach, S., Al-Mallah, M., Berman, D., Budoff, M., Cademartiri, F., Callister, T., Chang, H. J., Cheng, V., Chinnaiyan, K., Chow, B. J., Cury, R., Delago, A., Dunning, A., Feuchtner, G., Gomez, M., Kaufmann, P., Kim, Y. J., Leipsic, J., . . . Hausleiter. (2013). Optimized prognostic score for coronary computed tomographic angiography: results from the CONFIRM registry (COronary CT Angiography EvaluatioN For Clinical Outcomes: An InteRnational Multicenter Registry). *Journal of the American College of Cardiology, 62*(5), 468-476.

Hadamitzky, M., Freissmuth, B., Meyer, T., Hein, F., Kastrati, A., Martinoff, S., Schömig, A., & Hausleiter, J. (2009). Prognostic value of coronary computed tomographic angiography for prediction of cardiac events in patients with suspected coronary artery disease. *Journal of the American College of Cardiology: Cardiovascular Imaging, 2*(4), 404-411.

Hadamitzky, M., Täubert, S., Deseive, S., Byrne, R. A., Martinoff, S., Schömig, A., & Hausleiter, J. (2013). Prognostic value of coronary computed tomography angiography during 5 years of follow-up in patients with suspected coronary artery disease. *European Heart Journal, 34*(42), 3277-3285.

Hajjiri, M. M., Leavitt, M. B., Zheng, H., Spooner, A. E., Fischman, A. J., & Gewirtz, H. (2009). Comparison of positron emission tomography measurement of adenosine-stimulated absolute myocardial blood flow versus relative myocardial tracer content for physiological assessment of coronary artery stenosis severity and location. *Journal of the American College of Cardiology: Cardiovascular Imaging, 2*(6), 751-758.

Hamasaki, S., Al Suwaidi, J., Higano, S. T., Miyauchi, K., Holmes, D. R., & Lerman, A. (2000). Attenuated coronary flow reserve and vascular remodeling in patients with hypertension and left ventricular hypertrophy. *Journal of the American College of Cardiology, 35*(6), 1654-1660.

Hamm, C. W., Bassand, J. P., Agewall, S., Bax, J., Boersma, E., Bueno, H., Caso, P., Dudek, D., Gielen, S., Huber, K., Ohman, M., Petrie, M. C., Sonntag, F., Uva, M. S., Storey, R. F., Wijns, W., & Zahger, D. (2011). ESC Guidelines for the management of acute coronary syndromes in patients presenting without persistent ST-segment elevation: The Task Force for the management of acute coronary syndromes (ACS) in patients presenting without persistent ST-segment elevation of the European Society of Cardiology (ESC). *European Heart Journal, 32*(23), 2999-3054.

Heijenbrok-Kal, M. H., Fleischmann, K. E., & Hunink, M. G. (2007). Stress echocardiography, stress single-photon-emission computed tomography and electron beam computed tomography for the assessment of coronary artery disease: a meta-analysis of diagnostic performance. *American Heart Journal, 154*(3), 415-423.

Henzlova, M. J., Duvall, W. L., Einstein, A. J., Travin, M. I., & Verberne, H. J. (2016). ASNC imaging guidelines for SPECT nuclear cardiology procedures: Stress, protocols, and tracers. *Journal of Nuclear Cardiology, 23*(3), 606-639.

Herzog, B. A., Husmann, L., Valenta, I., Gaemperli, O., Siegrist, P. T., Tay, F. M., Burkhard, N., Wyss, C. A., & Kaufmann, P. A. (2009). Long-term prognostic value of 13N-ammonia myocardial perfusion positron emission tomography added value of coronary flow reserve. *Journal of the American College of Cardiology, 54*(2), 150-156.

Hoffmann, U., Ferencik, M., Udelson, J. E., Picard, M. H., Truong, Q. A., Patel, M. R., Huang, M., Pencina, M., Mark, D. B., Heitner, J. F., Fordyce, C. B., Pellikka, P. A., Tardif, J. C., Budoff, M., Nahhas, G., Chow, B., Kosinski, A. S., Lee, K. L., & Douglas, P. S. (2017). Prognostic Value of Noninvasive Cardiovascular Testing in Patients With Stable Chest Pain: Insights From the PROMISE Trial (Prospective Multicenter Imaging Study for Evaluation of Chest Pain). *Circulation, 135*(24), 2320-2332.

Hou, Z. H., Lu, B., Gao, Y., Jiang, S. L., Wang, Y., Li, W., & Budoff, M. J. (2012). Prognostic value of coronary CT angiography and calcium score for major adverse cardiac events in outpatients. *Journal of the American College of Cardiology: Cardiovascular Imaging, 5*(10), 990-999.

Hsu, B., Chen, F. C., Wu, T. C., Huang, W. S., Hou, P. N., Chen, C. C., & Hung, G. U. (2014). Quantitation of myocardial blood flow and myocardial flow reserve with 99mTc-sestamibi dynamic SPECT/CT to enhance detection of coronary artery disease. *European Journal of Nuclear Medicine and Molecular Imaging, 41*(12), 2294-2306.

Hueb, W., Lopes, N., Gersh, B. J., Soares, P. R., Ribeiro, E. E., Pereira, A. C., Favarato, D., Rocha, A. S., Hueb, A. C., & Ramires, J. A. (2010). Ten-year follow-up survival of the Medicine, Angioplasty, or Surgery Study (MASS II): a randomized controlled clinical trial of 3 therapeutic strategies for multivessel coronary artery disease. *Circulation, 122*(10), 949-957.

Hulten, E. A., Carbonaro, S., Petrillo, S. P., Mitchell, J. D., & Villines, T. C. (2011). Prognostic value of cardiac computed tomography angiography: a systematic review and meta-analysis. *Journal of the American College of Cardiology, 57*(10), 1237-1247.

Hyafil, F., Gimelli, A., Slart, R.H.J.A., Georgoulias, P., Rischpler, C., Lubberink, M., Sciagra, R., Bucerius, J., Agostini, D., & Verberne H. J. (2019). EANM procedural guidelines for myocardial perfusion scintigraphy using cardiac-centered gamma cameras. *European J Hybrid Imaging, 3*, 11 (2019).

Jaarsma, C., Leiner, T., Bekkers, S. C., Crijns, H. J., Wildberger, J. E., Nagel, E., Nelemans, P. J., & Schalla, S. (2012). Diagnostic performance of noninvasive myocardial perfusion imaging using single-photon emission computed tomography, cardiac magnetic resonance, and positron emission tomography imaging for the detection of obstructive coronary artery disease: a meta-analysis. *Journal of the American College of Cardiology, 59*(19), 1719-1728.

Jadhav, S., Ferrell, W., Greer, I. A., Petrie, J. R., Cobbe, S. M., & Sattar, N. (2006). Effects of metformin on microvascular function and exercise tolerance in women with angina and normal coronary

arteries: a randomized, double-blind, placebo-controlled study. *Journal of the American College of Cardiology, 48*(5), 956-963.

Jahnke, C., Nagel, E., Gebker, R., Kokocinski, T., Kelle, S., Manka, R., Fleck, E., & Paetsch, I. (2007). Prognostic value of cardiac magnetic resonance stress tests: adenosine stress perfusion and dobutamine stress wall motion imaging. *Circulation, 115*(13), 1769-1776.

Jensen, J. M., Bøtker, H. E., Mathiassen, O. N., Grove, E. L., Øvrehus, K. A., Pedersen, K. B., Terkelsen, C. J., Christiansen, E. H., Maeng, M., Leipsic, J., Kaltoft, A., Jakobsen, L., Sørensen, J. T., Thim, T., Kristensen, S. D., Krusell, L. R., & Nørgaard, B. L. (2018). Computed tomography derived fractional flow reserve testing in stable patients with typical angina pectoris: influence on downstream rate of invasive coronary angiography. *European Heart Journal – Cardiovascular Imaging, 19*(4), 405-414.

Jespersen, L., Hvelplund, A., Abildstrøm, S. Z., Pedersen, F., Galatius, S., Madsen, J. K., Jørgensen, E., Kelbæk, H., & Prescott, E. (2012). Stable angina pectoris with no obstructive coronary artery disease is associated with increased risks of major adverse cardiovascular events. *European Heart Journal, 33*(6), 734-744.

Johnson, N. P., & Gould, K. L. (2015). Regadenoson versus dipyridamole hyperemia for cardiac PET imaging. JACC. *Cardiovascular imaging, 8*(4), 438–447.

Juarez-Orozco, L. E., Martinez-Manzanera, O., van der Zant, F. M., Knol, R. J. J. & Knuuti, J. (2020). Deep Learning in Quantitative PET Myocardial Perfusion Imaging: A Study on Cardiovascular Event Prediction. *Journal of the American College of Cardiology: Cardiovascular Imaging, 13*(1 Pt 1), 180-182.

Kajander, S., Joutsiniemi, E., Saraste, M., Pietilä, M., Ukkonen, H., Saraste, A., Sipilä, H. T., Teräs, M., Mäki, M., Airaksinen, J., Hartiala, J., & Knuuti, J. (2010). Cardiac positron emission tomography/computed tomography imaging accurately detects anatomically and functionally significant coronary artery disease. *Circulation, 122*(6), 603-613.

Kajander, S., Ukkonen, H., Sipilä, H., Teräs, M., & Knuuti, J. (2009). Low radiation dose imaging of myocardial perfusion and coronary angiography with a hybrid PET/CT scanner. *Clinical Physiology and Functional Imaging, 29*(1), 81-88.

Kajander, S. A., Joutsiniemi, E., Saraste, M., Pietilä, M., Ukkonen, H., Saraste, A., Sipilä, H. T., Teräs, M., Mäki, M., Airaksinen, J., Hartiala, J., & Knuuti, J. (2011). Clinical value of absolute quantification of myocardial perfusion with (15)O-water in coronary artery disease. *Circulation: Cardiovascular imaging, 4*(6), 678-684.

Kaski, J. C., Crea, F., Gersh, B. J., & Camici, P. G. (2018). Reappraisal of Ischemic Heart Disease. *Circulation, 138*(14), 1463-1480.

Kaufmann, P. A., & Buechel, R. R. (2016). Cardiac SPECT/CCTA hybrid imaging: One answer to two questions? *Herz, 41*(5), 391-397.

Kaufmann, P. A., Gnecchi-Ruscone, T., Schäfers, K. P., Lüscher, T. F., & Camici, P. G. (2000). Low density lipoprotein cholesterol and coronary microvascular dysfunction in hypercholesterolemia. *Journal of the American College of Cardiology, 36*(1), 103–109.

Kini, S., Bis, K. G., & Weaver, L. (2007). Normal and variant coronary arterial and venous anatomy on high-resolution CT angiography. *American Journal of Roentgenology, 188*(6), 1665-1674.

Kishi, S., Giannopoulos, A. A., Tang, A., Kato, N., Chatzizisis, Y. S., Dennie, C., Horiuchi, Y., Tanabe, K., Lima, J. A. C., Rybicki, F. J., & Mitsouras, D. (2018). Fractional Flow Reserve Estimated at Coronary CT Angiography in Intermediate Lesions: Comparison of Diagnostic Accuracy of Different Methods to Determine Coronary Flow Distribution. *Radiology, 287*(1), 76-84.

Knuuti, J., Ballo, H., Juarez-Orozco, L. E., Saraste, A., Kolh, P., Rutjes, A. W. S., Jüni, P., Windecker, S., Bax, J. J., & Wijns, W. (2018). The performance of non-invasive tests to rule-in and rule-out significant coronary artery stenosis in patients with stable angina: a meta-analysis focused on post-test disease probability. *European Heart Journal, 39*(35), 3322-3330.

Knuuti, J., Bengel, F., Bax, J. J., Kaufmann, P. A., Le Guludec, D., Perrone Filardi, P., Marcassa, C., Ajmone Marsan, N., Achenbach, S., Kitsiou, A., Flotats, A., Eeckhout, E., Minn, H., & Hesse, B.

(2014). Risks and benefits of cardiac imaging: an analysis of risks related to imaging for coronary artery disease. *European Heart Journal, 35*(10), 633-638.

Knuuti, J., Kajander, S., Mäki, M., & Ukkonen, H. (2009). Quantification of myocardial blood flow will reform the detection of CAD. *Journal of Nuclear Cardiology, 16*(4), 497-506.

Knuuti, J., Wijns, W., Saraste, A., Capodanno, D., Barbato, E., Funck-Brentano, C., Prescott, E., Storey, R. F., Deaton, C., Cuisset, T., Agewall, S., Dickstein, K., Edvardsen, T., Escaned, J., Gersh, B. J., Svitil, P., Gilard, M., Hasdai, D., Hatala, R., Mahfoud, F., Masip, J., Muneretto, C., Valgimigli, M., Achenbach, S., Bax, J. J., & Group, E. S. D. (2020). 2019 ESC Guidelines for the diagnosis and management of chronic coronary syndromes. *European Heart Journal, 41*(3), 407-477.

Korosoglou, G., Marwan, M., Giusca, S., Schmermund, A., Schneider, S., Bruder, O., Hausleiter, J., Schroeder, S., Leber, A., Limbourg, T., Gitsioudis, G., Rixe, J., Zahn, R., Katus, H. A., Achenbach, S., & Senges, J. (2018). Influence of irregular heart rhythm on radiation exposure, image quality and diagnostic impact of cardiac computed tomography angiography in 4,339 patients. Data from the German Cardiac Computed Tomography Registry. *Journal of Cardiovascular Computed Tomography, 12*(1), 34-41.

Laine, H., Raitakari, O. T., Niinikoski, H., Pitkänen, O. P., Iida, H., Viikari, J., Nuutila, P., & Knuuti, J. (1998). Early impairment of coronary flow reserve in young men with borderline hypertension. *Journal of the American College of Cardiology, 32*(1), 147-153.

Lanza, G. A., Buffon, A., Sestito, A., Natale, L., Sgueglia, G. A., Galiuto, L., Infusino, F., Mariani, L., Centola, A., & Crea, F. (2008). Relation between stress-induced myocardial perfusion defects on cardiovascular magnetic resonance and coronary microvascular dysfunction in patients with cardiac syndrome X. *Journal of the American College of Cardiology, 51*(4), 466-472.

Lanza, G. A., Colonna, G., Pasceri, V., & Maseri, A. (1999). Atenolol versus amlodipine versus isosorbide-5-mononitrate on anginal symptoms in syndrome X. *The American Journal of Cardiology, 84*(7), 854-856.

Lauer, M. S., Blackstone, E. H., Young, J. B., & Topol, E. J. (1999). Cause of death in clinical research: time for a reassessment? *Journal of the American College of Cardiology, 34*(3), 618-620.

Le, T. T., Huang, W., Bryant, J. A., Cook, S. A., & Chin, C. W. (2017). Stress cardiovascular magnetic resonance imaging: current and future perspectives. *Expert Review of Cardiovascular Therapy, 15*(3), 181-189.

Lee, J. M., Kim, C. H., Koo, B. K., Hwang, D., Park, J., Zhang, J., Tong, Y., Jeon, K. H., Bang, J. I., Suh, M., Paeng, J. C., Cheon, G. J., Na, S. H., Ahn, J. M., Park, S. J., & Kim, H. S. (2016). Integrated Myocardial Perfusion Imaging Diagnostics Improve Detection of Functionally Significant Coronary Artery Stenosis by 13N-ammonia Positron Emission Tomography. *Circulation: Cardiovascular imaging, 9*(9), e004768.

Leipsic, J., Abbara, S., Achenbach, S., Cury, R., Earls, J. P., Mancini, G. J., Nieman, K., Pontone, G., & Raff, G. L. (2014). SCCT guidelines for the interpretation and reporting of coronary CT angiography: a report of the Society of Cardiovascular Computed Tomography Guidelines Committee. *Journal of Cardiovascular Computed Tomography, 8*(5), 342-358.

Libby, P., Aikawa, M., & Schönbeck, U. (2000). Cholesterol and atherosclerosis. *Biochimica et Biophysica Acta, 1529*(1-3), 299-309.

Libby, P., & Pasterkamp, G. (2015). Requiem for the 'vulnerable plaque'. *European Heart Journal, 36*(43), 2984-2987.

Libby, P., & Theroux, P. (2005). Pathophysiology of coronary artery disease. *Circulation, 111*(25), 3481-3488.

Liga, R., Vontobel, J., Rovai, D., Marinelli, M., Caselli, C., Pietila, M., Teresinska, A., Aguadé-Bruix, S., Pizzi, M. N., Todiere, G., Gimelli, A., Chiappino, D., Marraccini, P., Schroeder, S., Drosch, T., Poddighe, R., Casolo, G., Anagnostopoulos, C., Pugliese, F., . . . Gaemperli, O. (2016). Multicentre multi-device hybrid imaging study of coronary artery disease: results from the EValuation of INtegrated Cardiac Imaging for the Detection and Characterization of Ischaemic Heart Disease

(EVINCI) hybrid imaging population. *European Heart Journal – Cardiovascular Imaging, 17*(9), 951-960.

Lipinski, M. J., McVey, C. M., Berger, J. S., Kramer, C. M., & Salerno, M. (2013). Prognostic value of stress cardiac magnetic resonance imaging in patients with known or suspected coronary artery disease: a systematic review and meta-analysis. *Journal of the American College of Cardiology, 62*(9), 826-838.

Liu, A., Wijesurendra, R. S., Liu, J. M., Forfar, J. C., Channon, K. M., Jerosch-Herold, M., Piechnik, S. K., Neubauer, S., Kharbanda, R. K., & Ferreira, V. M. (2018). Diagnosis of Microvascular Angina Using Cardiac Magnetic Resonance. *Journal of the American College of Cardiology, 71*(9), 969-979.

Liu, K., Daviglus, M. L., Loria, C. M., Colangelo, L. A., Spring, B., Moller, A. C., & Lloyd-Jones, D. M. (2012). Healthy lifestyle through young adulthood and the presence of low cardiovascular disease risk profile in middle age: the Coronary Artery Risk Development in (Young) Adults (CARDIA) study. *Circulation, 125*(8), 996-1004.

Lorenzoni, V., Bellelli, S., Caselli, C., Knuuti, J., Underwood, S. R., Neglia, D., Turchetti, G., & Investigators, E. (2019). Cost-effectiveness analysis of stand-alone or combined non-invasive imaging tests for the diagnosis of stable coronary artery disease: results from the EVINCI study. *The European Journal of Health Economics, 20*(9), 1437-1449.

Maffessanti, F., Patel, A. R., Patel, M. B., Walter, J. J., Mediratta, A., Medvedofsky, D., Kachenoura, N., Lang, R. M., & Mor-Avi, V. (2017). Non-invasive assessment of the haemodynamic significance of coronary stenosis using fusion of cardiac computed tomography and 3D echocardiography. *European Heart Journal – Cardiovascular Imaging, 18*(6), 670-680.

Majmudar, M. D., Murthy, V. L., Shah, R. V., Kolli, S., Mousavi, N., Foster, C. R., Hainer, J., Blankstein, R., Dorbala, S., Sitek, A., Stevenson, L. W., Mehra, M. R., & Di Carli, M. F. (2015). Quantification of coronary flow reserve in patients with ischaemic and non-ischaemic cardiomyopathy and its association with clinical outcomes. *European Heart Journal – Cardiovascular Imaging, 16*(8), 900-909.

Maron, D. J., Hochman, J. S., Reynolds, H. R., Bangalore, S., O'Brien, S. M., Boden, W. E., Chaitman, B. R., Senior, R., López-Sendón, J., Alexander, K. P., Lopes, R. D., Shaw, L. J., Berger, J. S., Newman, J. D., Sidhu, M. S., Goodman, S. G., Ruzyllo, W., Gosselin, G., Maggioni, A. P., Rosenberg, Y. (2020). Initial Invasive or Conservative Strategy for Stable Coronary Disease. *New England Journal of Medicine, 382*(15), 1395-1407.

Marwan, M., Pflederer, T., Schepis, T., Lang, A., Muschiol, G., Ropers, D., Daniel, W. G., Achenbach, S. (2010). Accuracy of dual-source computed tomography to identify significant coronary artery disease in patients with atrial fibrillation: comparison with coronary angiography. *European Heart Journal, 31*(18), 2230-2237.

Marwick, T. H., Case, C., Sawada, S., Rimmerman, C., Brenneman, P., Kovacs, R., Short, L., & Lauer, M. (2001). Prediction of mortality using dobutamine echocardiography. *Journal of the American College of Cardiology, 37*(3), 754-760.

Mason, P. J., Shah, B., Tamis-Holland, J. E., Bittl, J. A., Cohen, M. G., Safirstein, J., Drachman, D. E., Valle, J. A., Rhodes, D., Gilchrist, I. C. (2018). An Update on Radial Artery Access and Best Practices for Transradial Coronary Angiography and Intervention in Acute Coronary Syndrome: A Scientific Statement From the American Heart Association. *Circulation: Cardiovascular Interventions, 11*(9), e000035.

Mathew, R. C., Bourque, J. M., Salerno, M., & Kramer, C. M. (2019). Cardiovascular Imaging Techniques to Assess Microvascular Dysfunction. *Journal of the American College of Cardiology: Cardiovascular Imaging, 13*(7):1577-1590.

Maurovich-Horvat, P., Ferencik, M., Voros, S., Merkely, B., & Hoffmann, U. (2014). Comprehensive plaque assessment by coronary CT angiography. *Nature Reviews Cardiology, 11*(7), 390-402.

Mc Ardle, B. A., Dowsley, T. F., deKemp, R. A., Wells, G. A., & Beanlands, R. S. (2012). Does rubidium-82 PET have superior accuracy to SPECT perfusion imaging for the diagnosis of

obstructive coronary disease? A systematic review and meta-analysis. *Journal of the American College of Cardiology, 60*(18), 1828-1837.

Meijboom, W. B., Meijs, M. F., Schuijf, J. D., Cramer, M. J., Mollet, N. R., van Mieghem, C. A., Nieman, K., van Werkhoven, J. M., Pundziute, G., Weustink, A. C., de Vos, A. M., Pugliese, F., Rensing, B., Jukema, J. W., Bax, J. J., Prokop, M., Doevendans, P. A., Hunink, M. G., Krestin, G. P., & de Feyter, P. J. (2008). Diagnostic accuracy of 64-slice computed tomography coronary angiography: a prospective, multicenter, multivendor study. *Journal of the American College of Cardiology, 52*(25), 2135-2144.

Meijboom, W. B., Van Mieghem, C. A., van Pelt, N., Weustink, A., Pugliese, F., Mollet, N. R., Boersma, E., Regar, E., van Geuns, R. J., de Jaegere, P. J., Serruys, P. W., Krestin, G. P., & de Feyter, P. J. (2008). Comprehensive assessment of coronary artery stenoses: computed tomography coronary angiography versus conventional coronary angiography and correlation with fractional flow reserve in patients with stable angina. *Journal of the American College of Cardiology, 52*(8), 636-643.

Metz, L. D., Beattie, M., Hom, R., Redberg, R. F., Grady, D., & Fleischmann, K. E. (2007). The prognostic value of normal exercise myocardial perfusion imaging and exercise echocardiography: a meta-analysis. *Journal of the American College of Cardiology, 49*(2), 227-237.

Meyer, T. S., Martinoff, S., Hadamitzky, M., Will, A., Kastrati, A., Schömig, A., & Hausleiter, J. (2007). Improved noninvasive assessment of coronary artery bypass grafts with 64-slice computed tomographic angiography in an unselected patient population. *Journal of the American College of Cardiology, 49*(9), 946-950.

Min, J. K., Dunning, A., Lin, F. Y., Achenbach, S., Al-Mallah, M., Budoff, M. J., Cademartiri, F., Callister, T. Q., Chang, H. J., Cheng, V., Chinnaiyan, K., Chow, B. J., Delago, A., Hadamitzky, M., Hausleiter, J., Kaufmann, P., Maffei, E., Raff, G., Shaw, L. J., . . . Berman, D. S. (2011). Age- and sex-related differences in all-cause mortality risk based on coronary computed tomography angiography findings results from the International Multicenter CONFIRM (Coronary CT Angiography Evaluation for Clinical Outcomes: An International Multicenter Registry) of 23,854 patients without known coronary artery disease. *Journal of the American College of Cardiology, 58*(8), 849-860.

Min, J. K., Shaw, L. J., Devereux, R. B., Okin, P. M., Weinsaft, J. W., Russo, D. J., Lippolis, N. J., Berman, D. S., & Callister, T. Q. (2007). Prognostic value of multidetector coronary computed tomographic angiography for prediction of all-cause mortality. *Journal of the American College of Cardiology, 50*(12), 1161-1170.

Motoyama, S., Sarai, M., Harigaya, H., Anno, H., Inoue, K., Hara, T., Naruse, H., Ishii, J., Hishida, H., Wong, N. D., Virmani, R., Kondo, T., Ozaki, Y., & Narula, J. (2009). Computed tomographic angiography characteristics of atherosclerotic plaques subsequently resulting in acute coronary syndrome. *Journal of the American College of Cardiology, 54*(1), 49-57.

Murthy, V. L., Lee, B. C., Sitek, A., Naya, M., Moody, J., Polavarapu, V., Ficaro, E. P., & Di Carli, M. F. (2014). Comparison and prognostic validation of multiple methods of quantification of myocardial blood flow with 82Rb PET. *Journal of Nuclear Medicine, 55*(12), 1952-1958.

Murthy, V. L., Naya, M., Foster, C. R., Gaber, M., Hainer, J., Klein, J., Dorbala, S., Blankstein, R., & Di Carli, M. F. (2012). Association between coronary vascular dysfunction and cardiac mortality in patients with and without diabetes mellitus. *Circulation, 126*(15), 1858-1868.

Murthy, V. L., Naya, M., Foster, C. R., Hainer, J., Gaber, M., Di Carli, G., Blankstein, R., Dorbala, S., Sitek, A., Pencina, M. J., & Di Carli, M. F. (2011). Improved cardiac risk assessment with noninvasive measures of coronary flow reserve. *Circulation, 124*(20), 2215-2224.

Murthy, V. L., Naya, M., Taqueti, V. R., Foster, C. R., Gaber, M., Hainer, J., Dorbala, S., Blankstein, R., Rimoldi, O., Camici, P. G., & Di Carli, M. F. (2014). Effects of sex on coronary microvascular dysfunction and cardiac outcomes. *Circulation, 129*(24), 2518-2527.

Muzik, O., Duvernoy, C., Beanlands, R. S., Sawada, S., Dayanikli, F., Wolfe, E. R., & Schwaiger, M. (1998). Assessment of diagnostic performance of quantitative flow measurements in normal

subjects and patients with angiographically documented coronary artery disease by means of nitrogen-13 ammonia and positron emission tomography. *Journal of the American College of Cardiology, 31*(3), 534-540.

Mygind, N. D., Michelsen, M. M., Pena, A., Frestad, D., Dose, N., Aziz, A., Faber, R., Høst, N., Gustafsson, I., Hansen, P. R., Hansen, H. S., Bairey Merz, C. N., Kastrup, J., & Prescott, E. (2016). Coronary Microvascular Function and Cardiovascular Risk Factors in Women With Angina Pectoris and No Obstructive Coronary Artery Disease: The iPOWER Study. *Journal of the American Heart Association, 5*(3), e003064.

Nakamura, S., Kitagawa, K., Goto, Y., Omori, T., Kurita, T., Yamada, A., Takafuji, M., Uno, M., Dohi, K., & Sakuma, H. (2019). Incremental Prognostic Value of Myocardial Blood Flow Quantified With Stress Dynamic Computed Tomography Perfusion Imaging. *Journal of the American College of Cardiology: Cardiovascular Imaging, 12*(7 Pt 2), 1379-1387.

Nakashima, Y., Chen, Y. X., Kinukawa, N., & Sueishi, K. (2002). Distributions of diffuse intimal thickening in human arteries: preferential expression in atherosclerosis-prone arteries from an early age. *Virchows Archive, 441*(3), 279-288.

Nakashima, Y., Fujii, H., Sumiyoshi, S., Wight, T. N., & Sueishi, K. (2007). Early human atherosclerosis: accumulation of lipid and proteoglycans in intimal thickenings followed by macrophage infiltration. Ar*teriosclerosis, Thrombosis, and Vascular Biology, 27*(5), 1159-1165.

Nakazato, R., Arsanjani, R., Achenbach, S., Gransar, H., Cheng, V. Y., Dunning, A., Lin, F. Y., Al-Mallah, M., Budoff, M. J., Callister, T. Q., Chang, H. J., Cademartiri, F., Chinnaiyan, K., Chow, B. J., Delago, A., Hadamitzky, M., Hausleiter, J., Kaufmann, P., Raff, G., . . . Min, J. K. (2014). Age-related risk of major adverse cardiac event risk and coronary artery disease extent and severity by coronary CT angiography: results from 15 187 patients from the International Multisite CONFIRM Study. *European Heart Journal – Cardiovascular Imaging, 15*(5), 586-594.

Namdar, M., Hany, T. F., Koepfli, P., Siegrist, P. T., Burger, C., Wyss, C. A., Luscher, T. F., von Schulthess, G. K., & Kaufmann, P. A. (2005). Integrated PET/CT for the assessment of coronary artery disease: a feasibility study. *Journal of Nuclear Medicine, 46*(6), 930-935.

Nahser, P. J. Jr, Brown, R. E., Oskarsson, H., Winniford, M. D., Rossen, J. D. (1995). Maximal coronary flow reserve and metabolic coronary vasodilation in patients with diabetes mellitus. *Circulation, 91*(3), 635-640.

Neglia, D., Michelassi, C., Trivieri, M. G., Sambuceti, G., Giorgetti, A., Pratali, L., Gallopin, M., Salvadori, P., Sorace, O., Carpeggiani, C., Poddighe, R., L'Abbate, A., & Parodi, O. (2002). Prognostic role of myocardial blood flow impairment in idiopathic left ventricular dysfunction. *Circulation, 105*(2), 186-193.

Nesterov, S. V., Han, C., Mäki, M., Kajander, S., Naum, A. G., Helenius, H., Lisinen, I., Ukkonen, H., Pietilä, M., Joutsiniemi, E., & Knuuti, J. (2009). Myocardial perfusion quantitation with 15O-labelled water PET: high reproducibility of the new cardiac analysis software (Carimas). *European Journal of Nuclear Medicine and Molecular Imaging, 36*(10), 1594-1602.

Neumann, F. J., Sousa-Uva, M., Ahlsson, A., Alfonso, F., Banning, A. P., Benedetto, U., Byrne, R. A., Collet, J. P., Falk, V., Head, S. J., Jüni, P., Kastrati, A., Koller, A., Kristensen, S. D., Niebauer, J., Richter, D. J., Seferovic, P. M., Sibbing, D., Stefanini, G., . . . Zembala, M. O. (2019). 2018 ESC/EACTS Guidelines on myocardial revascularization. *European Heart Journal, 40*(2), 87-165.

Newby, D. E., Adamson, P. D., Berry, C., Boon, N. A., Dweck, M. R., Flather, M., Forbes, J., Hunter, A., Lewis, S., MacLean, S., Mills, N. L., Norrie, J., Roditi, G., Shah, A. S. V., Timmis, A. D., van Beek, E. J. R., Williams, M. C. (2018). Coronary CT Angiography and 5-Year Risk of Myocardial Infarction. *New England Journal of Medicine, 379*(10), 924-933.

Nielsen, L. H., Ortner, N., Nørgaard, B. L., Achenbach, S., Leipsic, J., & Abdulla, J. (2014). The diagnostic accuracy and outcomes after coronary computed tomography angiography vs. conventional functional testing in patients with stable angina pectoris: a systematic review and meta-analysis. *European Heart Journal – Cardiovascular Imaging, 15*(9), 961-971.

Nissen, L., Winther, S., Westra, J., Ejlersen, J. A., Isaksen, C., Rossi, A., Holm, N. R., Urbonaviciene, G., Gormsen, L. C., Madsen, L. H., Christiansen, E. H., Maeng, M., Knudsen, L. L., Frost, L., Brix, L., Bøtker, H. E., Petersen, S. E., & Bøttcher, M. (2018). Diagnosing coronary artery disease after a positive coronary computed tomography angiography: the Dan-NICAD open label, parallel, head to head, randomized controlled diagnostic accuracy trial of cardiovascular magnetic resonance and myocardial perfusion scintigraphy. *European Heart Journal – Cardiovascular Imaging, 19*(4), 369-377.

Nitenberg, A., Valensi, P., Sachs, R., Dali, M., Aptecar, E., Attali, J. R. (1993). Impairment of coronary vascular reserve and ACh-induced coronary vasodilation in diabetic patients with angiographically normal coronary arteries and normal left ventricular systolic function. *Diabetes, 42*(7), 1017-1025.

Nordström, J., Kero, T., Harms, H. J., Widström, C., Flachskampf, F. A., Sörensen, J., & Lubberink, M. (2017). Calculation of left ventricular volumes and ejection fraction from dynamic cardiac-gated 15 O-water PET/CT: 5D-PET. *EJNMMI Physics, 4*(1), 26.

Nørgaard, B. L., Leipsic, J., Gaur, S., Seneviratne, S., Ko, B. S., Ito, H., Jensen, J. M., Mauri, L., De Bruyne, B., Bezerra, H., Osawa, K., Marwan, M., Naber, C., Erglis, A., Park, S. J., Christiansen, E. H., Kaltoft, A., Lassen, J. F., Bøtker, H. E., & Achenbach, S. (2014). Diagnostic performance of noninvasive fractional flow reserve derived from coronary computed tomography angiography in suspected coronary artery disease: the NXT trial (Analysis of Coronary Blood Flow Using CT Angiography: Next Steps). *Journal of the American College of Cardiology, 63*(12), 1145-1155.

Nørgaard, B. L., Terkelsen, C. J., Mathiassen, O. N., Grove, E. L., Bøtker, H. E., Parner, E., Leipsic, J., Steffensen, F. H., Riis, A. H., Pedersen, K., Christiansen, E. H., Mæng, M., Krusell, L. R., Kristensen, S. D., Eftekhari, A., Jakobsen, L., & Jensen, J. M. (2018). Coronary CT Angiographic and Flow Reserve-Guided Management of Patients With Stable Ischemic Heart Disease. *Journal of the American College of Cardiology, 72*(18), 2123-2134.

Ong, P., Athanasiadis, A., Borgulya, G., Mahrholdt, H., Kaski, J. C., & Sechtem, U. (2012). High prevalence of a pathological response to acetylcholine testing in patients with stable angina pectoris and unobstructed coronary arteries. The ACOVA Study (Abnormal COronary VAsomotion in patients with stable angina and unobstructed coronary arteries). *Journal of the American College of Cardiology, 59*(7), 655-662.

Ong, P., Athanasiadis, A., & Sechtem, U. (2015). Pharmacotherapy for coronary microvascular dysfunction. *European Heart Journal – Cardiovascular Pharmacotherapy, 1*(1), 65-71.

Ong, P., Camici, P. G., Beltrame, J. F., Crea, F., Shimokawa, H., Sechtem, U., Kaski, J. C., & Bairey Merz, C. N. (2018). International standardization of diagnostic criteria for microvascular angina. *International Journal of Cardiology, 250*, 16-20.

Ostrom, M. P., Gopal, A., Ahmadi, N., Nasir, K., Yang, E., Kakadiaris, I., Flores, F., Mao, S. S., & Budoff, M. J. (2008). Mortality incidence and the severity of coronary atherosclerosis assessed by computed tomography angiography. *Journal of the American College of Cardiology, 52*(16), 1335-1343.

Otsuka, F., Kramer, M. C., Woudstra, P., Yahagi, K., Ladich, E., Finn, A. V., de Winter, R. J., Kolodgie, F. D., Wight, T. N., Davis, H. R., Joner, M., & Virmani, R. (2015). Natural progression of atherosclerosis from pathologic intimal thickening to late fibroatheroma in human coronary arteries: A pathology study. *Atherosclerosis, 241*(2), 772-782.

Otsuka, K., Fukuda, S., Tanaka, A., Nakanishi, K., Taguchi, H., Yoshiyama, M., Shimada, K., & Yoshikawa, J. (2014). Prognosis of vulnerable plaque on computed tomographic coronary angiography with normal myocardial perfusion image. *European Heart Journal – Cardiovascular Imaging, 15*(3), 332-340.

Patel, M. R., Peterson, E. D., Dai, D., Brennan, J. M., Redberg, R. F., Anderson, H. V., Brindis, R. G., & Douglas, P. S. (2010). Low diagnostic yield of elective coronary angiography. *New England Journal of Medicine, 362*(10), 886-895.

Pauly, D. F., Johnson, B. D., Anderson, R. D., Handberg, E. M., Smith, K. M., Cooper-DeHoff, R. M., Sopko, G., Sharaf, B. M., Kelsey, S. F., Merz, C. N., & Pepine, C. J. (2011). In women with

symptoms of cardiac ischemia, nonobstructive coronary arteries, and microvascular dysfunction, angiotensin-converting enzyme inhibition is associated with improved microvascular function: A double-blind randomized study from the National Heart, Lung and Blood Institute Women's Ischemia Syndrome Evaluation (WISE). *American Heart Journal, 162*(4), 678-684.

Pazhenkottil, A. P., Benz, D. C., Gräni, C., Madsen, M. A., Mikulicic, F., von Felten, E., Fuchs, T. A., Moch, B. H., Stehli, J., Lüscher, T. F., Gaemperli, O., Buechel, R. R., & Kaufmann, P. A. (2018). Hybrid SPECT Perfusion Imaging and Coronary CT Angiography: Long-term Prognostic Value for Cardiovascular Outcomes. *Radiology, 288*(3), 694-702.

Pazhenkottil, A. P., Nkoulou, R. N., Ghadri, J. R., Herzog, B. A., Buechel, R. R., Küest, S. M., Wolfrum, M., Fiechter, M., Husmann, L., Gaemperli, O., & Kaufmann, P. A. (2011). Prognostic value of cardiac hybrid imaging integrating single-photon emission computed tomography with coronary computed tomography angiography. *European Heart Journal, 32*(12), 1465-1471.

Pazhenkottil, A. P., Nkoulou, R. N., Ghadri, J. R., Herzog, B. A., Küest, S. M., Husmann, L., Wolfrum, M., Goetti, R., Buechel, R. R., Gaemperli, O., Lüscher, T. F., & Kaufmann, P. A. (2011). Impact of cardiac hybrid single-photon emission computed tomography/computed tomography imaging on choice of treatment strategy in coronary artery disease. *European Heart Journal, 32*(22), 2824-2829.

Pepine, C. J., Anderson, R. D., Sharaf, B. L., Reis, S. E., Smith, K. M., Handberg, E. M., Johnson, B. D., Sopko, G., & Bairey Merz, C. N. (2010). Coronary microvascular reactivity to adenosine predicts adverse outcome in women evaluated for suspected ischemia results from the National Heart, Lung and Blood Institute WISE (Women's Ischemia Syndrome Evaluation) study. *Journal of the American College of Cardiology, 55*(25), 2825-2832.

Piccinelli, M. (2020). Multimodality image fusion, moving forward. *Journal of Nuclear Cardiology, 27*(3), 973-975.

Pijls, N. H., van Schaardenburgh, P., Manoharan, G., Boersma, E., Bech, J. W., van't Veer, M., Bär, F., Hoorntje, J., Koolen, J., Wijns, W., & de Bruyne, B. (2007). Percutaneous coronary intervention of functionally nonsignificant stenosis: 5-year follow-up of the DEFER Study. *Journal of the American College of Cardiology, 49*(21), 2105-2111.

Pitkänen, O. P., Raitakari, O. T., Niinikoski, H., Nuutila, P., Iida, H., Voipio-Pulkki, L. M., Härkönen, R., Wegelius, U., Rönnemaa, T., Viikari, J., & Knuuti, J. (1996). Coronary flow reserve is impaired in young men with familial hypercholesterolemia. *Journal of the American College of Cardiology, 28*(7), 1705-1711.

Pizzi, C., Manfrini, O., Fontana, F., & Bugiardini, R. (2004). Angiotensin-converting enzyme inhibitors and 3-hydroxy-3-methylglutaryl coenzyme A reductase in cardiac Syndrome X: role of superoxide dismutase activity. *Circulation, 109*(1), 53-58.

Plana, J. C., Mikati, I. A., Dokainish, H., Lakkis, N., Abukhalil, J., Davis, R., Hetzell, B. C., & Zoghbi, W. A. (2008). A randomized cross-over study for evaluation of the effect of image optimization with contrast on the diagnostic accuracy of dobutamine echocardiography in coronary artery disease The OPTIMIZE Trial. *Journal of the American College of Cardiology: Cardiovascular Imaging, 1*(2), 145-152.

Pries, A. R., & Reglin, B. (2017). Coronary microcirculatory pathophysiology: can we afford it to remain a black box? *European Heart Journal, 38*(7), 478-488.

Pries, A. R., Reglin, B., & Secomb, T. W. (2005). Remodeling of blood vessels: responses of diameter and wall thickness to hemodynamic and metabolic stimuli. *Hypertension, 46*(4), 725-731.

Rajappan, K., Rimoldi, O. E., Camici, P. G., Bellenger, N. G., Pennell, D. J., & Sheridan, D. J. (2003). Functional changes in coronary microcirculation after valve replacement in patients with aortic stenosis. *Circulation, 107*(25), 3170-3175.

Reeh, J., Therming, C. B., Heitmann, M., Højberg, S., Sørum, C., Bech, J., Husum, D., Dominguez, H., Sehestedt, T., Hermann, T., Hansen, K. W., Simonsen, L., Galatius, S., & Prescott, E. (2019). Prediction of obstructive coronary artery disease and prognosis in patients with suspected stable angina. *European Heart Journal, 40*(18), 1426-1435.

Rispler, S., Keidar, Z., Ghersin, E., Roguin, A., Soil, A., Dragu, R., Litmanovich, D., Frenkel, A., Aronson, D., Engel, A., Beyar, R., & Israel, O. (2007). Integrated single-photon emission computed tomography and computed tomography coronary angiography for the assessment of hemodynamically significant coronary artery lesions. *Journal of the American College of Cardiology, 49*(10), 1059-1067.

Rizvi, A., Han, D., Danad, I., Ó Hartaigh, B., Lee, J. H., Gransar, H., Stuijfzand, W. J., Roudsari, H. M., Park, M. W., Szymonifka, J., Chang, H. J., Jones, E. C., Knaapen, P., Lin, F. Y., Min, J. K., & Peña, J. M. (2018). Diagnostic Performance of Hybrid Cardiac Imaging Methods for Assessment of Obstructive Coronary Artery Disease Compared With Stand-Alone Coronary Computed Tomography Angiography: A Meta-Analysis. *Journal of the American College of Cardiology: Cardiovascular Imaging, 11*(4), 589-599.

Rochitte, C. E., George, R. T., Chen, M. Y., Arbab-Zadeh, A., Dewey, M., Miller, J. M., Niinuma, H., Yoshioka, K., Kitagawa, K., Nakamori, S., Laham, R., Vavere, A. L., Cerci, R. J., Mehra, V. C., Nomura, C., Kofoed, K. F., Jinzaki, M., Kuribayashi, S., de Roos, A., Laule, M., Tan, S. Y., Hoe, J., Paul, N., Rybicki, F. J., Brinker, J. A., Arai, A. E., Cox, C., . . . Lima, J. A. (2014). Computed tomography angiography and perfusion to assess coronary artery stenosis causing perfusion defects by single photon emission computed tomography: the CORE320 study. *European Heart Journal, 35*(17), 1120-1130.

Roffi, M., Patrono, C., Collet, J. P., Mueller, C., Valgimigli, M., Andreotti, F., Bax, J. J., Borger, M. A., Brotons, C., Chew, D. P., Gencer, B., Hasenfuss, G., Kjeldsen, K., Lancellotti, P., Landmesser, U., Mehilli, J., Mukherjee, D., Storey, R. F., & Windecker, S. (2016). 2015 ESC Guidelines for the management of acute coronary syndromes in patients presenting without persistent ST-segment elevation: Task Force for the Management of Acute Coronary Syndromes in Patients Presenting without Persistent ST-Segment Elevation of the European Society of Cardiology (ESC). *European Heart Journal, 37*(3), 267-315.

Rossi, A., Dharampal, A., de Feyter, P. J. (2014). Coronary CT angiography for patients with suspected coronary artery disease. *Heart (British Cardiac Society), 100*(12), 976-984.

Russo, G., Di Franco, A., Lamendola, P., Tarzia, P., Nerla, R., Stazi, A., Villano, A., Sestito, A., Lanza, G. A., Crea, F. (2013). Lack of effect of nitrates on exercise stress test results in patients with microvascular angina. *Cardiovascular Drugs and Therapy, 27*(3), 229-334.

Sand, N. P. R., Veien, K. T., Nielsen, S. S., Nørgaard, B. L., Larsen, P., Johansen, A., Hess, S., Deibjerg, L., Husain, M., Junker, A., Thomsen, K. K., Rohold, A., & Jensen, L. O. (2018). Prospective Comparison of FFR Derived From Coronary CT Angiography With SPECT Perfusion Imaging in Stable Coronary Artery Disease: The ReASSESS Study. *Journal of the American College of Cardiology: Cardiovascular Imaging, 11*(11), 1640-1650.

Sara, J. D., Widmer, R. J., Matsuzawa, Y., Lennon, R. J., Lerman, L. O., & Lerman, A. (2015). Prevalence of Coronary Microvascular Dysfunction Among Patients With Chest Pain and Nonobstructive Coronary Artery Disease. *Journal of the American College of Cardiology: Cardiovascular Interventions, 8*(11), 1445-1453.

Saraste, A., Kajander, S., Han, C., Nesterov, S. V., & Knuuti, J. (2012). PET: Is myocardial flow quantification a clinical reality? *Journal of Nuclear Cardiology, 19*(5), 1044-1059.

Saraste, M., Koskenvuo, J., Knuuti, J., Toikka, J., Laine, H., Niemi, P., Sakuma, H., & Hartiala, J. (2001). Coronary flow reserve: measurement with transthoracic Doppler echocardiography is reproducible and comparable with positron emission tomography. *Clinical Physiology, 21*(1), 114-122.

Sato, A., Nozato, T., Hikita, H., Miyazaki, S., Takahashi, Y., Kuwahara, T., Takahashi, A., Hiroe, M., & Aonuma, K. (2010). Incremental value of combining 64-slice computed tomography angiography with stress nuclear myocardial perfusion imaging to improve noninvasive detection of coronary artery disease. *Journal of Nuclear Cardiology, 17*(1), 19-26.

Schaap, J., de Groot, J. A., Nieman, K., Meijboom, W. B., Boekholdt, S. M., Kauling, R. M., Post, M. C., Van der Heyden, J. A., de Kroon, T. L., Rensing, B. J., Moons, K. G., & Verzijlbergen, J. F.

(2014). Added value of hybrid myocardial perfusion SPECT and CT coronary angiography in the diagnosis of coronary artery disease. *European Heart Journal – Cardiovascular Imaging, 15*(11), 1281-1288.

Schaap, J., de Groot, J. A., Nieman, K., Meijboom, W. B., Boekholdt, S. M., Post, M. C., Van der Heyden, J. A., de Kroon, T. L., Rensing, B. J., Moons, K. G., & Verzijlbergen, J. F. (2013). Hybrid myocardial perfusion SPECT/CT coronary angiography and invasive coronary angiography in patients with stable angina pectoris lead to similar treatment decisions. *Heart, 99*(3), 188-194.

Scheffel, H., Stolzmann, P., Alkadhi, H., Azemaj, N., Plass, A., Baumueller, S., Desbiolles, L., Leschka, S., Kozerke, S., Falk, V., Boesiger, P., Wyss, C., Marincek, B., & Donati, O. F. (2010). Low-dose CT and cardiac MR for the diagnosis of coronary artery disease: accuracy of single and combined approaches. *The International Journal of Cardiovascular Imaging, 26*(5), 579-590.

Schelbert, H. R. (2010). Anatomy and physiology of coronary blood flow. *Journal of Nuclear Cardiology, 17*(4), 545-554.

Schenker, M. P., Dorbala, S., Hong, E. C., Rybicki, F. J., Hachamovitch, R., Kwong, R. Y., & Di Carli, M. F. (2008). Interrelation of coronary calcification, myocardial ischemia, and outcomes in patients with intermediate likelihood of coronary artery disease: a combined positron emission tomography/computed tomography study. *Circulation, 117*(13), 1693-1700.

Schlaifer, J. D., Wargovich, T. J., O'Neill, B., Mancini, G. B., Haber, H. E., Pitt, B., & Pepine, C. J. (1997). Effects of quinapril on coronary blood flow in coronary artery disease patients with endothelial dysfunction. TREND Investigators. Trial on Reversing Endothelial Dysfunction. *The American Journal of Cardiology, 80*(12), 1594-1597.

Schroeder, S., Achenbach, S., Bengel, F., Burgstahler, C., Cademartiri, F., de Feyter, P., George, R., Kaufmann, P., Kopp, A. F., Knuuti, J., Ropers, D., Schuijf, J., Tops, L. F. & Bax, J. J. (2008). Cardiac computed tomography: indications, applications, limitations, and training requirements: Report of a Writing Group deployed by the Working Group Nuclear Cardiology and Cardiac CT of the European Society of Cardiology and the European Council of Nuclear Cardiology. *European Heart Journal, 29*(4), 531-556.

SCOT-HEART investigators (2015). CT coronary angiography in patients with suspected angina due to coronary heart disease (SCOT-HEART): an open-label, parallel-group, multicentre trial. *Lancet, 385*(9985), 2383-2391.

Sechtem, U., Brown, D., Godo, S., Lanza, G. A., Shimokawa, H., & Sidik, N. (2020). Coronary microvascular dysfunction in stable ischaemic heart disease (non-obstructive coronary artery disease and obstructive coronary artery disease). *Cardiovascular Research, 116*(4), 771-786.

Senior, R., Becher, H., Monaghan, M., Agati, L., Zamorano, J., Vanoverschelde, J. L., Nihoyannopoulos, P., Edvardsen, T., Lancellotti, P. (2017). Clinical practice of contrast echocardiography: recommendation by the European Association of Cardiovascular Imaging (EACVI) 2017. *European Heart Journal – Cardiovascular Imaging, 18*(11), 1205-1205af.

Shah, S. J., Lam, C. S. P., Svedlund, S., Saraste, A., Hage, C., Tan, R. S., Beussink-Nelson, L., Ljung Faxén, U., Fermer, M. L., Broberg, M. A., Gan, L. M., & Lund, L. H. (2018). Prevalence and correlates of coronary microvascular dysfunction in heart failure with preserved ejection fraction: PROMIS-HFpEF. *European Heart Journal, 39*(37), 3439-3450.

Shaw, L. J., Berman, D. S., Picard, M. H., Friedrich, M. G., Kwong, R. Y., Stone, G. W., Senior, R., Min, J. K., Hachamovitch, R., Scherrer-Crosbie, M., Mieres, J. H., Marwick, T. H., Phillips, L. M., Chaudhry, F. A., Pellikka, P. A., Slomka, P., Arai, A. E., Iskandrian, A. E., Bateman, T. M., Heller, G. V., . . . Douglas, P. S. (2014). Comparative definitions for moderate-severe ischemia in stress nuclear, echocardiography, and magnetic resonance imaging. *Journal of the American College of Cardiology: Cardiovascular Imaging, 7*(6), 593-604.

Shaw, L. J., Bugiardini, R., & Merz, C. N. (2009). Women and ischemic heart disease: evolving knowledge. *Journal of the American College of Cardiology, 54*(17), 1561–1575.

Shaw, L. J., & Iskandrian, A. E. (2004). Prognostic value of gated myocardial perfusion SPECT. *Journal of Nuclear Cardiology, 11*(2), 171-185.

Shrestha, U., Sciammarella, M., Alhassen, F., Yeghiazarians, Y., Ellin, J., Verdin, E., Boyle, A., Seo, Y., Botvinick, E. H., & Gullberg, G. T. (2017). Measurement of absolute myocardial blood flow in humans using dynamic cardiac SPECT and ^{99m}Tc-tetrofosmin: Method and validation. *Journal of Nuclear Cardiology, 24*(1), 268-277.

Sianos, G., Morel, M. A., Kappetein, A. P., Morice, M. C., Colombo, A., Dawkins, K., van den Brand, M., Van Dyck, N., Russell, M. E., Mohr, F. W., & Serruys, P. W. (2005). The SYNTAX Score: an angiographic tool grading the complexity of coronary artery disease. *EuroIntervention, 1*(2), 219-227.

Sicari, R., Nihoyannopoulos, P., Evangelista, A., Kasprzak, J., Lancellotti, P., Poldermans, D., Voigt, J. U., & Zamorano, J. L. (2009). Stress Echocardiography Expert Consensus Statement--Executive Summary: European Association of Echocardiography (EAE) (a registered branch of the ESC). *European Heart Journal, 30*(3), 278-289.

Sicari, R., Pasanisi, E., Venneri, L., Landi, P., Cortigiani, L., & Picano, E. (2003). Stress echo results predict mortality: a large-scale multicenter prospective international study. *Journal of the American College of Cardiology Cardiology, 41*(4), 589-595.

Smulders, M. W., Jaarsma, C., Nelemans, P. J., Bekkers, S. C. A. M., Bucerius, J., Leiner, T., Crijns, H. J. G. M., Wildberger, J. E., & Schalla, S. (2017). Comparison of the prognostic value of negative non-invasive cardiac investigations in patients with suspected or known coronary artery disease-a meta-analysis. *European Heart Journal – Cardiovascular Imaging, 18*(9), 980-987.

Steel, K., Broderick, R., Gandla, V., Larose, E., Resnic, F., Jerosch-Herold, M., Brown, K. A., & Kwong, R. Y. (2009). Complementary prognostic values of stress myocardial perfusion and late gadolinium enhancement imaging by cardiac magnetic resonance in patients with known or suspected coronary artery disease. *Circulation, 120*(14), 1390-1400.

Stocker, T. J., Deseive, S., Leipsic, J., Hadamitzky, M., Chen, M. Y., Rubinshtein, R., Heckner, M., Bax, J. J., Fang, X. M., Grove, E. L., Lesser, J., Maurovich-Horvat, P., Otton, J., Shin, S., Pontone, G., Marques, H., Chow, B., Nomura, C. H., Tabbalat, R., & Hausleiter, J (2018). Reduction in radiation exposure in cardiovascular computed tomography imaging: results from the PROspective multicenter registry on radiaTion dose Estimates of cardiac CT angIOgraphy iN daily practice in 2017 (PROTECTION VI). *European Heart Journal, 39*(41), 3715-3723.

Suzuki, H., Takeyama, Y., Koba, S., Suwa, Y., & Katagiri, T. (1994). Small vessel pathology and coronary hemodynamics in patients with microvascular angina. *International Journal of Cardiology, 43*(2), 139-150.

Takx, R. A., Blomberg, B. A., El Aidi, H., Habets, J., de Jong, P. A., Nagel, E., Hoffmann, U., & Leiner, T. (2015). Diagnostic accuracy of stress myocardial perfusion imaging compared to invasive coronary angiography with fractional flow reserve meta-analysis. *Circulation: Cardiovascular imaging, 8*(1), e002666.

Tanaka, M., Fujiwara, H., Onodera, T., Wu, D. J., Matsuda, M., Hamashima, Y., & Kawai, C. (1987). Quantitative analysis of narrowings of intramyocardial small arteries in normal hearts, hypertensive hearts, and hearts with hypertrophic cardiomyopathy. *Circulation, 75*(6), 1130-1139.

Taqueti, V. R., & Di Carli, M. F. (2018). Coronary Microvascular Disease Pathogenic Mechanisms and Therapeutic Options: JACC State-of-the-Art Review. *Journal of the American College of Cardiology, 72*(21), 2625-2641.

Taqueti, V. R., Hachamovitch, R., Murthy, V. L., Naya, M., Foster, C. R., Hainer, J., Dorbala, S., Blankstein, R., & Di Carli, M. F. (2015). Global coronary flow reserve is associated with adverse cardiovascular events independently of luminal angiographic severity and modifies the effect of early revascularization. *Circulation, 131*(1), 19-27.

Taylor, C. A., Fonte, T. A., & Min, J. K. (2013). Computational fluid dynamics applied to cardiac computed tomography for noninvasive quantification of fractional flow reserve: scientific basis. *Journal of the American College of Cardiology, 61*(22), 2233-2241.

Thomson, L. E., Wei, J., Agarwal, M., Haft-Baradaran, A., Shufelt, C., Mehta, P. K., Gill, E. B., Johnson, B. D., Kenkre, T., Handberg, E. M., Li, D., Sharif, B., Berman, D. S., Petersen, J. W.,

Pepine, C. J., & Bairey Merz, C. N. (2015). Cardiac magnetic resonance myocardial perfusion reserve index is reduced in women with coronary microvascular dysfunction. A National Heart, Lung, and Blood Institute-sponsored study from the Women's Ischemia Syndrome Evaluation. *Circulation: Cardiovascular imaging, 8*(4), e002481.

Tomaniak, M., Katagiri, Y., Modolo, R., Silva, R., Khamis, R. Y., Bourantas, C. V., Torii, R., Wentzel, J. J., Gijsen, F. J. H., van Soest, G., Stone, P. H., West, N. E. J., Maehara, A., Lerman, A., van der Steen, A. F. W., Lüscher, T. F., Virmani, R., Koenig, W., Stone, G. W., . . . Onuma, Y. (2020). Vulnerable plaques and patients: state-of-the-art. *European Heart Journal, 41*(31), 2997-3004.

Tonino, P. A., De Bruyne, B., Pijls, N. H., Siebert, U., Ikeno, F., van' t Veer, M., Klauss, V., Manoharan, G., Engstrøm, T., Oldroyd, K. G., Ver Lee, P. N., MacCarthy, P. A., & Fearon, W. F. (2009). Fractional flow reserve versus angiography for guiding percutaneous coronary intervention. *New England Journal of Medicine, 360*(3), 213-224.

Toth, G., Hamilos, M., Pyxaras, S., Mangiacapra, F., Nelis, O., De Vroey, F., Di Serafino, L., Muller, O., Van Mieghem, C., Wyffels, E., Heyndrickx, G. R., Bartunek, J., Vanderheyden, M., Barbato, E., Wijns, W., & De Bruyne, B. (2014). Evolving concepts of angiogram: fractional flow reserve discordances in 4000 coronary stenoses. *European Heart Journal, 35*(40), 2831-2838.

Trägårdh, E., Tan, S. S., Bucerius, J., Gimelli, A., Gaemperli, O., Lindner, O., Agostini, D., Übleis, C., Sciagrà, R., Slart, R. H., Underwood, S. R., Hyafil, F., Hacker, M., & Verberne, H. J. (2017). Systematic review of cost-effectiveness of myocardial perfusion scintigraphy in patients with ischaemic heart disease: A report from the cardiovascular committee of the European Association of Nuclear Medicine. Endorsed by the European Association of Cardiovascular Imaging. *European Heart Journal – Cardiovascular Imaging, 18*(8), 825-832.

Uusitalo, V., Kamperidis, V., de Graaf, M. A., Maaniitty, T., Stenström, I., Broersen, A., Dijkstra, J., Scholte, A. J., Saraste, A., Bax, J. J., & Knuuti, J. (2017). Coronary computed tomography angiography derived risk score in predicting cardiac events. *Journal of Cardiovascular Computed Tomography, 11*(4), 274-280.

van Assen, M., De Cecco, C. N., Eid, M., von Knebel Doeberitz, P., Scarabello, M., Lavra, F., Bauer, M. J., Mastrodicasa, D., Duguay, T. M., Zaki, B., Lo, G. G., Choe, Y. H., Wang, Y., Sahbaee, P., Tesche, C., Oudkerk, M., Vliegenthart, R., & Schoepf, U. J. (2019). Prognostic value of CT myocardial perfusion imaging and CT-derived fractional flow reserve for major adverse cardiac events in patients with coronary artery disease. *Journal of Cardiovascular Computed Tomography, 13*(3), 26-33.

van de Hoef, T. P., van Lavieren, M. A., Damman, P., Delewi, R., Piek, M. A., Chamuleau, S. A., Voskuil, M., Henriques, J. P., Koch, K. T., de Winter, R. J., Spaan, J. A., Siebes, M., Tijssen, J. G., Meuwissen, M., & Piek, J. J. (2014). Physiological basis and long-term clinical outcome of discordance between fractional flow reserve and coronary flow velocity reserve in coronary stenoses of intermediate severity. *Circulation: Cardiovascular Interventions, 7*(3), 301-311.

van Dijk, R., van Assen, M., Vliegenthart, R., de Bock, G. H., van der Harst, P., & Oudkerk, M. (2017). Diagnostic performance of semi-quantitative and quantitative stress CMR perfusion analysis: a meta-analysis. *Journal of Cardiovascular Magnetic Resonance, 19*(1), 92.

van Werkhoven, J. M., Heijenbrok, M. W., Schuijf, J. D., Jukema, J. W., van der Wall, E. E., Schreur, J. H., & Bax, J. J. (2010). Combined non-invasive anatomical and functional assessment with MSCT and MRI for the detection of significant coronary artery disease in patients with an intermediate pre-test likelihood. *Heart, 96*(6), 425-431.

van Werkhoven, J. M., Schuijf, J. D., Gaemperli, O., Jukema, J. W., Boersma, E., Wijns, W., Stolzmann, P., Alkadhi, H., Valenta, I., Stokkel, M. P. M., Kroft, L. J., de Roos, A., Pundziute, G., Scholte, A., van der Wall, E. E., Kaufmann, P. A., & Bax, J. J. (2009). Prognostic value of multislice computed tomography and gated single-photon emission computed tomography in patients with suspected coronary artery disease. *Journal of the American College of Cardiology, 53*(7), 623-632.

Vanhoutte, P. M., Shimokawa, H., Feletou, M., & Tang, E. H. (2017). Endothelial dysfunction and vascular disease - a 30th anniversary update. *Acta Physiologica, 219*(1), 22-96.

Vartiainen, E., Puska, P., Pekkanen, J., Tuomilehto, J., & Jousilahti, P. (1994). Changes in risk factors explain changes in mortality from ischaemic heart disease in Finland. *BMJ, 309*(6946), 23-27.

Vermeltfoort, I. A., Raijmakers, P. G., Odekerken, D. A., Kuijper, A. F., Zwijnenburg, A., & Teule, G. J. (2009). Association between anxiety disorder and the extent of ischemia observed in cardiac syndrome X. *Journal of Nuclear Cardiology, 16*(3), 405-410.

Virmani, R., Kolodgie, F. D., Burke, A. P., Farb, A., & Schwartz, S. M. (2000). Lessons from sudden coronary death: a comprehensive morphological classification scheme for atherosclerotic lesions. *Arteriosclerosis, Thrombosis, and Vascular Biology, 20*(5), 1262-1275.

Vogel, R., Indermühle, A., Reinhardt, J., Meier, P., Siegrist, P. T., Namdar, M., Kaufmann, P. A., & Seiler, C. (2005). The quantification of absolute myocardial perfusion in humans by contrast echocardiography: algorithm and validation. *Journal of the American College of Cardiology Cardiology, 45*(5), 754-762.

von Spiczak, J., Manka, R., Gotschy, A., Oebel, S., Kozerke, S., Hamada, S., & Alkadhi, H. (2018). Fusion of CT coronary angiography and whole-heart dynamic 3D cardiac MR perfusion: building a framework for comprehensive cardiac imaging. *The International Journal of Cardiovascular Imaging, 34*(4), 649-660.

Waller, B. F., Orr, C. M., Slack, J. D., Pinkerton, C. A., van Tassel, J. & Peters, T (1992). Anatomy, histology, and pathology of coronary arteries: a review relevant to new interventional and imaging techniques--Part I. *Clinical Cardiology, 15*(6), 451-7.

Wang, L., Jerosch-Herold, M., Jacobs, D. R., Shahar, E., Detrano, R., Folsom, A. R., & Investigators, M. S. (2006). Coronary artery calcification and myocardial perfusion in asymptomatic adults: the MESA (Multi-Ethnic Study of Atherosclerosis). *Journal of the American College of Cardiology, 48*(5), 1018-1026.

Weintraub, W. S., Spertus, J. A., Kolm, P., Maron, D. J., Zhang, Z., Jurkovitz, C., Zhang, W., Hartigan, P. M., Lewis, C., Veledar, E., Bowen, J., Dunbar, S. B., Deaton, C., Kaufman, S., O'Rourke, R. A., Goeree, R., Barnett, P. G., Teo, K. K., Boden, W. E., & Mancini, G. B. (2008). Effect of PCI on quality of life in patients with stable coronary disease. *New England Journal of Medicine, 359*(7), 677-687.

Werner, R. A., Chen, X., Rowe, S. P., Lapa, C., Javadi, M. S. & Higuchi, T (2019). Moving into the next era of PET myocardial perfusion imaging: introduction of novel 18 F-labeled tracers. *The international Journal of Cardiovascular Imaging, 35*(3), 569-577.

Williams, M. C., Hunter, A., Shah, A. S. V., Assi, V., Lewis, S., Smith, J., Berry, C., Boon, N. A., Clark, E., Flather, M., Forbes, J., McLean, S., Roditi, G., van Beek, E. J. R., Timmis, A. D., & Newby, D. E. (2016). Use of Coronary Computed Tomographic Angiography to Guide Management of Patients With Coronary Disease. *Journal of the American College of Cardiology, 67*(15), 1759-1768.

Wilson, P. W., D'Agostino, R. B., Levy, D., Belanger, A. M., Silbershatz, H., & Kannel, W. B. (1998). Prediction of coronary heart disease using risk factor categories. *Circulation, 97*(18), 1837-1847.

Windecker, S., Stortecky, S., Stefanini, G. G., da Costa, B. R., daCosta, B. R., Rutjes, A. W., Di Nisio, M., Silletta, M. G., Siletta, M. G., Maione, A., Alfonso, F., Clemmensen, P. M., Collet, J. P., Cremer, J., Falk, V., Filippatos, G., Hamm, C., Head, S., Kappetein, A. P., . . . Juni, P. (2014). Revascularisation versus medical treatment in patients with stable coronary artery disease: network meta-analysis. *BMJ, 348*, g3859.

Wood, D. A., Kotseva, K., Connolly, S., Jennings, C., Mead, A., Jones, J., Holden, A., De Bacquer, D., Collier, T., De Backer, G., Faergeman, O., & Group, E. S. (2008). Nurse-coordinated multidisciplinary, family-based cardiovascular disease prevention programme (EUROACTION) for patients with coronary heart disease and asymptomatic individuals at high risk of cardiovascular disease: a paired, cluster-randomised controlled trial. *Lancet, 371*(9629), 1999-2012.

Wykrzykowska, J. J., Arbab-Zadeh, A., Godoy, G., Miller, J. M., Lin, S., Vavere, A., Paul, N., Niinuma, H., Hoe, J., Brinker, J., Khosa, F., Sarwar, S., Lima, J., & Clouse, M. E. (2010). Assessment of in-stent restenosis using 64-MDCT: analysis of the CORE-64 Multicenter International Trial. *American Journal of Roentgenology, 194*(1), 85-92.

Xaplanteris, P., Fournier, S., Pijls, N. H. J., Fearon, W. F., Barbato, E., Tonino, P. A. L., Engstrøm, T., Kääb, S., Dambrink, J. H., Rioufol, G., Toth, G. G., Piroth, Z., Witt, N., Fröbert, O., Kala, P., Linke, A., Jagic, N., Mates, M., Mavromatis, K., . . . De Bruyne, B. (2018). Five-Year Outcomes with PCI Guided by Fractional Flow Reserve. *New England Journal of Medicine, 379*(3), 250-259.

Yahagi, K., Kolodgie, F. D., Otsuka, F., Finn, A. V., Davis, H. R., Joner, M., & Virmani, R. (2016). Pathophysiology of native coronary, vein graft, and in-stent atherosclerosis. *Nature Reviews Cardiology, 13*(2), 79-98.

Yao, S. S., Bangalore, S., & Chaudhry, F. A. (2010). Prognostic implications of stress echocardiography and impact on patient outcomes: an effective gatekeeper for coronary angiography and revascularization. *Journal of the American Society of Echocardiography, 23*(8), 832-839.

Yao, S. S., Qureshi, E., Sherrid, M. V., & Chaudhry, F. A. (2003). Practical applications in stress echocardiography: risk stratification and prognosis in patients with known or suspected ischemic heart disease. *Journal of the American College of Cardiology, 42*(6), 1084-1090.

Yokoyama, I., Momomura, S., Ohtake, T., Yonekura, K., Nishikawa, J., Sasaki, Y., & Omata, M. (1997). Reduced myocardial flow reserve in non-insulin-dependent diabetes mellitus. *Journal of the American College of Cardiology, 30*(6), 1472-1477.

Zhang, X., Li, Q., Zhao, J., Li, X., Sun, X., Yang, H., Wu, Z., & Yang, J. (2014). Effects of combination of statin and calcium channel blocker in patients with cardiac syndrome X. *Coronary Artery Disease, 25*(1), 40-44.

Ziadi, M. C., Dekemp, R. A., Williams, K. A., Guo, A., Chow, B. J., Renaud, J. M., Ruddy, T. D., Sarveswaran, N., Tee, R. E., & Beanlands, R. S. (2011). Impaired myocardial flow reserve on rubidium-82 positron emission tomography imaging predicts adverse outcomes in patients assessed for myocardial ischemia. *Journal of the American College of Cardiology, 58*(7), 740-748.

Zimmermann, F. M., Ferrara, A., Johnson, N. P., van Nunen, L. X., Escaned, J., Albertsson, P., Erbel, R., Legrand, V., Gwon, H. C., Remkes, W. S., Stella, P. R., van Schaardenburgh, P., Bech, G. J., De Bruyne, B., & Pijls, N. H. (2015). Deferral vs. performance of percutaneous coronary intervention of functionally non-significant coronary stenosis: 15-year follow-up of the DEFER trial. *European Heart Journal, 36*(45), 3182-3188.

UNIVERSITY OF TURKU

Painosalama Oy, Turku, Finland 2020

ISBN 978-951-29-8298-1 (PRINT)
ISBN 978-951-29-8299-8 (PDF)
ISSN 0355-9483 (Print)
ISSN 2343-3213 (Online)